Measuring and modeling the impact of roadway runoff on a headwater tributary of the Cahaba River

by

Catherine Gail Butler

A thesis submitted to the Graduate Faculty of
Auburn University
in partial fulfillment of the
requirements for the Degree of
Master of Science

Auburn, Alabama
August 1, 2015

Key words: Stormwater runoff, Water Quality, Headwaters
Field Investigation, SWMM

Approved by

Jose Goes Vasconcelos Neto, Chair, Assistant Professor of Civil Engineering
Xing Fang, Arthur H. Feagin Chair Professor of Civil Engineering
Wesley Zech, Brasfield & Gorrie Associate Professor of Construction Engineering and Management

Abstract

Stormwater runoff from highways has been a relevant focus of study both in terms of its characterization during construction phases as well as during the operational years. Highways have been thought to have adverse impacts on the water quality of nearby water bodies in terms of parameters such as solids, turbidity and metals, among others. This thesis presents results of a 24-month long monitoring of the Little Cahaba Creek (LCC), a perennial headwater tributary of the Cahaba River, located north of Trussville, AL. In this study, levels of nitrate, total nitrogen, total phosphorous, turbidity, and total suspended solids (TSS) were monitored and recorded upstream and downstream of Interstate-59 (I-59) on a biweekly basis. In addition to the biweekly samples taken at each site, two Water Quality Sondes were deployed at the upstream and downstream sites. The turbidity readings from these Sondes were converted to TSS using a turbidity-TSS relationship derived from samples collected in the stream in various flow conditions. The stream flow was continuously measured by two Area-Velocity Sensors each deployed at sites upstream and downstream from the crossing with I-59. The stream flow data, along with the rain gauge and TSS measurements, were entered into PC-Stormwater Management Model (PCSWMM), a decision support system and processing tool for EPA's Stormwater Management Model (SWMM5). The LCC SWMM5 model was calibrated for various hydrological characteristics from 6/12/2014 to 12/31/2014. The model calibration detected the sensitive parameters: subcatchment flow length width, % impervious, Horton's maximum and minimum infiltration rates, and channel roughness. Once calibration was completed, the validation period, 1/1/2015 to 3/26/2015, showed a satisfactory relationship for the upstream site but not for the downstream site. Limited available rain gauge data (due to equipment failure-may have restricted more adequate calibration and validation results). Through continuous recording and analyzing the levels of these nutrients and water quality indicators in the LCC, this study hopes to provide a better understanding of the impact of highway runoff on receiving water bodies in the context of post-construction stormwater

management of highways, as well as expand the SWMM knowledge base to include more detailed studies on the impacts of roadways on small stream waters or headwaters.

Acknowledgments

I would like to thank my advisor, Professor Jose Neto Vasconcelos, for his support and guidance over the last two years. He gave me this opportunity to grow in knowledge of the field of hydrology as well as in life. Thank you for your patience through our long meetings and discussions. I will carry with me the knowledge and wisdom you have passed on to me for the rest of my life.

I would also like to thank Mitchell Moore and all of the student workers on this project: Holly Guest, Robyn Manhard, Nikki Zeaser, Tyler Werk, Morgan Bell, Julianne Bolls, and Jacob Beatty. I would have not have made it through this project with my sanity if it was not for your outside help and work in the lab.

Lastly, I would like to thank my friends and family to whom I owe a great deal to because of their support and encouragement through the last two years. Thank you for being patient with me and standing by my side through the ups and downs. Your friendship has been my rock when all I wanted to do was fall over. I am beyond blessed to have the support that I have had from my parents, family, and friends, especially over the last months leading to the end of my thesis.

A special thank you goes to Katie and Winifred Rutenbar. Thank you for helping edit my thesis. Both of your revisions made my paper stronger. Also, thank you, Brian Spencer, my best friend and my companion, for helping me up when I fall and encouraging me to do my best. Thank you all. I would not have made it to the end without your love and support.

Table of Contents

List of Tables

List of Figures

List of Abbreviations

AADT	Annual Average Daily Traffic
ADT	Average Daily Traffic
AOI	Area of Intent
AV	Area-Velocity
BMP	Best Management Practices
Cd	Cadmium
Cr	Chromium
Cu	Copper
DEM	Digital Elevation Model
EMC	Event-mean Concentration
GIS	Geographic Information System
GSSHA	Gridded Surface Subsurface Hydrologic Analysis
GW	Groundwater
HEC-HMS	Hydrologic Engineering Center's Hydraulic Modeling System
IC	Ion-Chromatograph
LCC	Little Cahaba Creek
N	Nitrogen
NO	Nitric Oxide
NO_2	Nitrite

NO_3	Nitrate
NH_3	Ammonia
NPDES	National Pollutant Discharge Elimination System
NRCS	Natural Resources Conservation Service
NSE	Nash-Sutcliff Efficiency
NURP	Nationwide Urban Runoff Program
Pb	Lead
RMSE	Root Mean Square Error
SRTC	Sensitivity-based Radio Tuning Calibration
SWMM	Stormwater Management Model
SWMP	Stormwater Management Plan
TDS	Total Dissolved Solids
TKN	Total Kjeldahl Nitrogen
TN	Total Nitrogen
TOC	Time of Concentration
TOC	Total Organic Carbon
TP	Total Phosphorus
TSS	Total Suspended Solids
TVS	Total Volatile Solids
USGS	United States Geological Survey
Zn	Zinc

Chapter 1

Introduction: Aspects of stormwater management considering the urbanization process and stormwater management related to roadway development

Stormwater management is a priority for both rural and urban areas for roadway development. Most often, stormwater management is viewed as a group of institutional, managerial and engineering approaches that has a main objective of maintaining the integrity and stability of receiving water bodies and related ecosystems which are affected by stormwater runoff. Stormwater management aims, among other objectives, to prevent fish kills, deconstruction of the surrounding habitats, and contamination of drinking water. Uncontrolled stormwater can also lead to drastic changes in the course of a stream bed or the surrounding habitats due to overwhelming volume in the stream channel's limited capacity (EPA, 2005). Management of stormwater runoff from developed subcatchments is imperative to controlling the impacts on water quality.

Even though there have been numerous studies conducted on stormwater runoff, relatively less research has been performed in the context of roadway development. There have also been multiple conclusive studies produced to model the impacts of stormwater runoff on water bodies (e.g. rivers, streams, lakes, etc.) and the impacts of the surrounding environments (i.e. sediment discharge and flow rates). However, this work narrows the focus of modeling water bodies to modeling the impacts of roadways on small stream waters or headwaters.

Stormwater runoff due to roadways is considered highly variable in time and in space (Thomas et al. 1994). As a result, the amount of suspended solids within the runoff from a given stretch of roadway can range anywhere from 10 ppm to 2000 ppm (Thomas et al. 1994). Stormwater runoff, if left unmanaged, can cause pollutants to exceed their maximum admissible concentration set by the United States Environmental Protection Agency (EPA). Understanding the behavior of highway stormwater runoff and the impacts from stormwater runoff are an important step in developing best management practices (BMPs) to ensure the quality of receiving water bodies.

Over time, stormwater runoff produces a large amount of flow directly to surface water that can be detrimental to the existing environment (EPA, 2005). This motivated the establishment of the National Pollutant Discharge Elimination System (NPDES) Phase II Stormwater program, which requires contractors to develop and implement a stormwater management plan (SWMP). Included in this plan are BMPs that must be maintained and updated to provide effective erosion and sediment control as well as control of discharge and water quality impacts. These BMPs are carried out through the six minimum control measures of a stormwater management plan (SWMP):

1. Public education and outreach;
2. Public participation/involvement;
3. Illicit discharge detection and elimination;
4. Construction site runoff control;
5. Post-construction runoff control; and
6. Good housekeeping/pollution prevention for municipal operations (EPA 2005).

1.1. Literature Review

Development or secondary development of roadways creates a difficult balance between stimulating economic growth and protecting the surrounding environment through SWMPs. Wheeler et al. (2006) noted that construction and urbanization are persistent threats, both immediate and long term, to a stream's ecosystem's physical, chemical and biological impacts. A stream's ecosystem is sensitive to even low levels (<10%) of watershed urbanization (Wheeler et al. 2006). The understanding of these impacts of urbanization and roadways on the surrounding environment are crucial when designing and implementing a SWMP.

This literature review covers the hydrological impacts of roadways on watersheds, stormwater runoff pollutants and the quantification of highway runoff impacts on receiving water bodies through multiple case studies. These three sections provide a comprehensive overview of the overall impact urbanization has on the surrounding environment. The last two sections will cover the difficulties involved with modeling natural waters and their application to PC-Stormwater Management Model (PCSWMM).

1.1.1. Hydrological impacts of roads to watersheds

Highways have three main development stages which account for short- and long- term impacts on waterbodies: highway construction, highway presence and urbanization (Angermeirer et al. 2004). The initial stage, highway construction, includes the short term impacts of the construction processes. Generally, these impacts are only temporary and physical (e.g. sediment loading), but the highway presence has sustained impacts on natural water bodies. This phase includes the impact of chemical pollutants, possibly through highway maintenance and/or from vehicular traffic, as well as the impact arising from stream channel alterations. Lastly, the urbanization phase includes the impact of the economic growth and the variety of chemical and physical impacts that cannot be fully monitored and controlled.

Development in watersheds increases stormwater runoff due to the introduction of impervious surfaces having direct impacts on the aquatic population (Gubernick et al. 2003; Wheeler et al. 2006). Due to this harsh impact on the environment, many studies have been conducted to better understand the problems caused by roadways and urbanization. Structures where the roadway crosses over the stream, such as bridges and culverts, affect the aquatic populations by impeding passage during low flow, perched outlets, and over time as culverts may become filled with debris and sediment. Such structures can also cause large amounts of scouring and destruction of the surrounding vegetation if not properly sized (Gubernick et al 2003). Non-vegetative habitats have been proven to shorten aquatic animals' life spans (Duncan et al. 2010).

Additionally, groundwater can be impacted by the reduction of base flow due to decreased time of concentration of stormwater across receiving water bodies (Arnold and Gibbons 1996; Pouraghniaei 2002). Groundwater recharge can be reduced by the reduction of infiltration through the watershed system, which is largely caused by the increase in impervious surfaces fromroadway construction (Pouraghniaei 2002). A study done in Orange County, N.C. proved that the discharge per square mile can increase up to six times the amount from a forested basin ($0.45 ft^3/s/mi^2$) to an area with approximately 50% impervious area ($2.78\ ft^3/s/mi^2$) (Herrera 2007).

In summary, surface water and groundwater are both susceptible to the impacts of roadways and urbanization (Stephenson et al. 1999). However, through the application of the appropriate mitigation measures, such as stormwater retention or treatment and vegetative

buffers, the impact of highways on natural streams can be reduced (Wheeler et al 2006). This includes increasing stream stability and, more importantly, improvements in sustaining the existing water quality (Selvakumar et al. 2010).

1.1.2. Stormwater runoff pollutants

Hydrological impacts are not the only concerns threatening receiving water bodies; more than that, the presence of pollutants in stormwater runoff negatively impact receiving water bodies. Studies have established that pollutants such as solids, metals and nutrients are found in stormwater runoff from roadways and are often associated with traffic, the type of roadway maintenance, and the roadway itself (Bian and Zhu 2008; Barrett et al. 1995a; Cape 2004; Herrera 2007; Viklander 1998). Barrett et al. (1995a,b) has listed several categories of constituents that are important to monitor including: suspended solids, oxygen demand, nutrients, heavy metals, organic compounds, petroleum products, and bacteria. If these constituents are left untreated, they can impair water quality thus posing a danger to aquatic organisms. The presence of solids, dissolved oxygen and nutrients in stormwater are discussed further in the following sections.

Physical Parameters

The physical impact of highways extends to the buildup of contaminants on impervious surfaces and the subsequent washoff into channels (Duncan 1995). The buildup of contaminants is a dynamic process that will vary between contributing and non-contributing areas. Pollutants build up over dry periods, and then they are partially or almost completely flushed offsite through an urban stormwater system. This is why stormwater pollution can be detrimental to nearby waterbodies (Duncan et al. 2010).

Traffic loads can be particularly impactful on sediment loads. Although the channel flow, velocity, shear stress, and channel friction can yield very different effects on water quality, the type of geography and the amount of traffic has a consistent effect on the environment (Harned 1988). Viklander (1998) monitored a roadway in Sweden and found that as traffic loads increased so did the amount of sediment found on the roadway. Sweeping and flushing techniques are often used to clear roadways from solids and debris that may cause pollutants buildup. However, a study done in Germany found that sweeping devices mainly remove coarser

material, while contaminates tend to bond to finer particles (Grottker, 1987). Studies done on the particle size distribution, have found that particles smaller than 75 μm contained the most heavy metals (Viklander, 1998).

Solids that accumulate on roadways can originate from many different types of roadway activities. Herrera et al. (2007) list some of these activities as rust and wear of vehicles; sand applied to improve vehicle traction on snow and ice; erosion of the surrounding landscape; road particle from the roadway itself; and atmospheric deposition (Thomson et al. 1996). Other than solids, these roadway activities can produce significant amounts of various metals, ionic species, and nutrients.

Although solids have an impact on the morphology of a water body, solids may also provide insight into the amount of nutrients or metals in a water body (Sansalone et al. 1997). Thomson et al. (1996) has shown that the buildup of solids in various forms, TSS, total dissolved solids (TDS), total volatile solids (TVS), and total organic carbon (TOC), can explain the presence of certain metal, ionic species and nutrients such as cadmium, zinc, iron, arsenic, chloride, and sulfate. Hydrological sampling of metals and other constituents can be expensive and using these surrogate parameters (e.g. TSS, TDS, etc.) allows for more affordable and readily available stormwater monitoring techniques (Sansalone et al. 1998).

In addition to the buildup of contaminants on impervious surfaces, washoff is the process by which dry deposition is removed from the impervious surfaces by rainfall and runoff. Therefore, washoff is strongly associated with rainfall intensity. This “first flush” of pollutants is defined by both the storm and the watershed characteristics (Barrett et al. 1995b). Duncan (1995) states that the “first flush” by nature is a characteristic of a small catchment and that the first flush increases with the degree of urbanization.

Consequently, the frequency, intensity, and duration of rainfall have a large impact on sediment transport or washoff (Herrera et al. 2007). Rainfall is able to more effectively transport finer particles from the pavement to receiving water bodies, where pollutants bind more readily to these finer particles as previously stated (Sansalone 1998). Irish et al. (1995) describes antecedent dry periods and volume of runoff from previous storms as controlling the constituent loading.

In the situation of large storms containing large amounts of stream flow, erosion can occur releasing suspended sediment (soil particles) into water bodies (Wheeler et al. 2006). By

increasing the volume and velocity of the stormwater runoff pouring into the receiving water body, downstream flooding and erosion takes place, such as stream bank scouring. Erosion is caused largely in part by the reduction or lack of vegetation surrounding the water body.

Chemical Parameters

Observing and recognizing the impact of nutrient levels on surrounding waterbodies has become an integral part in assessing the impact of stormwater runoff. Monitoring nutrient levels in stormwater runoff has become more readily practiced mainly due to the increase in the ease of technology that is used to detect nutrient levels. Other than monitoring nutrient levels to comply with EPA regulations, the nutrient levels greatly impact the living aquatic system in a water body. Nutrients can be present in many dissolved forms. Nitrogen can be present as ammonia (NH_3), nitrite (NO_2), nitrate (NO_3) and total Kjeldahl nitrogen (TKN). Phosphorous is mainly measured as orthophosphate phosphorous (Herrera 2007). Increased nutrient levels can cause excessive plant growth in waterbodies, which can deplete the oxygen supply in the water. This process, known as eutrophication, can have toxic effects on the aquatic life (Rabalais et al. 2001).

In a study conducted by Harned (1988) on eight sampling sites, alkalinity, specific conductance, and concentrations of calcium, sodium, and chloride were measurably greater at highway site areas than at the undeveloped sites. These findings suggested that the increase in water quality levels resulted from the salinization of roadways used to mitigate the impact of icy roadways on traffic. Salinization and other roadway maintenance methods can highly impact the nutrient loads deposited into the stream. Vaze and Chiew (2004) concluded that stormwater runoff from urbanized areas resulted in much greater concentrations of suspended sediment, nutrients, and other constituents than unimpaired and rural areas.

Similarly to heavy metals, nutrients attach to sediment particles that can then be carried further downstream (Herrera 2007; Harned 1988; Chui 1981). In the case of a flooding, the concentration of nutrients can be diluted. The study conducted by Vaze and Chiew (2004) found that mainly all the dissolved species of total nitrogen (TN) and total phosphorus (TP) were attached to sediments between 11 and 150 µm. While most street sweepers remove course particles (>300µm), most of the pollutant is found on the smaller particles (11-150 µm) suggesting that roadway maintenance may consider reducing these smaller particles as well

(Harned 1988). Although nutrients may attach to suspended sediment, an effective reduction in sediment loads does not necessarily mean a similar reduction in nutrient loads (Vaze and Chiew 2004).

Roadways and vehicular traffic can be potential sources of various pollutants from tire wear, brake linings, oil leakage, pavement degradation, and atmospheric deposition (Sansalone and Buchberger 1997). Atmospheric deposition or vehicle exhaust can also contribute to an increased amount of nitrogen and phosphorous species. Wu et al. (1998) discovered that atmospheric deposition can contribute 10-30% of runoff pollutant loadings for TSS, TP and NO_{3+2}-N; 30-50 % for copper (Cu), chromium (Cr), lead (Pb), and orthophosphate (OP); and 70-90% for TKN and NH_3-N. These constituents may have originated in both dry and wet weather conditions. Additionally, vehicle traffic can be contributing to the levels on nutrients in a stream. Vehicle exhaust contains nitrogen oxides, such as NO and NO_2, and NH_3 (AQEG 2004), therefore vehicle exhaust may contribute to the increase in nitrogen in runoff (Capea et al. 2004).

A parameter that can be heavily affected by sediment-laden runoff due to large amounts of rainfall is dissolved oxygen (DO). The increase of turbidity can block the sunlight from reaching the benthic zone of the water body, which in turn slows down or halts the aquatic plant photosynthesis. Higher turbidity levels also increase the water temperature by the “suspended particles absorbing more heat” and this reaction “in turn reduces the concentration of DO because warm water holds less DO than cold” (EPA 2012).

Other constituents in surface water runoff can also have a negative impact on DO levels (Herrera et al. 2007). While nutrients such as phosphorus, nitrogen and ammonia are a vital part of plant life in streams, rivers and lakes, they can have a detrimental impact on dissolved oxygen (Rabalais et al. 1994; Turner and Rabalais 1994). High levels of phosphorous contribute to excessive algae growth, which leads to oxygen deficiencies, which is further discussed in the later part of this chapter (Rabalais et al. 2001).

1.1.3. Highway runoff impacts on receiving water bodies

This section covers the impact of TSS and nutrients on surrounding water bodies from a quantitative perspective. Many studies conducted on the quantification of the quality of stormwater runoff to waterbodies (Gould et al. 2010; Herrera 2007; Wheeler et al. 2006;

Stephenson 1999; Barret et al. 1995b; Harned 1988) are used to discuss the impacts of highways on receiving waterbodies.

The most common water quality parameter monitored is solids. Other than the readily available collection material and ease of data analyzation, the ability for suspended solids to bond to pollutants makes this one of the most commonly monitored parameters. Monitoring the amount of sediment allows for an approximation of the range of toxic pollutants that are present in the water body. TSS display the "first flush" effect which means that there is typically a higher concentration during the beginning of the runoff event (Barrett et al. 1995a). Barrett et al. (1995a) also found that the first flush effect was more pronounced during short storm events with constant rainfall intensities. Plots of TSS loads indicated a linear increase between the TSS load and the flow volume. TSS loads for first flush were 56% of the total storm runoff (21mm) (Irish et al. 1995). Moreover, the study showed that metal loads (Cu, iron (Fe), Pb, and Zinc (Zn)) linearly increased with the flow volume as well, averaging a first flush of 57% of the total storm runoff. Although these values are during traffic conditions, the values for non-traffic condition were overall greater. Metals concentrations can be two to five times greater than downstream of a roadway (Barrett et al. 1995b). Viklander (1998) found that a 75 µg particle size carried approximately 0.35µg/g of cadmium (Cd), 140 µg/g of (Cu), 73 µg/g of (Pb), and 250µg/g of (Zn)collected by a sweeping machine.

In North Carolina six highway construction sites were monitored for TSS loads. The pre-construction phase sediment export was 0.01-0.20 tons/ac-yr, during the construction phase 1.23-7.91 tons/ac-yr were exported, and during the post-construction phase the sediment export decreased to 0.17-0.44 ton/ac-yr (Line et al. 2009). Although there was a significant decrease in sediment transport, the pre-existing conditions were still not satisfied at the conclusion of the study. Highly turbid waters, during and after the construction phase, can easily collect heavy metals which do not breakdown. The heavy metals are deposited on the sediment in the benthic zone and can contribute to the chemical and physical degradation of the benthic habitat (EPA 2012). Figure 1.1 is a whisker plot for various major land use types from the National Stormwater Quality Database of TSS (Pitt et al. 2004). The figure includes samples taken from Birmingham and Huntsville AL, as well as other parts of the country. Freeways possessed a higher average of TSS than all the other land uses.

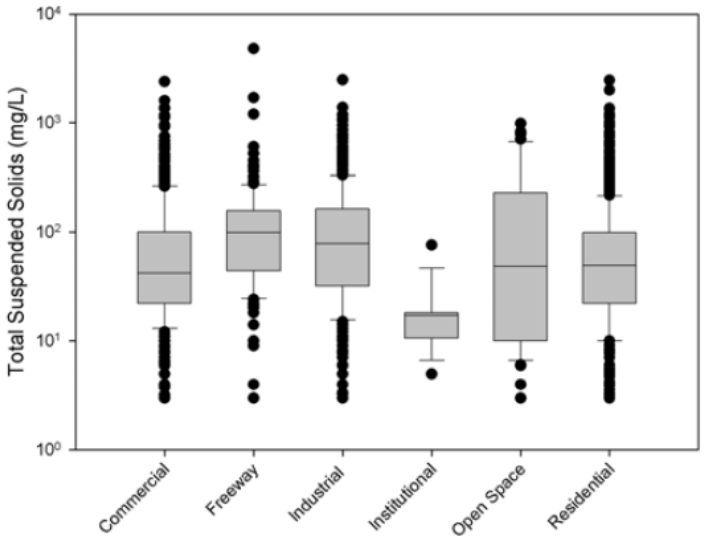

Figure 1.1: Example stormwater data sorted by land use for TSS concentrations (no mixed land use data included in plots) (Pitt et al. 2004).

Over time, channel beds are eroded with increased direct stormwater runoff from roadways and the sediment is transported downstream to another location. Often this will lead to a change in the aquatic habitat and food chain in a stream. Scouring due to high flows can cause a significant disturbance in the water quality of the stream. Stream channel erosion can account for two-thirds of the measured sediment yield (Trimble 1997). Additionally, erosion is caused due to the reduction or lack of vegetation surrounding roadways and water bodies. As mentioned earlier, higher turbidity levels increase the water temperature because "suspended particles absorb more heat". The lack of vegetation leads to a reduction in the amount of dissolved oxygen (DO) due to the warm water that holds less DO than the cold water (EPA 2012).

Analyzing the impact of roadways on receiving water bodies is critical due to the fact that the concentrations of nutrients are typically higher in urban highway runoff than in unimpaired and rural areas. In a study conducted by Bian and Zhu (2008) on road-deposited sediment, the mean concentrations of phosphorous and nitrogen located in high volume areas were approximately 4.45 and 3.52 mg/g, respectively. In the background level areas, the mean concentrations of TP and TN were 2.76 and 2.28 mg/g, respectively.

Nutrients are similar to solids, as they also show characteristics of the first flush effect (Irish et al. 1995; Barrett et al. 1995b; Herrera 2007). Nutrients such as phosphate and nitrogen can represent up to 60% of the pollutant load contained in the first flush storm runoff. These

nutrient concentrations can possess a more complex temporal variation (Barrett et al. 1995b). Nitrate for example, can continue to increase even under no-traffic conditions. This may be caused by the nitrification process that occurs as well as the lack of need for vehicle-induced winds and movement form tires (Irish et al. 1995). Nitrate is also supplied by the releasing of NH_3 into the sediment through denitrification. Macroinvertebrate diversity has been proven to decrease downstream of nutrient point sources (Cole 1973).

Studies by Vaze and Chiew (2002 & 2004) set out to determine nutrient loads associated with different particle sizes on roadways with an ADT of 3000. Vaze and Chiew (2004) discovered that 60-80% of phosphorous and 50-60% of nitrogen from roadway samples were associated with sediment particles. Furthermore, they concluded more than 60% of the total TP from roadway stormwater samples was attached to particles between 11 and 150 µm for wet sieve analysis and about 50% of the total TN was attached to particles between 53 and 300 µm for the dry sieve analysis.

Capea et al. (2004) measured NH_3 and NO_2 levels from 1 m to 10 m away from the roadway. They found that on average NH_3 concentrations were 0.17 to 9.80 $\mu g/m^3$ and NO_2 concentrations were 2.6 to 59.5 $\mu g/m^3$ at the edge of the traffic lane. These values were only reduced 30 to 40% at 10 m from the road. Capea et al (2004) also found that NH_3 concentrations exhibited a seasonal pattern, increasing in the summer months then decreasing in the winter months. The increase in traffic amount from tourist travel during the summer probably contributed to this difference in concentration levels.

Additional causes for an increase in nutrient levels can originate from atmospheric deposition, fertilizer applications, and land use, as well as average daily traffic (ADT) between storms, and antecedent dry periods (Herrera 2007; Wilson et al. 2014). Nutrient concentrations found from western Washington highway runoff were roughly on average 1.8 mg/L of NH_3-N, 1.7mg/L of NO_3+NO_2-N, 6.5 mg/L of TN, 0.8 of TKN, 0.10 mg/L of OP and 1.1 mg/L of TP. These runoff nutrient values were within or similar to the range of values presented in national data (Driscoll et al. 1990; Barrett et al. 1995a,b; Yonge et al. 2000, 2002; Herrera 2007).

Increases in nutrients (various forms of nitrogen and phosphorous) over time can lead to eutrophication of water bodies (Barrett et al. 1995b). Eutrophication will deplete the oxygen in the water body harming, if not resulting in killing fish. In some cases where nutrients level were greater downstream, increased numbers of algae, algal abundance, species diversity and the

relative abundance of filamentous organism were found (Dussart 1984). In this case, the existence of the highway introduced nutrients to this area that was otherwise nutrient poor. Although pollutants did not exceed existing EPA criteria levels at the time, organism such as macroinvertebrates and macrophytes can indicate toxic conditions for that particular region (Peterson et al. 1985). Although, Dupuis et al. (1985) discovered that highway runoff from traffic densities ranging from 12,000 to 20,000 ADT had little impact on the aquatic organism of the receiving water body, for the reason above, the effects of highway runoff are spatially dependent on local hydrological conditions for both surface water and groundwater (Barrett 1995).

Furthermore, Kayhanian et al. (2003) concluded that although Annual ADT (AADT) was found to have a significant effect on concentrations of most constituents in highway runoff, other factors are capable of influencing the accumulation and runoff of pollutants from highways such as antecedent dry period, seasonal cumulative rainfall, total event rainfall and maximum, rain intensity, drainage area, and land use. Based on Kayhanian et al. (2003) results from monitoring several sites in California both urban and nonurban highways, the surrounding and contributing land use effects on runoff water quality are less consistent and less important than AADT and the other factors listed above. Figure 1.2 is a comparison of the event mean concentrations (EMCs) for all of the Caltrans highway runoff data with median EMCs for the median and 90^{th} percentile ranked sites for the Nationwide Urban Runoff Program (NURP). According to the 2003 study, the California roadway study areas are below the national EMC for TSS and phosphate species and above the NURP for NO_3-N and TKN.

As mentioned earlier, the presence of the first flush effect depends on the constituent being measured as well as the rainfall characteristics (Maestre et al. 2004; Pitt et al. 2004). Table 1.1 list the ratios of the medians of the first flush and the composite data sets for each constituent and land use determined by the Mann-Whitney and Fligner-Policello non-parametric tests. The '>' symbol indicates that the median of the first flush data set is higher than for the composite storm data set. The '=' symbol indicates that there is not enough information to reject the null hypothesis. Events without enough data for the analysis are represented with an 'X' (Pitt et al. 2004).

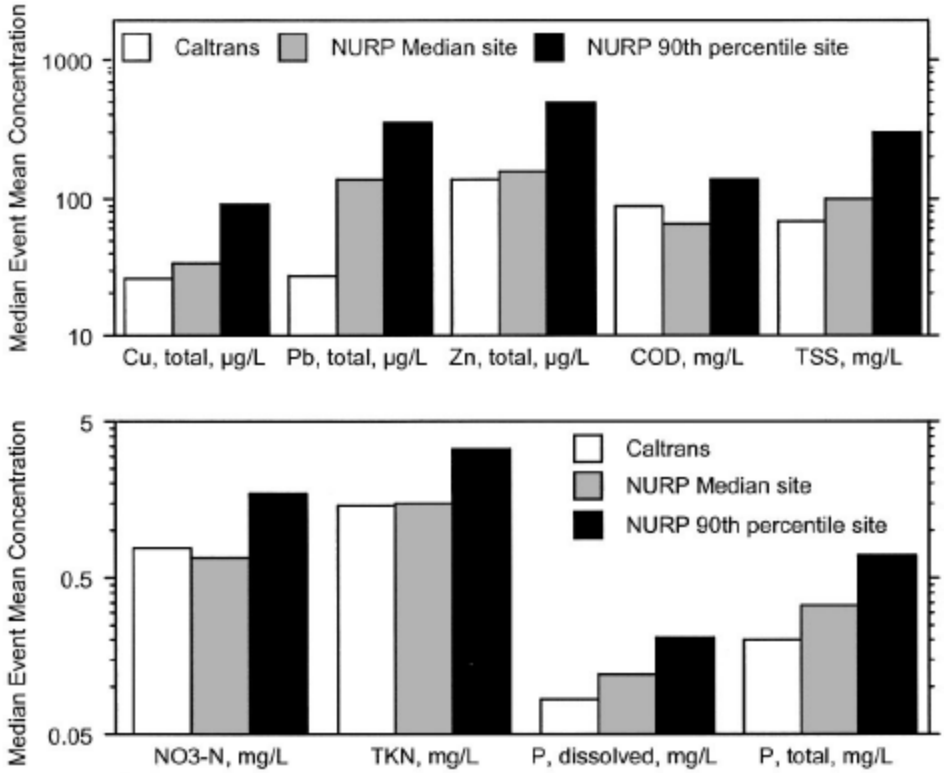

Figure 1.2: Comparisons of Caltrans median EMCs and NURP results for (top) trace metals and conventional pollutants, and (bottom) nutrients (Kayhanian et al. 2003).

Table 1.1: Presence of significant first flush (ratio of first flush to composite median concentrations).

Parameter	Commercial	Industrial	Institutional	Open Space	Residential	All Combined
Turbidity	= (1.32)	X	X	X	= (1.24)	= (1.26)
pH	= (1.03)	= (1.00)	X	X	= (1.01)	= (1.01)
COD	> (2.29)	> (1.43)	> (2.73)	= (0.67)	> (1.63)	> (1.71)
TSS	> (1.85)	= (0.97)	> (2.12)	= (0.95)	> (1.84)	> (1.60)
BOD_5	> (1.77)	> (1.58)	> (1.67)	= (1.07)	> (1.67)	> (1.67)
TDS	> (1.82)	> (1.32)	> (2.66)	= (1.07)	> (1.52)	> (1.55)
O&G	> (1.54)	X	X	X	= (2.05)	> (1.60)
Fecal Coliform	= (0.87)	X	X	X	= (0.98)	= (1.21)
Fecal Strep.	= (1.05)	X	X	X	= (1.30)	= (1.11)
Ammonia	> (2.11)	= (1.08)	> (1.66)	X	> (1.36)	> (1.54)
NO_2 NO_3	> (1.73)	> (1.31)	> (1.70)	= (0.96)	> (1.66)	> (1.50)
Total N	= (1.35)	= (1.79)	X	= (1.53)	= (0.88)	= (1.22)
TKN	> (1.71)	> (1.35)	X	= (1.28)	> (1.65)	> (1.60)
Total P	> (1.44)	= (1.42)	= (1.24)	= (1.05)	> (1.46)	> (1.45)
P Dissolved	= (1.23)	= (1.04)	= (1.05)	= (0.69)	> (1.24)	= (1.07)
Phosphate Ortho	X	= (1.55)	X	X	= (0.95)	= (1.30)
Cd	> (2.15)	= (1.00)	X	= (1.30)	> (2.00)	> (1.62)
Cr	> (1.67)	= (1.36)	X	= (1.70)	= (1.24)	> (1.47)
Cu	> (1.62)	> (1.24)	= (0.94)	= (0.78)	> (1.33)	> (1.33)
Pb	> (1.65)	> (1.41)	> (2.28)	= (0.90)	> (1.48)	> (1.50)
Ni	> (2.40)	= (1.00)	X	X	= (1.20)	> (1.50)
Zn	> (1.92)	> (1.540	> (2.48)	= (1.25)	> (1.58)	> (1.59)

1.1.4. Aspects of hydrological and water quality data collection in watersheds

In order to minimize confusion and a lack of crucial data, a monitoring plan needs to be designed and implemented early on in the project to obtain data needed to address the various project concerns and objectives (Young et al. 1996; Southerland 2006). However, the monitoring plan cannot always account for unforeseen problems and sensor malfunctions that may occur during the data collection period of the project. Moreover, calibrated parameters based on macroscale discretization may not be as adequate as a smaller delineation, which can accommodate the variations between subcatchments (Sun et al. 2014a). Microdelineation, in which each subcatchment was defined for a unique soil and land-use combination, will reduce the uncertainty of flow prediction along with having accurate field data. Over simplifying the parameters will not accurately represent the watershed. Instead over simplification could lead a user to false conclusions about the drainage system (James 2005).

For instance, discretization of rainfall data dictates how well a model predicts flow or pollutant concentrations. Since storm events are dynamic in nature, storms can appear at different times across a subcatchment making it difficult to track runoff and channel flow (James 2005). Storm duration and intensity varies from event to event, which makes predicting rainfall measurement concentration as a function of time difficult (Kim et al. 2005). Small rain events during the summer season in the southeast region of the United States are quick moving with high intensities and short durations. During the winter season in the southeastern region, rain events have long durations with smaller intensities, affecting distribution and the representation of the rain gauge data collection. Many time errors in flow can be traced back to poorly represented rainfall data collection, which result from improper calibration, malfunctions, poor location of rain gauges, equipment limitations, and data collection and reduction. James (2005) suggests having three rain gauges in order to adequately calculate the speed and direction of a storm cell through the watershed. Calculating this in a program such as RAINPACK™ can assist in generating discretized time series of a runoff module.

In addition to meteorological constraints, physical constraints are also a concern. Physical constraints on stormwater quality monitoring can be due to the size of the watershed, the time of concentration, and peak flow, as well as downstream access issues and numerous outfalls (Strecker et al. 2001). Small to medium sized watersheds are easier to monitor. This is due to the ease of tracking the smaller system compared to a large urban watershed. The larger watershed

system may be verified by mapping or by municipal connections possibly resulting in multiple downstream connections that were not a part of the natural watershed. Monitoring a smaller watershed may also be more cost effective when deploying equipment. Nevertheless, watersheds with short time of concentrations (TOC) and high peak flows can cause damage to equipment; inaccuracies in automatic samplers becoming triggered in low flow conditions; and error in flow measurement due to unsteady flow conditions (Strecker et al. 2001).

Furthermore, selecting the appropriate equipment can be challenging (Strecker et al. 2001). Equipment that can withstand stream or sewer system flow should be implemented, especially for long-term operation (Southerland 2006; Sun et al 2014b). When evaluating the purchase of certain equipment, the following options should be considered: evaluate alternative means for acquiring the information needed to support project objectives, consider a phase approach that addresses only the important stormwater questions to obtain useful results within resource limitation, and utilize available data from other local monitoring sites (Young et al. 1996; Strecker et al. 2001). Using these basic concepts, the correct equipment can be implemented to observe hydrological and water quality interactions.

1.1.5. Modeling Watersheds

The golden rule for model calibration is to calibrate the most sensitive parameters considering a pre-determined objective function. Without a defined objective function, model calibration efforts are limited. Creating the perfect model is not the objective of this literary work. The objective of this thesis is to create a model that best represents the area of interest (AOI) and the major processes involved through thorough site investigation and parameter calibration as well as to provide a better understanding of modeling headwaters.

There are many complexities and concerns involved in modeling natural watersheds. James (2005) states that a model is measured by its reliability, and to achieve reliability in the LCC model, the project required the use of observed data, such as flow and rainfall measurements. This section covers these modeling concerns and their significance: watershed delineation, defining critical structural elements, adequate available field data, establishing a relationship between land use and water quality, tracking the relationship between surface water and groundwater, defining groundwater parameters, discretization of surface runoff parameters, determining parameter relationships, parameter uncertainty, and water quality calibration. These

difficulties and uncertainties behind the listed model building processes are only a portion of all the possible concerns with watershed modeling. Other concerns associated with watershed modeling not listed are outside the scope of this thesis.

One of the first steps to create a model is watershed delineation. The size and nature of the receiving water body of interest helps define the optimal scale and detail of the water quality model (Duncan 1995). A model can be delineated using two types of delineation: macroscale and microscale (Sun et al. 2014a). Macroscale delineation is also known as lumped parameter modeling, where subcatchment boundaries are developed by existing land area and sewer network map. The macroscale delineated subcatchments contain more than one land use or soil property, and the inferred parameters are given an area-weighted averaged over the existing surface conditions, whereas microscale delineation is distributed parameter modeling dividing subcatchments by distinct soil and land use combinations. Microscale delineation better replicates the heterogeneity across the subcatchment to reduce model uncertainty.

Furthermore, in the process of creating a reliable model, certain elements in the watershed must be identified such as: dams, ponds, storage tanks, pump wells and pump stations, the largest diameter conveyances, the tributaries, diversions, outfalls, weirs and gates (Tsihrintzis et al. 1998; James 2005). The connection between these elements and the drainage system must be replicated when spatially discretizing a model. As the model takes on more and more elements, the complexity of the model increases as well. However, only the most significant elements should be incorporated into the watershed model. The models relative sensitivity decreases with increasing complexity thus making the ‘subspace intensity’ less important (James 2005).

Modeling and calibrating headwaters is complex and therefore requires local field data to calibrate and validate a model (Sun et al. 2014a). The model can only be as reliable as the observed field data being used. The majority of field data should already be collected before being model calibration. Calibration is needed for predictions of specific regions regarding effects of pollutants on water bodies (Tsihrintzis et al. 1998). An undeveloped watershed in the Southwest Region of the United States does not have the same characteristics as an undeveloped watershed in the Southeast Region.

Therefore, the model needs quality flow measurements and rainfall data to optimize the calibration of the model. A study done by Huynh-Ba et al. (2004) chose six sites based off their

location to improve the relationship of the hydrological elements within the watershed. Monitoring these six sites led to a better understanding of the watershed and to better input parameters of the Hydrologic Engineering Center's Hydraulic Modeling System (HEC-HMS) model. Another field site monitoring was conducted by Kim et al. (2005), where eight sites were monitored to detect the first flush of pollutants from runoff (i.e. TSS, COD, TOC, TKN, TP, oil and grease, hardness, and alkalinity). The model was used to quantify stormwater pollutant concentrations applied to a variety of rainfall and runoff conditions. Without observed data, there would be a high uncertainty associated with the model.

Stephenson et al. (1989) points out that stormwater parameters such as infiltration rates and subcatchment roughness cannot be measured directly and thus need calibration. In the watershed model, Stephenson et al. (1989) also found that peak flow rates were better predicted by a coarser model with a larger discretization, and the runoff volumes were more accurately predicted by the finely discretized model. Parameters such as Manning's n, catchment length or infiltration rate must be altered with finer levels of discretization.

However, recent studies conducted using LIDAR for SWMM models, have proved that when a finer DEM is defined, a finer discretized model can provide adequate and in some cases more accurate results (Haile and Rientjes 2005). When higher resolution of watershed attribute information detailing first-order hydrological channel features on steep shadowed mountain slopes or zero-order hill-slope depressions beneath forest canopies is needed, LIDAR technology may be more suitable to produce DEMs for watershed models such as SWMM (Hopkinson et al. 2009). A loss of detailed topographic properties may affect flood simulations (Haile and Rientjes 2005; Meierdiercks et al. 2010; Sansalone et al. 2013). Nevertheless, before a finer discretization approach can be implemented, the physical structures and characteristics of a watershed and the drainage connectivity must be defined and correctly replicated (James 2005).

Additionally, the relationship between parameters such as the infiltration rate and runoff volume can impact a model significantly. Weak or tenuous correlations between model parameters and reality can be a result of unaccounted pervious or impervious areas (e.g. roves, driveways, roads, etc.) that affects runoff (Jones et al. 2003; USEPA, 1983). For that reason there is importance in understanding the reason a derived parameter from available data is not yielding the anticipated outcome (Bumgardner et al. 1984; Scott Dierks, SWMM Knowledge Base on Model Calibration Oct. 2004). Understanding the basis of model calibration results leads to

greater insight into a parameter's function relating to the local region (Gregory and Cunningham 2004; Motiee et al. 2006).

Tracking the interactions between surface water and groundwater can also be a potential challenge in developing headwater models (Peart et al. 2007). Since headwater streams are mainly dependent on groundwater supply, the contribution of groundwater is a driving force during the model calibration. The groundwater compartment receives infiltration from the land surface compartment and transfers a portion of the inflow to the transport compartment. This transport compartment contains a network of conveyance, storage, regulation and treatment elements that manage the movement of parameters through the aquifer (e.g. flow, nutrients, etc.) (Cambez et al. 2008; Rossman and Supply 2005).

Defining certain groundwater/aquifer parameters for modeling may not be as straight forward as defining surface water parameters, especially with lack of local soil characteristics or land use data. Finding the sensitive parameters through calibration will reduce the amount of time and effort put into calibrating and verifying the model (Tshirintzis 1998). Recognizing the sensitive parameters in a watershed model can also help prioritize sampling frequencies and locations as well as accuracy of determination (James 2005).

The complexity of a model is directly related to the number of uncertain input parameters (James 2005). The amount of sensitive, principle parameters being calibrated should be limited in order to reduce model complexity. In order to minimize principle parameters, Tsitrintzis et al. (1998) suggest that objectives for calibration should include: hydrological timing and shape, runoff volume and peak discharge. By narrowing the principle parameters to be calibrated and by focusing on these calibration objectives, the model should be a better representation of the actual watershed. Introducing more measurement error also adds unnecessary detail to the model (Duncan 1995). Therefore, the amount of error can be reduced by eliminating insensitive model parameters whenever possible.

In the study conducted by Tsitrintzis et al. (1998), the comparison of rain gauge data from three different stations proved that spatial variation was insignificant. In other words, depending on the location and region in which the watershed is located, certain model input parameters may not need to be discretized on a finer scale. As mentioned earlier, the local characteristics of the region may need to be evaluated separately from other existing models (Kim et al 2005).

There is also a significant amount of uncertainty associated with water quality relationships. In a model created by Gould et al. (2010), the Soil Water Assessment Tool (SWAT) was used to establish the relationship between land use, land management activities, and water quality processes. The calibration and validation procedures were done using flow, turbidity and TSS data collected at the study sites. Without local field data, the model would have been approximated and possibly over simplified and assessing the impacts from change in land use would not have been accurate.

Effectively setting up the watershed model through the physical and meteorological parameters, paves the way for the calibration of pollutants. The calibration of pollutants such as TSS, metals and nutrients are dependent on the flow calibration. Therefore, there can be many issues associated with calibrating water quality parameters within modeling programs. For instance, modeling and treating TP and TN can prove to be highly variable and the source of TP and TN cannot always be easily defined and successfully implemented in water quality modeling (Kim et al. 2005; Tobio et al. 2015). Nutrients are dependent on surrounding land use characteristics (Vieux and Vieux 2007). Land use characteristics and rainfall washoff highly impact the supply and transport of nutrients (Chua et al. 2009). Furthermore, the quality of nutrient measurements highly affects the quality of simulated data. The reason for poor data collection could be caused by the grade of instruments analyzing the water samples or the precision in which these water quality evaluation methods are performed (Rice et al. 2012).

TSS can also be difficult to calibrate due to the complexity of flow and erosion processes (Gassman et al. 2007). There is a direct relationship between the level of flow and the level of suspended sediment in a stream reach (Gould et al. 2010). Additionally, the TSS event loads also depend on the rainfall depth and intensity, but not necessarily on the antecedent conditions as discovered by Borris et al. (2014). The process of calibrating TSS is heavily dependent on the hydrological calibration of the model; without model verification the results may just be speculation. Therefore, the model needs to be supported with accurate flow measurements.

As much as inaccuracies can be present in flow measurements, there can also be inaccuracies found in TSS field measurements. Inaccuracies in field measurements are a significant concern for modeling TSS loads through a watershed system. An investigation conducted by Packman et al. (2006) found that turbidity provides a satisfactory estimate of TSS in urbanized streams (Hannouche et al. 2012). Likewise, Acheampong et al. (2012) has

suggested that turbidity could be used as a surrogate parameter for suspended solids. However, limited studies have been conducted to correlate turbidity and TSS for headwater streams (Packman et al. 2006). This leaves limited validation for using turbidity to model TSS.

Nevertheless, to accurately depict sediment loads in headwater streams, calibration of the washoff and buildup parameters is critical as well as reliable field data. This research conducted on the LCC hopes to provide a reliable hydrologic model, as well as a reliable TSS relationship.

1.1.6. SWMM Modeling

The following section covers the background of the decision support system and processing tool for SWMM5, which is PCSWMM. The EPA's Stormwater Management Model (SWMM5) was used to provide a view of the hydrological functions in the LCC headwater as well as the present sediment loading. PCSWMM is used mainly for continuous modeling through the estimation of runoff, sediment wash-off, and sediment removal rates for the entire length of a given precipitation record. Behind these hydrological calculations is a computation engine that routes water through conduits, nodes, weirs, orifices, storage/treatment units, flow dividers, pumps, outfalls, and outlets. As with most hydrological models there is a warm-up period in PCSWMM as well as a calibration and verification period; because of these model periods, PCSWMM is best used as a continuous model.

Since being developed in 1996, PCSWMM and other commercial implementations of SWMM have provided a much needed improvement to the model's ability to describe the hydrology of watersheds. Widely recognized for its ability to integrate geographic information systems (GIS) with SWMM5, PCSWMM's GIS engine is optimized for many common data processing and topological operations relating to stormwater, wastewater and watershed modeling. This feature allows the user to access all common projections, datum and units as well as allowing the user to re-project vector layers to any of the supported projections. Users can easily project any SWMM layer into ArcMap or AutoCAD. PCSWMM can be used to import Hydrologic Engineering Centers River Analysis System (HEC-RAS) data files as well (Finney et al. 2011).

Within the SWMM engine, several different attributes are calculated and implemented. For instance, modeling the interactions between sediment transport and runoff can be generated through the use of the 'Land use Editor', which is where the user can specify the buildup and

washoff functions. SWMM5 provides one of the easiest models to track washoff and buildup when total runoff volumes and pollutant loads are available (Tsihrintzis et al. 1998). Figure 1.3 is a representation of the typical movement of stormwater runoff in an urban system.

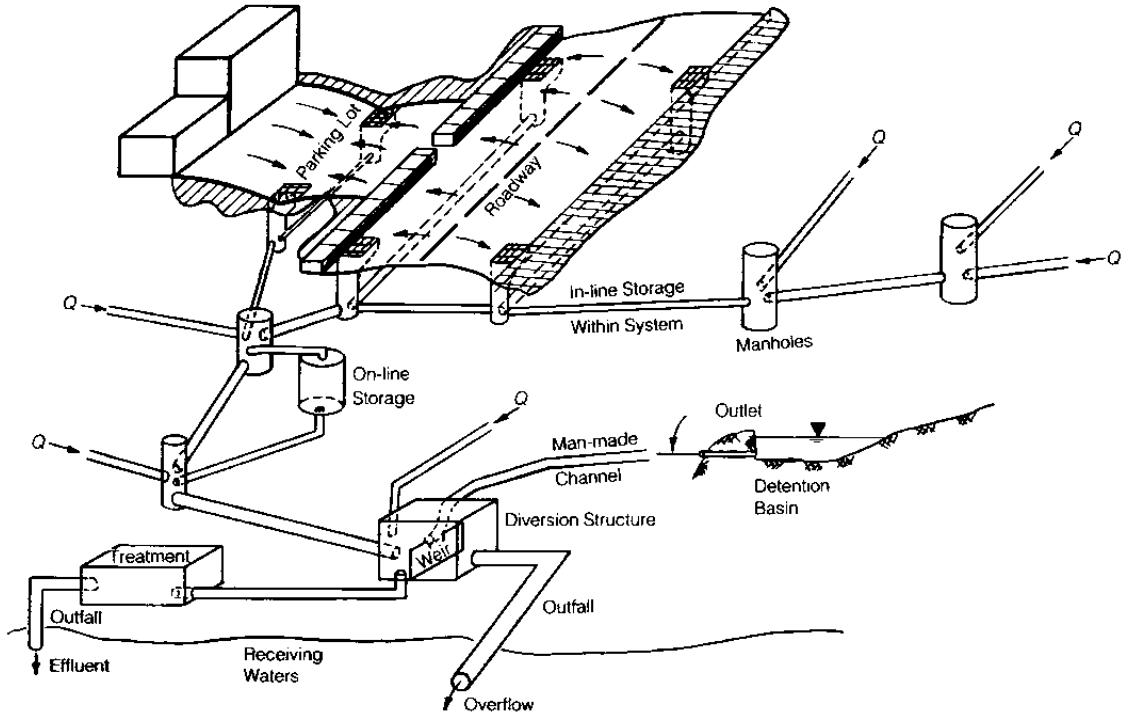

Figure 1.3: Fundamental representation of urban stormwater runoff in SWMM (Rossman and Supply 2005).

Another important attribute is the groundwater component. The groundwater (GW) component can control a significant amount of the base flow during hot summer months, where just using precipitation and upstream storage systems may not support the model's base flow. Figure 1.4 represents the groundwater processed used in SWMM5 (Rossman and Supply 2005). The groundwater flow in SWMM5 is assumed to be a unidirectional flow. Davis et al. (2007) stresses the importance of GW modeling (interflow) in order to obtain a realistic watershed when calibrating in a stormwater model.

PCSWMM has been used for many projects such as modeling stormwater runoff of remediation areas, E. coli levels, estimating metal concentrations, modeling Low Impact Development (LID) alternatives to stormwater management, and evaluating thermal impacts on ponds, as well as determining the reliability of design storms (Irvine et al. 1998; Malik and James 2007; Shamsi 2012; Perrelli and Irvine 2013; Sabouri et al. 2013).

Although PCSWMM is designed to carry out many different hydrological and transport models, PCSWMM, such as other model, does make use of certain assumptions. One assumption

is in the evapotranspiration model. PCSWMM does not directly account for evapotranspiration from vegetated surfaces or the influence of crop coverage on soil moisture and infiltration rates (Chin et al. 2006), as does the Soil Water Assessment Tool (SWAT).

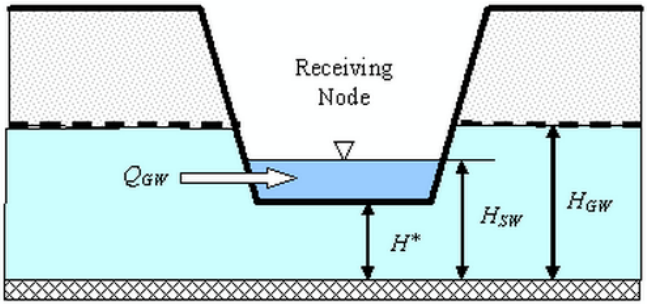

Figure 1.4: Groundwater schematic as used in SWMM5 (Rossman and Supply 2005).

Where:

Q_{GW} = groundwater flow (cfs per acre or cms per hectare)

H_{GW} = height of saturated zone above bottom of aquifer (ft or m)

H_{SW} = height of surface water at receiving node above aquifer bottom (ft or m)

H^* = threshold groundwater height (ft or m)

Another assumption of PCSWMM's hydraulic formulation is that flow across an area occurs only as overland flow thus the complete and potential impact of flow may be difficult to quantify, for example, over estimating the runoff (Rees and Schoen 2009). Figure 1.5 illustrates the overland flow process used in SWMM5. Although, this assumption has been proven to lead to minimal impacts on the travel time and peak flow once these relative impacts are recognized, PCSWMM can overestimate infiltration, leading to a greater influence on the recession limb of the hydrograph (Rees and Schoen 2009). Despite the limitations, PCSWMM is a reputable model for depicting the hydrological processes of a watershed (Chin et al. 2006; Rees and Schoen 2009; Finney et al. 2013).

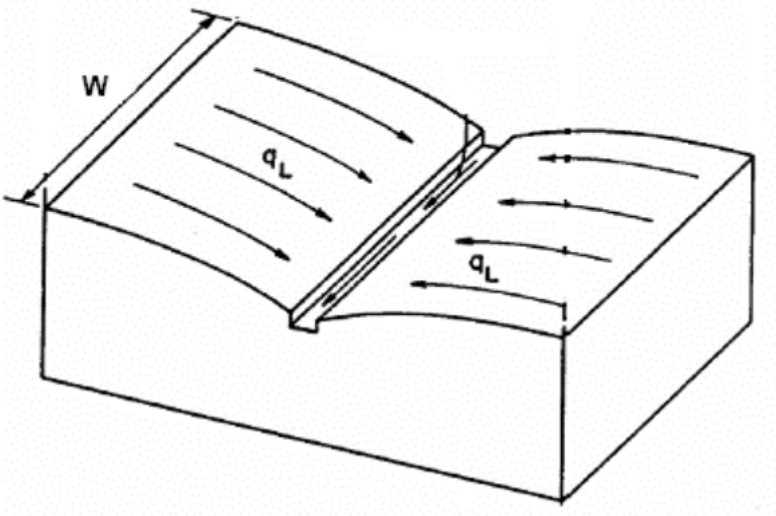

Figure 1.5: Overland Flow Schematic (Gironàs et al. 2009)

Different assumptions can be implemented through the selection of the flow routing method. For the process of Dynamic Wave routing, which is heavily impacted by the water depths maintained at nodes, the excess volume is assumed to pond over the mode with a constant surface area. This surface area is an input value supplied for junctions. Figure 1.6 shows the different surcharge and flooding assumptions SWMM.

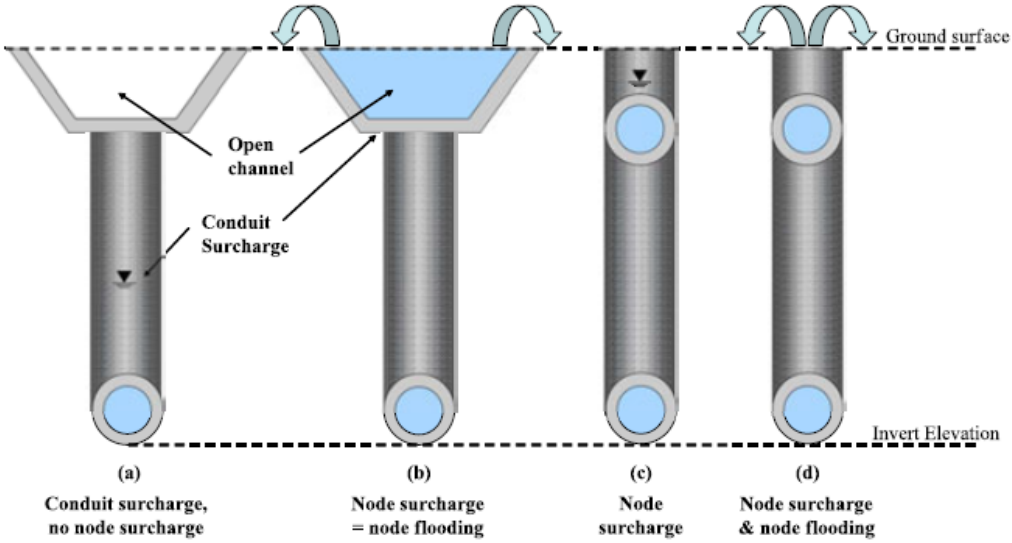

Figure 1.6: Examples of Surcharge and Flooding Processes in SWMM (Gironàs et al. 2009)

An assumption affecting the process of water quality routing is that a conduit behaves as a continuously stirred tank reactor (CSTR) (Rossman and Supply 2005). Even though a plug flow reactor may be a more realistic assumption, the difference is projected to be small if the travel time through the conduit is on the same order as the routing time step.

In support of PCSWMM's reliability, many sensitivity and calibration studies have been conducted (Rees and Schoen 2009; Finney et al. 2013; Davis et al. 2007; Malik and James 2007; Sun et al. 2014). Rees and Schoen (2009) measured the sensitivity of a model by evaluating changes to the Cumulative Runoff versus Flow Rate relationship. The default parameters that proved to be insensitive to both volume and flow rate were: Manning's n for pervious and impervious surfaces, surface width (ft), evaporation rate (in/d), f_c (in/h), f_o (in/h), infiltration decay rate (min^{-1}), infiltration regeneration rate (min^{-1}), depression storage, impervious (in), and depression storage, pervious (in). Similar results for the detection of insensitive parameters were found for the aquifer defaults parameters and the GW coefficients during calibration (David et a. 2007).

Other studies conducted on PCSWMM were a comparison of SWMM5 to HEC-RAS, where SWMM5 produced similar results to HEC-RAS using dynamic wave routing (Finney et al. 2013). Moreover, Sun et al. (2014a) measured how the level of catchment discretization influenced PCSWMM uncertainty. Microdelineation was found to reduce the amount of uncertainty of flow predictions significantly more those predictions from the macrodelineation. Cambez et al. (2008) also found satisfactory results for the hydraulic model calibration and verification when using SWMM5.

PCSWMM has also been widely used to simulate the quantity and quality of urban stormwater runoff (Tsihrintzis et al. 1998). Malik and James (2007) developed PCSWMM to gauge the reliability of design storms used to size urban stormwater system elements. A study conducted by Zhang and Shuster (2014) on a small catchment in Ohio examined the accuracy in runoff simulations for both SWMM and Gridded Surface Subsurface Hydrologic Analysis (GSSHA). This study found that even though SWMM does not account for spatial variations of evapotranspiration (ET) in topography and soil, SWMM possess certain advantages as the un-calibrated results were broadly more accurate than those from GSSHA. SWMM generated similar flows to GSSHA in low flow conditions as well.

Furthermore, Wan and James (2002) and Muleta (2012) used parameter-optimization approaches and uncertainty analysis to improve the reliability of SWMM, such as a genetic algorithm method and Bayesian methodology, respectively. Calibrated parameters in the Wan and James (2002) study were found to be within 97% of the target dataset. These findings further support the application of PCSWMM across a wide variety of hydrologic situations.

Although a large number of studies have been conducted on watersheds, there has been a lack of research aimed at calibrating small headwater watersheds. From a thorough investigation of various hydrological resource engines, there has been a significant amount of research and modeling done on urban watersheds but far less work has been focused on headwater watersheds, especially through the application of SWMM. The PCSWMM modeling conducted by this investigation hopes to provide a description of the complex processes of the LCC headwater focusing on the ability of describing peak rain events, thereby adding to the quantity of research done on modeling headwaters.

1.2.Knowledge Gaps

As the literature review indicates, there have been multiple conclusive studies produced to model the impacts on water bodies (e.g. rivers, streams, lakes, etc.) and the impacts of the surrounding environments such as runoff, sediment discharge and flow rates. Yet, there have been fewer studies on impacts of runoff from roadways, particularly from the standpoint of streams receiving such flows. This thesis intends to address this particular knowledge gap in the case of a small headwaters watershed in Alabama. In particular, to address this knowledge gap, this study focuses on:

1. Performing a long term hydrological and water quality monitoring for a perennial, headwater watershed.
2. Modeling the impact of roadways on small stream waters or headwaters.
3. Deriving generic observations from this small watershed that can be applied to other related watersheds.

1.3. Chapter Summary

In this chapter, the hydrological and environmental impacts of roadways on watersheds were reviewed as well as studies quantifying the impacts of highway runoff. The knowledge gap from available studies on long term modeling the impact of roadways on headwater tributaries is presented above. In the following chapter, the objective to provide insight on these knowledge gaps is outlined. The objective of this thesis aims to provide more understanding and quantification of highway runoff on headwater tributaries similar to the LCC.

Following the Scope and Objective section of this thesis will be the Methodology, Results, and Conclusion. Each of these sections will provide support and guidance for the research objectives and the characterization of the LCC headwater tributary.

Chapter 2
Scope and Objectives

The modeling of the Little Cahaba Creek (LCC) watershed prior to construction on other streams of similar characteristics on the LCC's alignment has four main objectives.

1. Provide field measurements of hydrologic and water quality characteristics for the LCC watershed analysis and documentation for long term modeling.
2. Assess the ability to model this watershed, including roadway impacts using a SWMM model approach. The observed field data should allow insight for potential impacts of Interstate-59 (I-59).
3. Supply guidance on assessing impacts of stormwater runoff from roads in receiving water bodies.
4. Verifying the accuracy of the modeling efforts for similar headwater watersheds in the path of BNB.

The importance this watershed has is related to the planned construction of the Birmingham Northern Beltline (BNB), a 52-mile-long northern by-pass roadway around Birmingham, Alabama. This new roadway will connect to the existing I-59 within the LCC watershed, and knowledge of pre-development conditions within this watershed is of fundamental importance for the future stormwater management in this site.

Chapter 3

Methodology

3.1. Field data collection and analysis

In conjunction with the research objectives listed in chapter 2, the following field measurements and data collections were implemented to adequately quantify the impact of the roadway on the LCC. Nonetheless the continuous monitoring, analyzing, and modeling of the LCC in this chapter can act as an outline for similar headwater watersheds withstanding possible impacts from roadways. These efforts to quantify the impact of roadways on the LCC include tasks such as continuous monitoring of surface water flow, stream and groundwater levels, stream velocity, rainfall, nutrients, pH levels, and solids. All of these characteristics were used in developing the LCC SWMM5 model in PCSWMM. The methodology for the LCC model is discussed following the description of the field data collection and analysis.

3.1.1. Site description

The Little Cahaba Creek (LCC) watershed is composed of 7 miles^2 (18km^2) of mainly rural land use as well as some residential areas with large lot areas. The area surrounding the stream is mainly composed of dense brush and trees. The LCC watershed is located northeast of Trussville, Alabama, in a town called Argo. The coordinates for the outfall of the watershed is 33.667313°, -86.544747°. I-59 passes through the middle of the LCC watershed, intersecting the creek and its intermittent tributaries at multiple locations. Also, the 52-mile-long Birmingham Northern Beltline will connect to I-59 within the area of LCC watershed.

Figure 3.1 shows the portion of the LCC watershed and I-59 that was the central focus in this investigation. Also shown in Figure 3.1 are the site locations where the hydrological and water quality sensors were placed. One observation site was located downstream from I-59. The other observation site is located directly upstream and northwest of I-59. An additional site was chosen to determine the excess amount of TSS at an intermittent tributary upstream. This additional site is referred to as the secondary upstream tributary. Two other sites were also used for data collection for water quality characterization, but they are not presented in Figure 3.1.

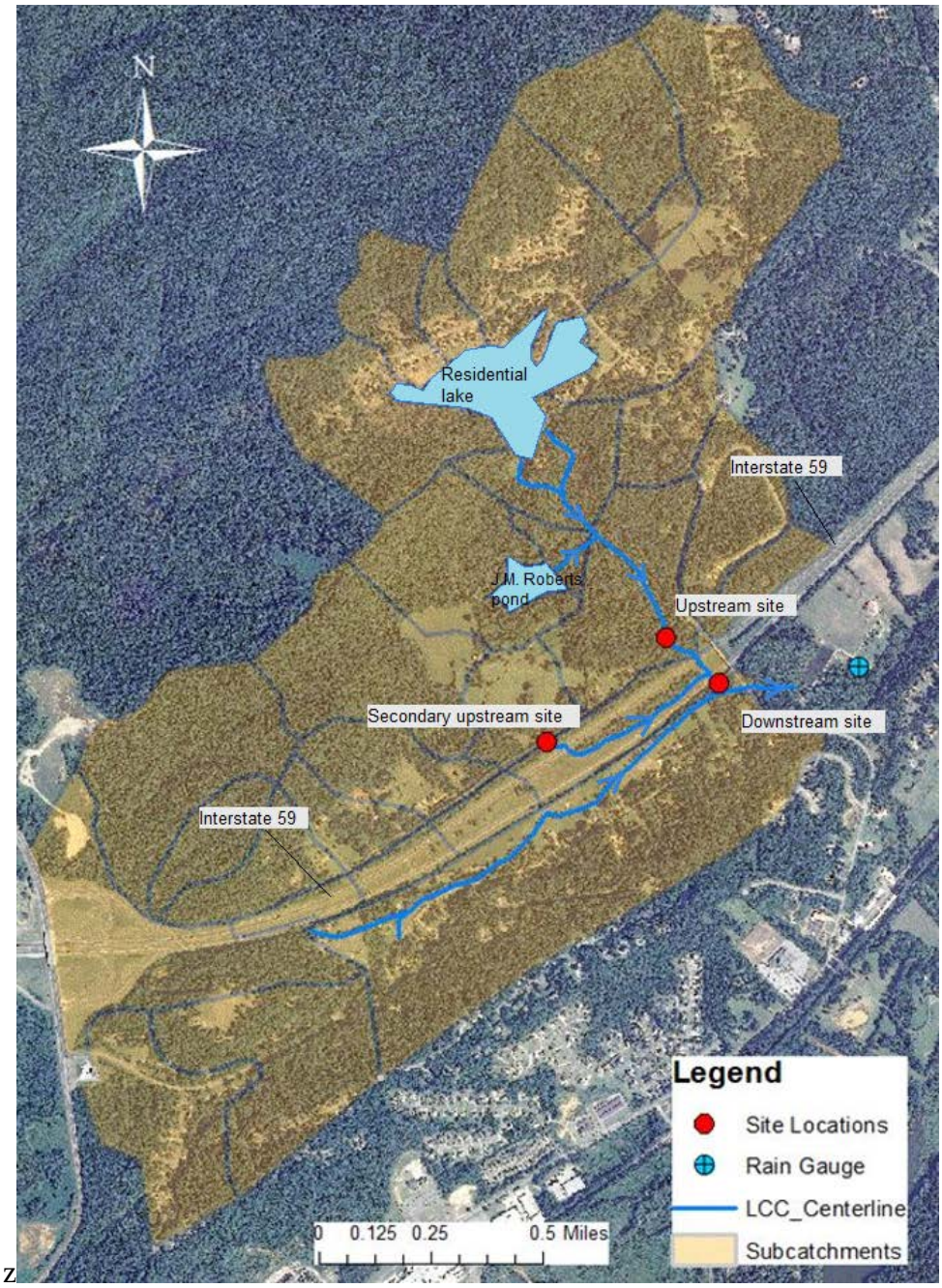

Figure 3.1: LCC watershed used for SWMM model showing site locations as well as rain gauges (Butler 2015).

The LCC between the downstream and upstream locations is a perennial stream due mainly to the constant supply of water fed by ground water and stormwater retention ponds upstream. There are two water bodies that feed the headwaters of LCC. The first is a residential lake that covers approximately 35.4 acres and the second is the J.M. Roberts Pond, which covers approximately 6.8 acres.

Most of the surrounding soil is composed of Hydrologic Soil Group A and B, which possess moderate to high infiltration rates (NRCS 2011). Soil types such as Bodine, Birmingham and Sullivan make up most of the subcatchments that pours into the site downstream of the interstate. Figure 3.2 shows the division of soil types as mapped out and labeled by the National Cooperative Soil Survey. The northwestern section of Figure 3.2 includes many ridges where Bodine and Birmingham soils are prevalent.

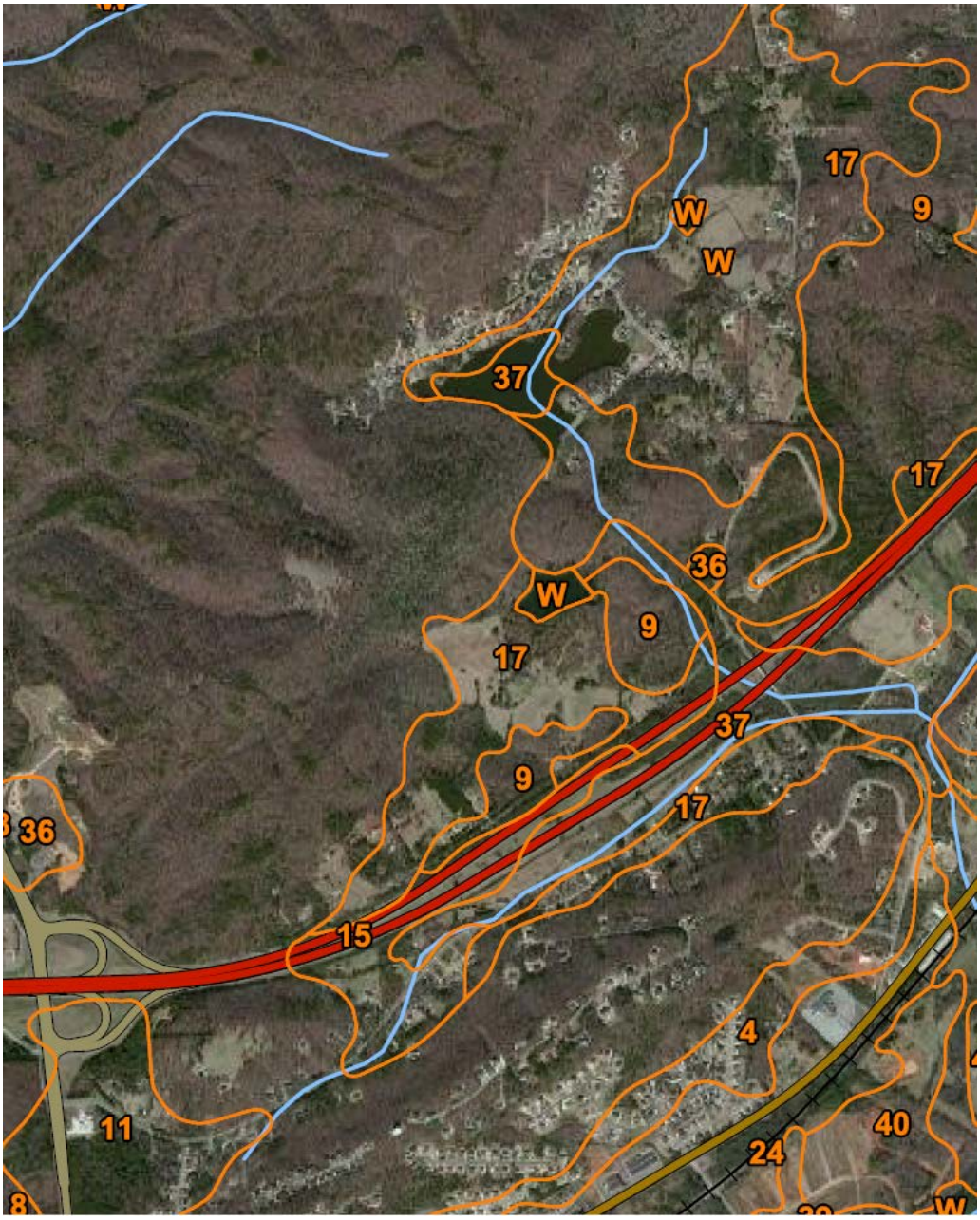

Figure 3.2: USDA Web Soil Survey results for portions of the LCC watershed (NRCS 2011).

The region's climate records show that the average rainfall in the Birmingham area varies between 3 in. to 6 in. (7.62 cm to 15.24 cm) per month, with typical lows in the summer (NOAA 2002). The average annual precipitation between 1971 and 2000 was 53.99 inches. The region's temperature ranges from 30°F to 70°F in the winter months and 48°F to 90°F in the summer, excluding abnormal weather days (NOAA 2002).

3.1.2. Hydrological characterization and hydrological data gathering

The field investigation began January of 2013 with preliminary scouting to survey the area. Two sites along the perennial branch of the creek were chosen in February, 2013 to monitor for pH, turbidity, nutrients, TSS, other secondary parameters and eventually flow rate, velocity and water levels. These sites were chosen to provide an initial estimate of the pre-existing conditions for the quantity and quality of stormwater runoff before the construction of the new interstate in that area. Data was collected in two week intervals for 12 months for pH, turbidity, nutrients and TSS. This data will be used as a baseline to compare with conditions during and following the roadway construction.

In addition, turbidity was also measured by the use of an ISCO 6100 series auto-sampler positioned at each site. These instruments were programed to be activated for a specific amount of rainfall, 0.1 in every 15 min., through the use of a rain gauge connected to the system. Once activated, the instrument pumps 600 mL of sample water every 15 minutes. There were 24 bottles collected over the span of 6 hours. Due to interception of rainfall by the tree canopy or other foliage, the rain gauges were not always activated at the same time. These samples were also brought to the Auburn University laboratory to be measured for TSS and turbidity in accordance to the Standard Methods Procedures (method 2540).

Various hydrological parameters were also monitored including stream level, stream flow and velocity, and cross-sectional areas at the two sites. The monitoring of these parameters was accomplished through the use of an area velocity sensor. Figure 3.1 shows the location of the two sites. The stream in Figure 3.1 is flowing northwest to southeast where I-59 crosses the creek at several locations and contributes substantial runoff. Figure 3.3 shows the location of all the sensors at the upstream and downstream sites as well as the median tributary.

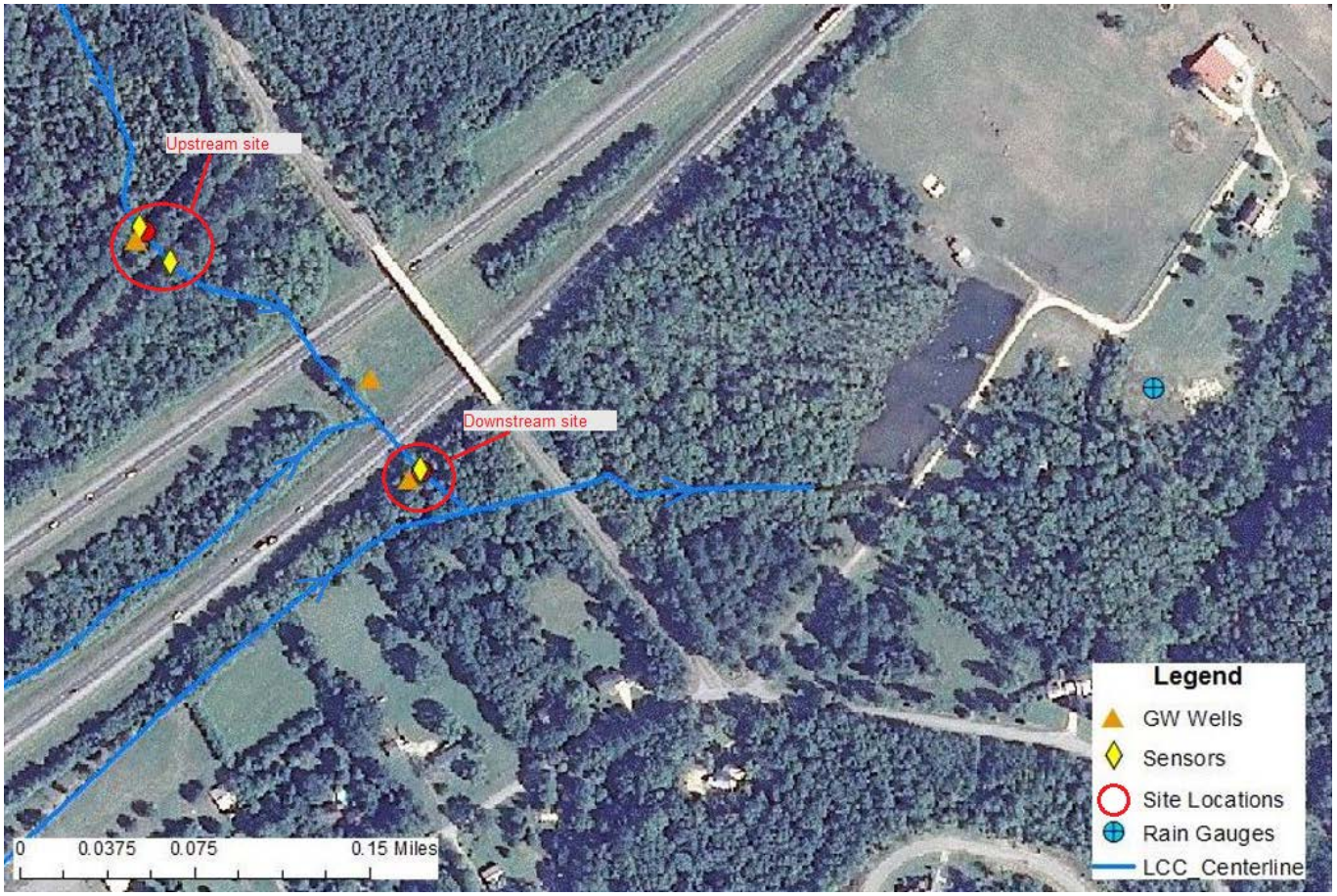

Figure 3.3: LCC Upstream and Downstream Sensor Locations for Area Velocity Sensors, Auto-Samplers, Water Quality Sondes, Hobo level Loggers (used in groundwater wells); Rain Gages.

3.1.2.1 Location for all sensor deployment: Strategy for deployment

The stream was surveyed at both sites, upstream and downstream of the deployed sensors. Figure 3.4 shows the equipment setup at the site downstream of the I-59 crossing. The photograph is taken from above the culvert nearest the roadway. By monitoring upstream of the roadway, the impact of the interstate is not only determined but also the impacts of other land uses upstream from the I-59 (e.g. open terrain and residential development).

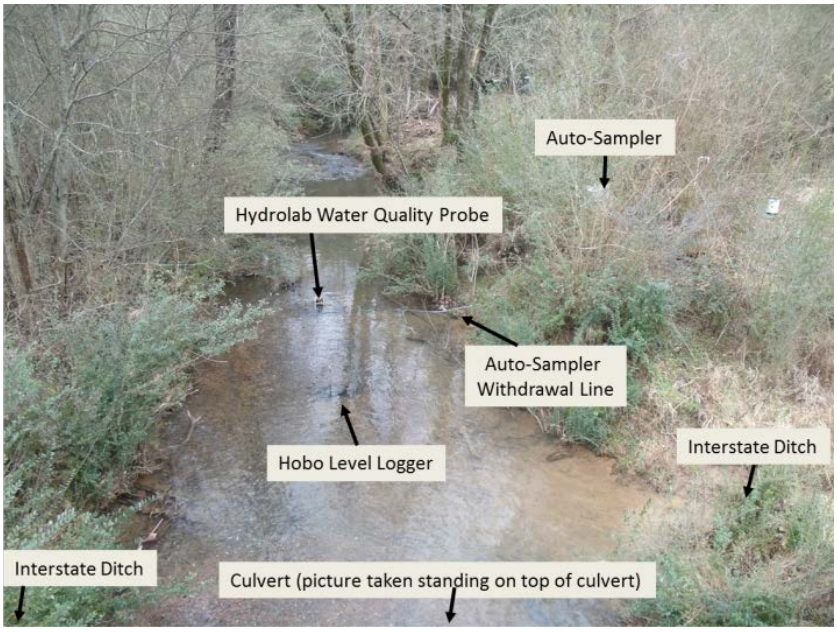

Figure 3.4: Downstream site monitoring equipment is identified by text boxes and arrows; for scale, the width of this stream is approximately 18 ft (5.5 m).

Once the perennial section of the LCC was chosen as one of the official site locations, the deployment of the sensors was decided based on the water level and sunlight exposure within that section of the stream. The hydraulics and hydrology of the stream was also taken into consideration. The HOBO Level Loggers should not be exposed to direct sunlight; however, the level loggers needed to be secured in the middle of the stream cross-section in order to have minimal interference with the internal sensor. A cement block was used along with a rod buried one foot into the streambed through one of the cement block holes. The level logger was then placed in a metal wireframe pouch that was 8 inches long and 5 inches wide. The pouch was secured to the rod by sliding the steel rod through the additional space in the pouch. The pouch then rested on the bottom of the streambed.

The deployment of the auto-sampler was limited to the length of the tubing which collected the water. The tube was only 50 ft long, therefore the auto-sampler needed to be placed near the stream, but not where water could reach the auto-sampler in case of large storm events. The auto-sampler was placed on the high side of the creek, and then secured to the large wooden box that holds the battery that powers the auto-sampler. The auto-sampler was also attached to the rain gauge. The rain gauge needed to be exposed to direct rainfall that was not intercepted by the tree canopy or other tree brush.

The area velocity deployment was more complex than the HOBO level logger and the environmental probe. The area velocity sensor had to point upstream as well as having to be placed near bottom of the streambed. The area velocity sensor used a built in pressure sensor along with the Doppler sensor to read the air bubbles traveling from upstream towards the sensor. Hence, there could be no obstruction in front of the area velocity sensor.

3.1.2.2 Rainfall Collection

In order to adequately monitor the LCC and calibrate the PCSWMM model, the rainfall was recorded at two different locations with HOBO RG3 rain gauges. The first rain gauge location was approximately 0.32 miles east of the downstream site and 0.43 miles southeast of the upstream site (Please refer to Figure 3.3 on page 31). The second location was behind a gas station 2.4 miles northeast of the downstream site. Both rain gauges are within the LCC watershed. However, since the chosen monitoring sites upstream and downstream of the interstate were a substantial distance away from the second rain gauge, the second rain gauge was not considered as a sufficient representation of the precipitation in that area when applied to PCSWMM. Figure 3.3 shows the location of the rain gauges.

The rain gauges were installed by using a 4”x4” wooden post oriented vertically, mounted with a 2’x2’ plywood board. The plywood board secured to the tall wooden post was reinforced by aligning and bolting another 2’x2’ plywood board with 2 inches of clearance to allow for adjustments in case of warping and other possible instability issues. Figure 3.5 shows the installation of the rain gauge located behind the gas station on Liles Lane. Both of the rain gauges had a bull’s eye level that prevented them from becoming unknowingly unleveled. If the rain gauges were unleveled, this would prevent the bucket inside the rain gauge from tipping once full of precipitation, thus leading to inaccurate data.

Figure 3.5: Installed Rain Gauge behind the gas station on Liles Lane off I-59. The 4x4 post holding up the platform is approximately 6ft high. A ladder is used to access the rain gauge.

To validate the rain gauge's accuracy and performance, the collected data was compared to off-site gauges monitored by the State Climate Office of North Carolina. These rain gauges used for calibration were located in Birmingham, Pinson, Center Point and Trussville, Alabama. If the start of a long rain event was within 30 minutes of one of the gauges used for calibration the data was accepted. If the start of the recorded rain event was not within 30 minutes of one of the rain gauges listed above, the following was taken into consideration: storm duration, storm frequency in that area, time of year, and the storm intensity.

Some malfunctioning occurred with the rain gauges which resulted in periods of missing rainfall data. In order to account for these periods of missing rainfall, nearby rain gauges of the State Climate Office of North Carolina were used as points of interpolation. The following stations were used to interpolate for the missing rainfall: Argo 1.5 NW and Trussville 6.6 NNE. These daily averages were taken and matched with the durations from those of the Birmingham Municipal Airport hourly data. By using a uniform distribution for those durations, this method provided an indicator that the rainfall data needed to be manually entered.

3.1.2.3 Atmospheric Temperature and Pressure

Atmospheric temperature and pressure were measured by the HOBO water level logger devices. The level loggers record the absolute pressure, which is later converted to the water level readings by the provided software. The level logger uses the HOBOware Pro software for operation. This software automatically converts the pressure readings into water level readings. For the sake of accuracy, the software also compensates for temperature, fluid density, and barometric pressure. In order to compensate for the barometric pressure changes, the loggers are also used as a barometric reference by placing them in air. The temperatures were obtained from these level loggers placed above ground level.

Each logger comes with a calibration certification. The range of temperatures available for most all of the deployed level loggers is 32-122°F (Nominal). The level of accuracy for the temperature sensor is +/- 0.79°F. The daily average temperatures ranged from a maximum of 88°F to a minimum of 14°F. During the summer months (between May and September) the temperature was typically around 80°F. The range calibrated for the pressure head fell between 10-30psi. The maximum error associated with the raw pressure accuracy is +/- 0.09 psi. The pressure heads that were recorded by the level logger provided critical insight into the relationship between the surface water and groundwater levels.

3.1.2.4 Stream and Groundwater levels

The stream levels were recorded by the level loggers deployed in the stream. There are two level loggers deployed in the stream, one at the upstream site and one located at the downstream site. The typical water level accuracy associated with these devices is +/- 0.5 cm. When the data was collected from the level logger in the stream, the current stream level needed to be measured using the original reference point, as well as the date and time of collection. The reference water level was used to run the barometric pressure compensation assistant that accounts for the changes in pressure.

The level loggers recording the groundwater levels were deployed in shallow wells approximately 20 ft below ground level. These wells were installed next to the streams, as shown in Figure 3.6. The water levels between the stream and the water in the well was measured with the implementation of a surveyor’s total station. The same process for the surface water barometric pressure compensation was used for the groundwater well barometric compensation.

Figure 3.6: Installation of the groundwater well at the downstream site of the interstate; also picture is the auto sampler and the wooden box used to shelter the auto-sampler battery.

The groundwater levels at the upstream site were typically similar to the water levels in the stream, meaning that when the surface water levels peaked, so did the ground water levels within 0.2 ft of the other. The difference was in the recession of the peak flows. The groundwater took longer to return to the base flow. The downstream site had a different relationship. When the groundwater levels peaked, the stream water levels were up to 3 magnitudes greater. Unlike the recession relationships from the upstream site, the recovery at the downstream site for the surface water and the groundwater were similar. The recession was also more abrupt than the upstream groundwater recession.

3.1.2.5 Stream Velocity and Flow Measurements

Stream flow measurements were calculated and recorded using the 2150 Area Velocity (AV) Flow module in Figure 3.7, part of the ISCO 2100 Series, which was deployed most recently on July 7th, 2014. This device can hold approximately 79,000 readings (equivalent of nine months of data). The AV sensor records water level and velocity of open channel flow streams. These values are viewed in the separately purchased software Flowlink®.

Figure 3.7: Area-Velocity Sensor attached to a thin metal sheet secured to a cinder block located upstream of interstate.

The water level is measured by an internal differential pressure transducer which is a small “piezo-resistive chips that detects the difference of the pressures felt on the inner and outer face” (Teledyne 2012). The AV sensor must be calibrated with the reference cross-section at which the sensor is deployed. The stream level and zero level offset, if applicable, must also be entered into the program settings when first installing the sensor. If there is a build-up of silt around the sensor, that value will need to be accounted for as well. Since both of the AV sensors deployed at the upstream and downstream sites were installed above the streambed floor at the center of the channel, the offset distance the AV Sensor was entered into the Flowlink® program. These water level measurements were cross-referenced with the stream level measurements from the HOBO level loggers.

As mentioned previously, the AV sensor measures velocity by using ultrasonic sound waves and the Doppler Effect. As stated in the Teledyne Operation Guide, the Doppler Effect is “the frequency of a sound wave passed from one body to another is relative to both their motions”. As two waves approach one another, the frequency increases; thus, as they move apart, the frequency decreases. The sound waves generated by the transducers bounce off the particles or air bubbles in the stream and reflect to the AV sensor.

The AV sensor uses the area velocity flow rate conversion method to calculate the flow rate in the stream. Since the AV sensor has the reference cross-sectional area that was measured for the program set up, the flow rate can simply be calculated by using the user defined cross-

sectional area and the stream flow velocity measured by the sound wave frequencies. The AV sensor flow rate calculations are used in the PCSWMM model for calibration of the stream hydrology.

3.1.3. Water Quality Characterization

Water quality parameters were collect by two different methods. The first method was to collect grab samples approximately every two weeks following the procedure outlined in Pitt (2007). These samples were analyzed in the Auburn University Hydraulics lab following Hach instructions. The second method used to collect water quality data was through the use of three Hydrolab DS5 Water Quality Sondes. These Sondes were deployed for 3 weeks at a time, and then switched out in order to be calibrated.

3.1.3.1 Study sites/sensor sites

The study sites, as mentioned earlier, are upstream and downstream of I-59. Grab samples were collected at both sites and one environmental probe was placed at each site. An additional Sonde was deployed at the tributary connecting to the LCC in the median of I-59. This Sonde was placed in the tributary upstream of the interstate to account for the additional sediment loads that occur downstream during large rain events. Otherwise, we were uncertain what was causing the large additional sediment load at the downstream site during rain events.

3.1.3.2 Selected Parameters: Nitrogen and Phosphorous Species

Nitrogen and phosphorus species were measured from the grab samples that were collected every 2 weeks. Samples were collected, preserved and tested with a Hach DR/890 colorimeter, for a full year from March 2013 to March 2014. The samples were collected in accordance with the procedure outlined in Pitt (2007). The major nitrogen species collected included NO_3, NO_2, and NH_3. This work measured NO_3, NO_2, NH_3, and total nitrogen using Hach methods 8192, 8507, 8155 and 10071 respectively. Phosphorus species consisted of ortho-phosphate and poly-phosphate. Similar to our analysis of nitrogen, we measured ortho- and poly-phosphate, as well as total phosphate in our lab, according to Hach methods 8048, 8180 and 8190 respectively.

The Hach DR/890 colorimeter tests have the following accuracy associated with each of the corresponding parameters: NO_3-N +/- 0.3 mg/L, NO_2-N ±0.001mg/L, NH_3-N ±0.02 mg/L, TN +/- 0.5 mg/L, PO_4^{-3} +/- 0.05 mg/L (both ortho-phosphate and poly-phosphate), and TP +/- 3.0 mg/L.

In order to guarantee quality control of nutrient concentration measurements, the samples tested for nitrogen and phosphorous species concentrations were analyzed in an ion-chromatograph (IC) column once every month. The point collection data was tested with an IC column from Dionex Products. The first full run of water samples and standards showed an average error of ~22%. The IC column was run with standards with the following concentration: 0.25 mg/L of NO_3, 1.0 mg/L of NO_3, 2.0 mg/L of NO_3 and 0.5 mg/L of PO_4, 1.5 mg/L of PO_4, and 3.0 mg/L of PO_4. All the standards had a R^2 coefficient in the range 0.9131 to 0.9999. As the investigation progressed, IC column and colorimeter results showed much increased consistency with an overall average R^2 value of 0.9858.

3.1.3.3 Water Sampling Techniques and sample preservation

Module 3 of Pitt (2007) Water Sample Collection Methods was followed to handle and preserve the samples adequately, ensuring the best analytical results. High density polyethylene plastic containers with screw lids were used to hold the water samples. The amount of sample collected was dependent on how many tests that were being performed. 1500 mL was collected per sample at each site. There was also a duplicate sample collect for each site in case there was a non-point source of contamination.

In order to avoid increases, transformations, and/or losses in pollutants concentrations the nutrient samples were analyzed as soon as possible. TP, TN and NH_3 could be preserved up to 28 days by adding sulfuric acid to reduce the pH to 2 (at least 2 mL). However, NO_3, NO_2, ortho-phosphate, and poly-phosphate need to be analyzed within 24 to 48 hours. All the samples had to be put on ice once they were collected (Pitt 2007). This was done on ice via a standard cooler cleaned with rubbing alcohol.

In preparation for each sample collection the sample bottles and glassware were cleaned using the ASTM (1996) standard D 5088-90. The equipment first has to be rinsed with water to remove any dirt or debris left behind. Then the bottle must be washed with a phosphate-free detergent solution using a scrub brush if necessary, followed by the rinse of “clean” water, e.g.

tap water. This rinse is then followed by a rinse with 10% hydrochloric acid, which is followed by a rinse of deionized water. The bottles and glassware are washed with an additional rinse of deionized water to insure the laboratory equipment is ready for new sample water.

3.1.3.4 Laboratory Techniques

In addition to the cleaning of the laboratory equipment, the HACH DR/890 colorimeter tests were carried out following the Hach Data logging Handbook for the DR/890 colorimeter. The manual covered chemical analysis techniques such as temperature consideration- making sure the samples were analyzed at room temperature; sample dilution techniques – this was seldom an issue; operating the Hach TenSette Pipets – e.g. maintaining a slow constant pressure when pressing down and releasing pipettes; the use of graduated cylinder – reading at the meniscus; and mixing water samples – assuring the sample is thoroughly mixed either by inverting or swirling the sample. There was also a prescribed technique for opening the pillow packets that were used for each of the tests.

Standards were also implemented to further assess the quality of the results. The following standards were applied to the Hach DR/890 colorimeter tests: 1 mg/L as N, 2.0 NO_3-N, 100 mg/L as NO_2, 1 mg/L as NH_3-N and 25 mg/L as P. These standards were chosen because they fell within the specific range for each of the corresponding test.

3.1.3.5 Water Quality Sonde Parameters and Overview of Measurement Method

Continuous water quality monitoring was implemented through the use of two Hydrolab DS5 Water Quality Sondes, deployed at the sites upstream and downstream of the perennial branch of the LCC. Recently, there was an additional probe deployed in the intermittent tributary upstream of the interstate. The hope of this third probe was to account for the additional sediment loads that occur at the downstream site during large rain events.

The Hydrolab program allowed the selection of specific parameters. Temperature (F), pH, Specific Conductivity (µS/cm), Dissolved Oxygen (LDO) (mg/L), Salinity (ppt), TDS (g/L), and Turbidity (NTU) were measured at 30 minute intervals. These parameters were continuously recorded in the environmental probes that stayed out in the field for a maximum of three weeks.

Although the probes were set to continuously monitor the stream's water quality, there were periods where there was no data for one or both of the probes. This was due to the probe

suddenly turning off due to battery depletion or the nearby electrical lines sending a voltage through the ground and water causing the probe to suddenly turn off.

The Water Quality Sonde data was compared with the point collection and auto sampler date analyzed in the on campus lab for the site upstream from the interstate and the site downstream from the interstate. The Water Quality Sonde was able to catch dynamic changes in turbidity. Where the point collection data and the auto-sampler data could only captured part of the turbidity, the Sonde was able to capture a more detailed picture of the stream's turbidity levels during the investigation.

3.1.3.6 Water Quality Sonde Deployment strategy

The deployment of the Hydrolab Environmental Water Quality Sonde needed to be free of obstruction by branches and other stream debris that could become caught on the sensor, thus affecting the turbidity and possibly the specific conductivity, salinity and pH values. The sensor needed to be exposed to the water but also be deep enough to not catch any passing debris. Additionally, the sensor needed to be secured to the streambed in case of a storm with extreme flow conditions that moved the sensor. Therefore the sensor was secured to the streambed using cement blocks that can be found in any landscaping store. These blocks were then braced with iron rods that were hammered one foot into the streambed.

Theft was another concern; therefore a PVC pipe with holes drilled on either side was used to contain both Sondes. The ends of the PVC pipe were closed off with rubber lids that were tightened with a metal strap. The probes were only displaced once since being deployed. This was during a major storm event that carried large pieces of debris through the stream.

3.1.3.7 Sonde Calibration and Data Gathering

Every 2 to 3 weeks the probes were accessed for data gathering and calibrated for each of the following parameters: LDO, pH, Turbidity, temperature and pressure. The calibration and data gathering process were conducted within the Hydras 3 LT software provided with the probe. The calibrated parameters were selected within this program. The user could create and store a template file to make deploying the probe more efficient. This template file could contain any of the parameters available in the Sonde (e.g. battery voltage, Temperature, Total Dissolved

Oxygen, Turbidity, etc.). Some of these parameters have a separate sensor, but all are calculated within the Sonde.

Each sensor has a specific set of calibration instructions. When calibrating the Sondes, the current readings display next to the newly calibrated value until the "Calibrated" option is selected. The Water Quality Sonde has the following errors associated with each of the corresponding parameters: LDO +/- 0.2 mg/L, pH ±0.2 pH units, Turbidity ± 1%, Atmospheric pressure ±0.05%, Conductivity± (0.5% of reading + 0.001 mS/cm), Temperature +/- 0.10 degrees C.

Furthermore, when downloading the measured parameters, all the data was downloaded at once. The measured data could only be downloaded when the Sonde was disconnected or no longer recording, unlike the area-velocity sensor, which downloaded data even while the sensor was still recording. Once the download was complete, the data was downloaded as a text file. From here, the file was converted to an Excel format which was the primary method of keeping track of data throughout the monitoring and analysis of the LCC.

3.2. Numerical Investigation using SWMM

3.2.1. Model Description and Design

The design of the SWMM model started with the focus of the watershed and which areas were important to bring to attention. Since most of the data collected was near the location of the upstream and downstream sites of the interstate, the area of intent (AOI) became that part of the watershed. Once the AOI was established for the model, the boundaries of the watershed could then be delineated.

3.2.2. Data Sources for Modeling

The supporting data sources were used in SWMM and ArcGIS to georeferenced JPEG images as well as to spatially supported images to ensure the accuracy of the model. The images of the watershed were mainly used for visual reference and are not necessary for the development of the nodes, channels, storages, and outfalls.

The data used for the digital elevation model (DEM) was taken from the Tiger Products Database of the United States Census Bureau. The Tiger DEM files are provided by counties. Since the LCC watershed is located in both Jefferson and Saint Clair Counties. As the watershed

is located in both of these counties, the DEM had to be joined to create one DEM. This DEM file was extracted and reduced in ArcGIS to focus on the area of the LCC. Once the DEM was corrected, contour lines were generated at 10 foot intervals and at 25 foot intervals in ArcMap. These contour lines would be used to define the subcatchment boundaries.

Another source of data that was utilized in the creation of the PCSWMM model was Global Mapper. A watershed was delineated in Global Mapper by first downloading the US Geological Survey Digital Elevation Data (NED) for a 30 m resolution from the USGS website. Once an elevation grid was provided, a watershed could be generated according to the following parameters: resolution (meters), stream threshold (drainage area), depression fill depth and digitizing tool operations. This Global Mapper generated watershed was used to validate and cross-reference the manually delineated watershed for PCSWMM.

The last source used as a check point was Google Earth. This source of information was used to account for natural drainage paths such as stormwater sewer systems and open channels carved from erosion.

3.2.3. Assumptions and parameters adopted for LCC modeling

The complexity of a model is determined by the amount of uncertainties of the input parameters. The complexity also depends on the level of discretization and the number of processes active (James 2005). Therefore, the assumptions applied to this model were given careful consideration as to how and when they would be implemented.

3.2.3.1 Subcatchment Division

Subcatchment division was decided according to the previously generated watershed in Global Mapper, as well as the natural flow characteristics, the topography, land use, and the soil characteristics. The slopes or topography of the area was used to define the subcatchments along with the use of the contour lines and DEM files listed above. Once the general outlines of the subcatchments were defined, natural runoff patterns were adjusted for each of the boundaries. Thirdly, land use was considered and where water would be redirected because of an obstruction or stormwater sewer system. For instance, the interstate redirects flow from the original flow path due to the separation of forested and residential areas. There are many open fields in this watershed and those farmlands advance the runoff causing more erosion. Lastly, soil site

characteristics from soil survey data were taken into consideration to delineate subcatchments that could not be observed through contour lines generated through DEMs. As show in Figure 3.8, overall 32 subcatchments were formed through the land and flow characteristics listed above. These subcatchments ranged from undeveloped forested areas to residential and roadway area. A majority of the subcatchments contain residential area and are also a mix of pastured land and undeveloped forested area. Therefore the soil characteristics did not vary significantly among the different subcatchments.

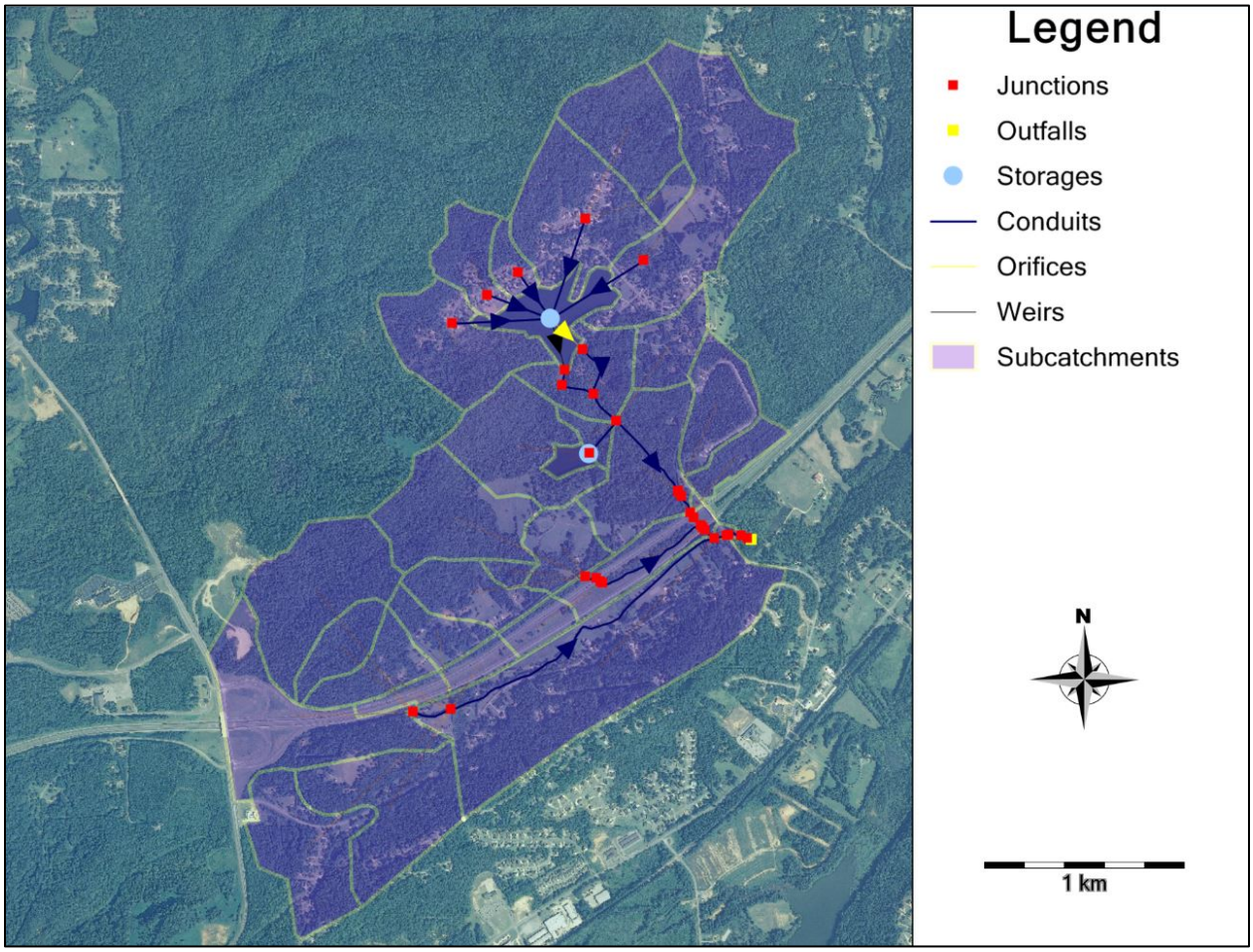

Figure 3.8: LCC watershed generated in SWMM5 showing the structural elements used for the simulations runs.

3.2.3.2 Soil Characteristics

The characteristics of the soil played a large part in the delineation of the watershed. Many soils in the LCC watershed had moderately high infiltration rates such as 1.98 to 5.95 in/hr; however, there were many areas which possessed a low infiltration rate such as 0.04 to

0.57 in/hr (NRCS 2011). These areas of low infiltration rates would need to be separated from the areas of high infiltration rates to adequately model the abstraction characteristics of each subcatchment. The subcatchments were also combined if they possessed similar soil characteristic, natural drainage paths, land use, and slopes. Since there is such a large degree of uncertainty within the delineation of the LCC watershed, a 'relatively simple [model] may be selected in situations where field data are lacking,' as suggested by James (2005).

3.2.3.3 Rainfall Characteristics

The recording of the amount of precipitation in the area was limited to the rain gauge located in the nearby farmland. Although this rain gauge was not located directly between the two primary sites upstream and downstream of the interstate, the rain gauge was within 0.43 miles of both sites, which was considered an adequate distance representative for both sites. By using one rain gauge, the storm cells were assumed uniform for the entire area. However, through the use of rain gauges as triggering mechanism for the auto-sampler, the rain over that area was discovered to vary in intensity and duration over a fraction of a mile. Using two or three rain gauges would have created a better situation for applying to the calibration of the PCSWMM model (James 2005).

Sun et al. (2014b) produced SWMM results that suggest the modeling program is limited when simulating small rain events. This limitation can be an issue when modeling small rain events (<1.94 mm/hr, or 0.076 in/hr). With this in mind, individual rain events that produced less than 0.1inches/hr were not considered. In order to be considered an individual rain event, there had to be an inter-event time of six hours.

3.2.3.4 Water Quality

SWMM and PCSWMM can stimulate movement of a number of user-defined pollutants such as inflow and transport. The following is required information for each pollutant: pollutant name, concentration units, concentration in rainfall concentration in groundwater, concentration in dry weather flow and first-order decay coefficient. Additionally, pollutants can be reliant or dependent on one another. For example the runoff concentration of phosphorous or nitrogen can be a fixed fraction of the runoff concentration of suspended solids. However, the scope of modeling nutrient cohesion to suspended solids is not covered in this paper.

In this model, suspended solids were tracked through the LCC watershed. Suspended solids were measured via grab samples and auto-sampler samples. Through measuring turbidity and total suspended solids for each auto-sampler sample, a distinct relationship was formed for the LCC watershed.

3.2.3.5 SWMM modeling assumptions and parameters

There are many features and elements to identify when creating a hydrological model of a watershed in PCSWMM, and these are characterized either through a field site inspection or using an updated virtual map with geographical information. According to Rossman and Supply (2005), these elements include dams, ponds, storage tanks, pump wells and pump stations, the largest diameter conveyances, tributaries, diversions, outfalls, weirs, and gates.

The simplest elements to assign were the conduits and their junctions. A centerline shapefile was created using ArcMap. This allowed for the use of the “snap-to-function” tool in PCSWMM when uploaded as a layer. The existing channelized sections and junctions of the LCC were clearly defined in the ArcMap program, which allowed for an accurate representation of the actual stream. The channel geometry was defined using the surveying data obtained from the total station. The channel geometry varied once the model was run. These variations are discussed in the section on Range of Variability.

There is only one outfall in the LCC watershed model. This outfall is located upstream of the mill creek dam just on the upstream of a property owner’s pond. This pond at the outfall sometimes causes a backwater effect upstream at the downstream site of the interstate. Initially, there were only two weirs as the exit flow for both of the storage elements. Since the flow at the outfall needed to be restricted, another weir and orifice were placed, leading to the outfall. The additional weir and orifice restricted the flow in order to mimic the stream flow of the LCC.

The LCC watershed AOI contained two storage elements. The first was a large residential lake that covers 35.4 acres. The second storage element was a smaller pond, called J.M. Roberts Pond, which covers 6.8 acres. The storage curves for these tanks were calculated through the use of ArcMap. Contour lines were developed in ArcMap at 10- ft intervals. The original depth of the storage unit could then be estimated. The calculated storage curves are provided below Table 3.1. The storage units had the largest impact on the calibration of the surface water flow.

Table 3.1: Storage curves for residential lake and JM Roberts Pond upstream of I-59 created in ArcMap 10

Residential Lake			JM Roberts Pond		
Elevation (ft)	**Depth (ft)**	**Area(ft^2)**	**Elevation (ft)**	**Depth (ft)**	**Area(ft^2)**
860	0	1543405	800	0	295271
850	10	1041057	795	5	221453
840	20	580181	790	10	166090

Another characteristic that needed to be specified were the subcatchment widths. This was done by creating a layer shapefile that represented the subcatchments overland flow path. Within the subcatchment boundaries, 1-3 flow path lines were drawn to represent the average area weighted values (Schmidt 2005). Once these paths were created, the file was applied to the flow length/width calculation tool to be generated and implemented into the subcatchment layer.

3.2.3.6 Surface Water Modeling

In order to model the surface water of the LCC, the dynamic wave routing was chosen. The reason the dynamic wave model was chosen over the kinematic wave routing was the lack of the kinematic wave method's ability to account for backwater effects, entrance/exit losses, flow reversal, or pressurized flow (Rossman and Supply 2005). A backwater situation was detected at the downstream site of the interstate. When large flows occurred, a constraint downstream caused a backwater effect to travel up to the upstream observation location. This occurrence could not be tracked using the Kinematic wave. Another advantage of using the dynamic wave routing method over the kinematic method is that the dynamic wave method produces the most theoretically accurate results by solving the complete one-dimensional Saint Venant flow equations, Equation 3.1 and 3.2, below:

$$\frac{\partial A}{\partial t} + \frac{\partial Q}{\partial x} = 0 \qquad 3.1$$

$$\frac{\partial Q}{\partial t} + \frac{\partial}{\partial x}\left(\frac{Q^2}{A}\right) + gA\frac{\partial H}{\partial x} + gA\left(S_f - H_L\right) = 0 \qquad 3.2$$

Where:

Q = flow rate through the conduit (cfs)

x = length of the conduit (ft)

H = hydraulic head of water in the conduit (ft)

A = cross sectional conduit area (ft^2)

t = simulation time (s)

S_f = friction slope

h_L = local energy loss per unit length of conduit (ft)

g = acceleration of gravity (ft/s^2)

3.2.3.7 Representing Groundwater-Surface Water Interaction

The groundwater interrelation was established in the aquifer editor. This relationship was not determined until once all of the other parameters were adjusted. SWMM computes the groundwater flow as a function of groundwater and surface water levels through the use of Equation $Q = A1(H_{GW} - H^*)^{B1} - A2(H_{SW} - H^*)^{B2} + A3(H_{GW}H_{SW})$ 3.3.

$$Q = A1(H_{GW} - H^*)^{B1} - A2(H_{SW} - H^*)^{B2} + A3(H_{GW}H_{SW}) \quad 3.3$$

Where:

Q_{GW} = groundwater flow (cfs per acre)

H_{GW} = height of saturated zone above bottom of aquifer (ft)

H_{SW} = height of surface water at receiving node above aquifer bottom (ft)

H* = threshold groundwater height (ft)

A1 = groundwater flow coefficient

B1 = groundwater flow exponent

A2 = surface water flow coefficient

B2 = surface water flow exponent

A3 = surface-GW interaction coefficient

The groundwater component of this model was quite complex to implement. The site upstream of the interstate shows characteristics of a receiving stream, while the downstream site shows characteristics of a giving stream. One single aquifer that fed the LCC watershed was initially assumed. Furthermore, an assumption that the water table was 20 -30 feet below the dam located further downstream from the downstream observation site was applied. The assumption that the bedrock is at a higher elevation in this area was applied as well due to the region's less

permeable soil, compared to a region such as the lower coastal plains of the southeastern United States (Moynihan 2013). Thus the aquifer is shallower due to the high bed flow.

Later, a second aquifer was assigned to specific subcatchments. The use of multiple aquifers proved to have a more accurate representation of the surface and groundwater flows (Moynihan 2013). The peak flows were reduced as well as correcting the recession curve. Each of the parameters used for the aquifers is listed in Table 3.2. All of the existing parameters for the aquifers were not changed from the default parameters. These values were validated with the soil properties of various soil types listed in Table 3.3 (Rossman and Supply 2005).

Table 3.2: Groundwater properties of the two aquifers in the PCSWMM model.

Aquifers	AQ1	AQ2	AQ3	AQ4
Porosity	0.43	0.43	0.43	0.43
Wilting Point	0.15	0.15	0.15	0.15
Conductivity (in/hr)	1	1	1	1
Bottom Elevation (ft)	674.79	684.79	735	750
Water Table Elevation (ft)	720	732	785.866	770.5

Other than the USDA soil survey data, there was no other soil survey data provided for this project. Therefore, altering these aquifer parameters would have only been speculation. However, the water table was best estimated by the geographical information provided by the Tiger/Line® shapefiles of the United States Census Bureau. The digital elevation model was downloaded for both Jefferson and Saint Clair County since parts of LCC watershed lie in both counties.

The Jefferson and Saint Clair County region is comprised mainly of limestone, chert, and sandstone from the Knox Group, Sequatchie Formation and Chickamauga Limestone, and Red Mountain Formation. This allows for a conveyance of groundwater through the region, which supports the perennial nature of the LCC.

Table 3.3: Aquifer properties for various soil types, taken from Rossman and Supply (2005).

Soil Texture Class	Hydraulic Conductivity, K (in/hr)	Porosity, φ (fraction)	Field Capacity (fraction)	Wilting Point (fraction)	Suction Head, Ψ (in)
Sand	4.74	0.437	0.062	0.024	1.93
Loamy sand	1.18	0.437	0.105	0.047	2.4
Sandy Loam	0.43	0.453	0.19	0.085	4.33
Loam	0.13	0.463	0.232	0.116	3.5
Silt Loam	0.26	0.501	0.284	0.135	6.69
Sandy Clay Loam	0.06	0.398	0.244	0.136	8.66
Clay Loam	0.04	0.464	0.31	0.187	8.27
Silty Clay Loam	0.04	0.471	0.342	0.21	10.63
Sandy Clay	0.02	0.43	0.321	0.221	9.45
Silty Clay	0.02	0.479	0.371	0.251	11.42
Clay	0.01	0.475	0.378	0.265	12.6

3.2.4. PCSWMM Calibration Process

The PCSWMM calibration processes varied parameters such as surface roughness, percent impervious and junction invert elevations (ft) during this process. Other parameters such as the saturated hydraulic conductivity, K_{sat} (in/hr), minimum infiltration rate (in/hr), decay constant (1/hr), and drying time (days) were not varied with the calibration process. The calibration of the PCSWMM model was carried out using the Sensitivity-based Ratio Tuning Calibration (SRTC) tool offered in the PCSWMM packet. The SRTC tool helped detect the sensitive and insensitive parameters of the LCC watershed model. The method to determine each parameter is described in the following sections.

3.2.4.1 Modeling Parameters

In order to run the model, an initial set of input parameters was defined. The initial parameter selection was based on the SWMM 5.0 Manual (Rossman and Supply 2005) and the NRCS soil characteristic survey for the Jefferson and Saint Clair county area. The saturated hydraulic conductivity was determined by defining the soils types for each subcatchment. This was done by overlaying the georeferenced NRCS soil map (Figure 3.2) in ArcMap with the delineated subcatchments, the different soil types were assigned to each subcatchment. For subcatchments with multiple soil types that were evenly distributed across the plan, the saturated hydraulic conductivities were averaged across the area to represent the minimum infiltration rate

(in/hr). Most subcatchments were composed of 2 to 3 different soil types. If the soil type covered more than 50% of the subcatchment, then that soil type was chosen as the predominant soil type and that infiltration rate represented the minimum infiltration for the subcatchment.

K_{sat} was determined through the application of the maximum infiltration rate on the Horton curve definition, since the Horton infiltration method was selected as the infiltration model in PCSWMM. Horton's equations were used to calculate the potential infiltration rate as a function of time and the potential cumulative infiltration as a function of time in Equation

$$f = f_c + (f_0 - f_c)e^{-kt}$$

3.4 and

$$F = \int_0^t f dt = f_c t + \frac{f_o - f_c}{k}(1 - e^{-kt})$$

3.5, respectively.

$$f = f_c + (f_0 - f_c)e^{-kt} \quad 3.4$$

$$F = \int_0^t f dt = f_c t + \frac{f_o - f_c}{k}(1 - e^{-kt}) \quad 3.5$$

Where:

F = cumulative infiltration at time t

f_p= the infiltration capacity (depth/time) at time t

k= a constant representing the rate of decrease in f capacity

f_c= a final or equilibrium capacity

f_o = the initial infiltration capacity

Most of the soils in the LCC watershed are considered to be dry soils with dense vegetation. Therefore the soils in the NRCS group A were multiplied by 2 to calculate the maximum infiltration rate. Table 3.4 represents the selected K_{sat} and minimum infiltration values as determined from the NRCS Soil map (Figure 3.2).

In addition to K_{sat}, the Horton's infiltration rate decay constant, k, the drying time and the depression storage values did not vary during the duration of the model (Rossman and Supply 2005). The default values assigned by SWMM were 2 ^{1}/hr and 7 days, for the decay constant and

the drying time, respectively. Typical values for the decay constant ranged between 2 and 7 ^{1}/hr, and typical values for the drying time ranged from 2 to 14 days. The default value for both impervious and pervious depression storage was 0.05. Overall, these parameters were determined during the calibration stage to be insensitive parameters; therefore, the initial default values were maintained.

Table 3.4: Determined Saturated Hydraulic Conductivity also known as theminimum infiltration rate as well as the maximum infiltration rate used in PCSWMM.

Subcatchment	Maximum Infiltration Rate (in/hr)	Minimum Infiltration Rate (in/hr)
S_1	5.24	2.62
S_2	1.58	0.79
S_4	3.00	1.285
S_5	1.58	0.79
S_6	5.24	2.62
S_7	5.24	2.62
S_8	5.24	2.62
S_9	5.24	2.62
S_10	2.55	1.28
S_11	5.24	2.62
S_12	3.54	1.77
S_13	2.55	1.28
S_14	4.04	2.02
S_15	4.04	2.02
S_16	4.04	2.02
S_17	3.54	1.77
S_18	2.55	1.28
S_19	5.24	2.62
S_20	2.55	1.28
S_21	4.04	2.02
S_22	5.24	2.62
S_23	3.00	0.65
S_24	4.04	2.02
S_25	5.24	2.62
S_26	4.04	2.02
S_27	4.04	2.02
S_28	3.00	1.28
S_29	4.04	2.02
S_30	2.55	1.28
S_31	3.00	1.28
S_32	2.55	1.28
S_33	4.04	2.02

Another parameter that was not altered once applied were the storage curves for the residential lake and the JM Roberts pond. As mentioned earlier in section '3.2.3.5', the storage had a large impact on the stream flow. The storage curves are represented in Table 3.1.

The surface elevations of the subcatchments also did not vary throughout the calibration process. Since the average invert elevation for the junctions was 726.8 feet, the surface elevations were initially approximated to be 60 feet above the receiving node invert elevation. Both the observed flow and stream flow level were kept constant during the calibration process. The stream flow rate was the primary parameter used to calibrate the model. As mentioned previously, the flow rate measurements came from the AV sensors, which are located upstream and downstream of I-59. The AV sensor exports Excel files through the Flow Link software. These Excel files were converted into data files, and, eventually, time series files, in order to be accessed in PCSWMM. Once these files were uploaded for both sites, the simulated stream flow rate could be compared and calibrated to this observed flow. The stream level was another method of calibrating the hydrological elements of the LCC model. The stream level was also measured by the AV sensor and converted to time series files in order to be used in the calibration of the model.

In addition to the hydrological parameters, the pollutant parameters were also modeled. Once the continuous Sonde turbidity was converted into TSS (mg/L) using the relationship discussed in the Results section of this paper, the time series files were uploaded into the PCSWMM time series manager. The initial pollutant parameters were taken from the SWMM5 Applications Manual (Gironàs et al. 2009). While these values were suggestions, this was a good starting point for the calibration of pollutants within the LCC.

The SWMM applications manual used the exponential buildup function (EXP). The buildup function is represented below in Equation $B= C_1(1 - e^{-C_2 t})$

3.6. The initial values for the maximum buildup rate and the buildup rate constant are listed in Table 3.5.

$$B = C_1(1 - e^{-C_2 t}) \quad 3.6$$

Where:

B = pollutant buildup remaining on the surface at time t (lbs);

C_1 = maximum buildup possible (lb/area-ft);

C_2 = buildup rate constant at a time t (1/day).

For the washoff process in SWMM5, the exponential function (EXP) was chosen over the event-mean concentration function due to the continuous data provided by the Water Quality Sonde (Gironàs et al. 2009). Without the continuous Sonde data for an estimation and calibration of the exponential function washoff variables, the event-mean concentration would have provided a more sufficient approach to the calibration of TSS in the LCC water quality model. The exponential washoff function is shown in Equation $W = C_1 \cdot q^{C_2} \cdot B$

3.7. The initial values for the washoff coefficient and the washoff exponent are listed in Table 3.6.

$$W = C_1 \cdot q^{C_2} \cdot B \qquad 3.7$$

Where:

W = rate of pollutant load washed off at time t in (lbs/hr);

C_1 = washoff coefficient in units of (in/hr)-C2(hr)-1;

C_2 = washoff exponent;

q = runoff rate per unit area at time t (in/hr);

B = pollutant buildup remaining on the surface at time t (lbs).

Table 3.5: Initial Values for the Exponential Buildup Function in SWMM.

Land Use	C_1 (lbs/area-ft)	C_2 (1/day)
Interstate	100	0.2
Residential	45	0.5
Undeveloped	20	1.0

Table 3.6: Initial Values for the Exponential Washoff Function in SWMM.

Land Use	C_1 (in/hr)$^{-C_2}$(hr)$^{-1}$	C_2
Interstate	60	2.2
Residential	50	1.8
Undeveloped	45	1.1

3.2.4.2 Range of Variability: roughness, imperviousness, invert elevations, buildup and washoff

Based on the literature by Chow et al. (1973), the Manning coefficient of roughness (n) for the streams and overland flow depended on the land use and function of the surface (e.g., interstate, residential, etc.). Chow et al. (1973) conducted a survey to thoroughly define n values by matching the channel bed slope and floodplain area to the best description of the surface condition and thus to determine n value. The default value for a smooth channel roughness was 0.01. The roughness was a sensitive parameter in the LCC model. Therefore, the SRTC tool was applied to obtain the optimum values of channel roughness.

The pervious and impervious roughness values for subcatchments were also calibrated in the SRTC tool. All of the roughness values for the watershed were optimized through a period of SWMM runs. The default values for n pervious and impervious subcatchment areas were 0.1 and 0.01, respectively. Eventually the n impervious values were changed to 0.005. This value better represented the characteristics of the watershed. Similarly, the value for pervious areas was changed to 0.2 across all subcatchments, and this corresponded to the majority of the areas in the LCC watershed.

Along with the coefficient of roughness, the percent impervious for the subcatchment area was also varied over the duration of the model. The default parameter given by SWMM was 25 % impervious for all subcatchments. The subcatchments containing the right-of-way for the interstate were eventually assigned a value of 85% for percent impervious. The subcatchments containing only forested or wooded area were assigned a percent impervious of 10-13%. Lastly, the subcatchments containing residential and business lots were assigned a value of 13-25% (Rossman and Supply 2005). The range of variability for percent imperious is 0 to 100%; however, with little impervious area in the LCC watershed, the percent impervious range for the LCC area was only 0 to 85%.

The junction invert elevations were varied, depending on the elevations from the surveying data as well elevation points created in ArcMap. The elevation points in ArcMap were based on the USGS DEM, which had a coarse accuracy. Therefore, there are uncertainties present in the invert elevation values. In order to avoid adverse slopes from occurring in the channel, each of the junctions invert elevations were closely examined to determine the best value. The channel slopes were checked over to avoid supercritical flow conditions in areas that were experiencing subcritical flow. The range of invert elevations were 718 ft (the outlet junction) to 850 ft (the subcatchments upstream of the residential lake).

During the calibration process, the need to control the outflow at the residential lake and pond as well as the outflow at the outfall became crucial. Since there are many cross-sections throughout the LCC acting as control structures, weirs and orifices were implemented to adjust this flow. Although the storage curves for the residential lake and JM Robert Pond were not varied, the flow control structures were, such as the weir and orifices.

The trapezoidal weir height at the residential pond was changed to 2 feet (from the measured 1.5 feet) and the length was changed to 45 ft (from the measured 3 ft) -to account for the wide, low flood plan surrounding the weir channel- with a side slope of 3.3%. The additional exit flow structure from the residential pond was an orifice with a width of 0.06 ft and a height of 0.06 ft. The weir at J.M. Roberts Pond was approximated to be 20 ft in length and 2 ft in height. The weir at the J.M. Roberts Pond acts like a dam. In addition to these structures, a weir and an orifice were implemented just upstream of the outfall. These structures were added to slow the flow through the southern channels of the LCC watershed. The weir height is 10 ft and the length is 30 ft. The reason for the large length is due to the nature of the floodplain area. This area is characterized mainly as a wetland area with a main channel flowing through the area. The orifice height is 2 ft and the width is set as 10 ft.

Lastly, the pollutant buildup and washoff values were determined using the specified range of variability from Rossman and Supply (2005) and Vanoni (1975) as well as Cambez et al. (2008). The range of maximum buildup for the LCC was initially determined from the nationwide study by Manning et al. (1977), where dust and dirt buildup rates were examined for different land uses. The land uses included residential, commercial and industrial. The difference between these land uses and those of the LCC were taken into consideration upon calibration. Furthermore, in conjunction with the sediment transport theory, the washoff exponent, C2, should range from 1.1 to 2.6, with most values near 2. High density residential or commercial areas tend to release pollutants faster than areas with individual lots (Vanoni 1975).

3.2.4.3 Calibration data range/validation data range

Calibration for the developed SWMM model was carried out by focusing on a series of rain events between 6/12/2014 and 12/31/2014. There was a large variety of rain events within this time period. During the summer months or dry season, there were several smaller rain events that produced peak flows of less than 10 cfs. There were multiple rain events in November and

December, the wet season, which exhibited large groundwater flow that sustained the base flow over a period of days.

Due to the lack of observed data, the hydrological validation range was from 1/1/2015 to 3/26/2015. Since these wet conditions in the LCC support high water tables levels, this time period was mainly composed of groundwater-influenced events. The groundwater levels were still high at this time; therefore, only wet season events could be validated from the existing data. The lack of summer validation data did not ease the challenge of calibrating summer events for the LCC.

Figure 3.9 provides a visual representation of the hydrological calibration and validation periods.

The calibration period for the calibration of TSS is also between 6/12/2014 and 12/31/2014. However, the validation period for TSS differs from the hydrological validation period due to the available data. Nevertheless, since the Environmental Probe was deployed since April 2013, the pollutant validation period was selected from 6/1/2013 to 6/11/2014. Even with this larger range of rain events, there were still only a few rain events in which the Water Quality Sonde was functioning properly and the downstream and upstream site data over-lapped. Nonetheless, there were only a handful of events to calibrate the upstream sensor site and even fewer to calibrate the downstream site. Consequently, the calibration and verification results for the TSS are not as satisfactory for the downstream site as the results were for the upstream site.

As mentioned previously, when calibrating the SWMM model for the best fit range of parameter, the range of variability for each parameter was considered by the SWMM 5.0 Manual. Initial calibration was conducted without the use of the SRTC tool of PCSWMM. Once more precise calibration was needed; the SRTC tool was applied to detect the sensitive parameters.

The SRTC tool can be used to verify results as well. The verification process in PCSWMM takes the changes made to the parameters through the radio-tuning tool and runs them once more through SWMM to validate the predicted results. This verification process is to analyze whether or not the parameter changes made through the SRTC tool had the desired effects on the model.

3.3. Chapter Summary

In summary, the methodology behind preparing the data for the creation and use of the LCC model was established by efficiently collecting and analyzing data from the AV sensors, rain gauges, HOBO level loggers, and the Water Quality Sondes. The numerical investigation of the hydrological and water quality data allowed for the characterization of the LCC model. The range in the LCC model parameters was defined by the LCC watershed characteristics and the by Rossman and Supply (2005). Chapter 4 will discuss the results from this calibration and validation period in

Figure 3.9, which compares the hydrological and water quality results for the LCC and the difference between the upstream and downstream sites.

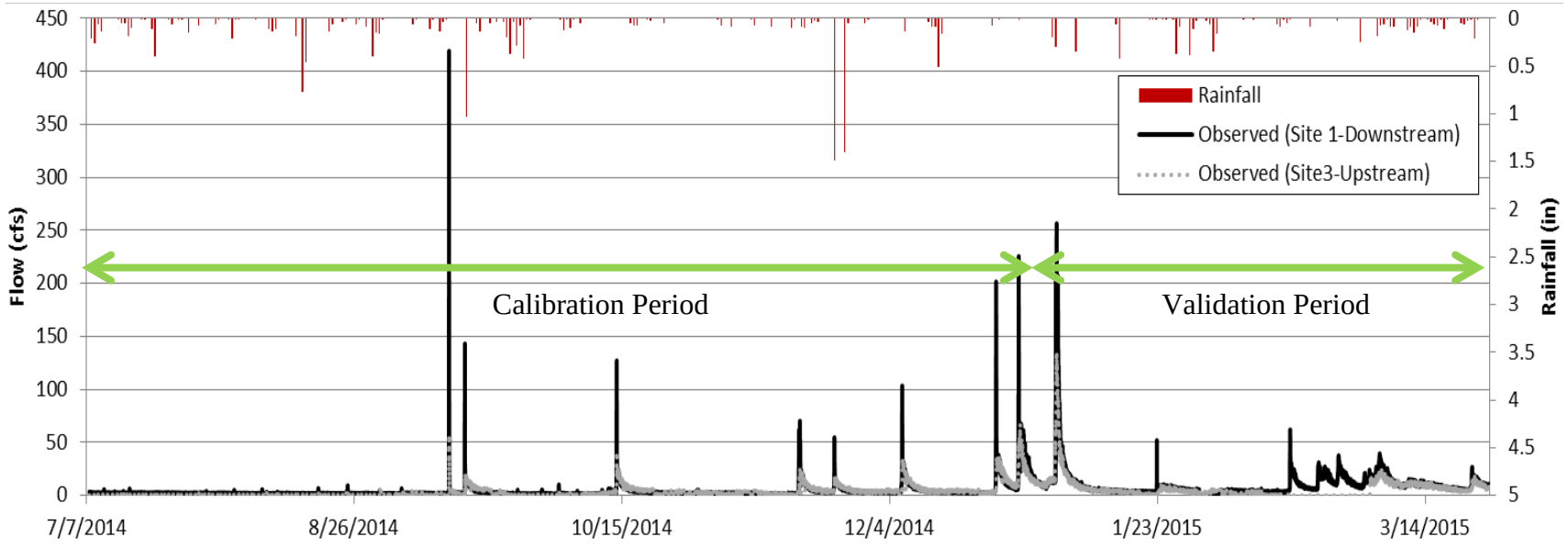

Figure 3.9: Visual Representation of the hydrological calibration and validation period.

Chapter 4

Results and Discussion

4.1. Measurements

4.1.1. Turbidity: continuous Sonde and point sample data

Initially in the LCC project, beginning in April 2013, turbidity was collected by means of point sample collections every two weeks. A map depicting the upstream and downstream sites is shown in Figure 4.1. All of these sites are perennial tributaries of the LCC watershed. Through the investigation of the LCC, the location downstream was established as the outlet point for the entire LCC watershed. At this site there is a low-head dam, which is now damaged as consequence of a large storm event during the earlier stages of the project.

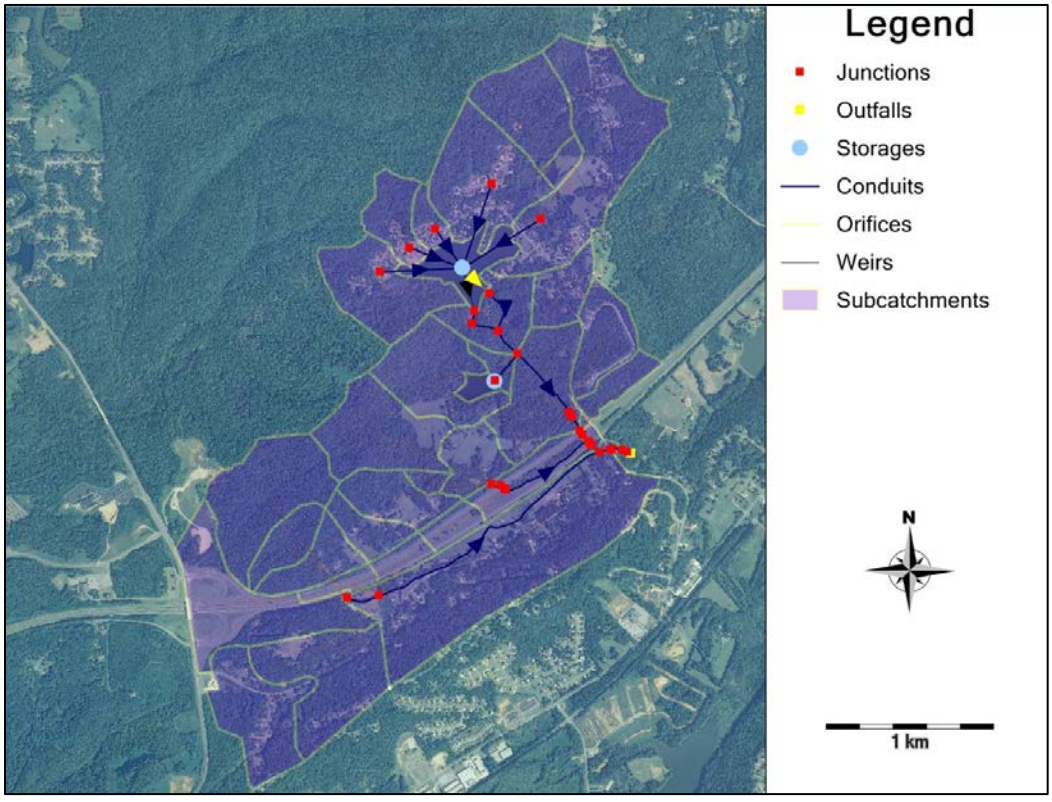

Figure 4.1: Map presenting upstream and downstream sites in the entire LCC Watershed corresponding to Table 4.1.

The downstream site was chosen for the nearby location to the interstate and to provide an undisturbed account of the runoff downstream of the interstate. The upstream site was chosen to represent the LCC stream characteristics upstream of the interstate. Since this branch was the only perennial branch crossing the interstate, downstream and upstream sites were selected for analysis.

From this collection of LCC site samples, the following summary of physical water quality parameters, shown in Table 4.1, was derived. Seldom were there samples collected during an actual rain event; therefore, the time period in which the samples were taken was compared. Samples taken within 72 hours of a rain event were separated from the samples that were not collected within 72 hours. This 72-hour period was established from observing generally the recession time of the LCC following rain events.

Table 4.1: Summary of water quality physical parameters from the LCC watershed monitoring program.

				Occurred within 72hrs of a Rain Event		Occurred After 72hrs of a Rain Event	
Physical Parameter	**Site**	**Average**	**Standard Deviation, σ**	**Average**	**Standard Deviation, σ**	**Average**	**Standard Deviation, σ**
TS (mg/L)	Downstream	118.8	32.6	111.1	36.6	127.8	24.1
	Upstream	116.6	32.8	112.9	38.6	120.9	23.5
TSS (mg/L)	Downstream	3.2	10.0	2.1	11.8	4.5	7.2
	Upstream	12.6	26.4	16.8	34.9	7.6	6.3
Turbidity (NTU)	Downstream	3.8	2.8	4.3	3.3	3.0	1.7
	Upstream	3.4	3.2	3.7	3.4	3.0	2.7
pH	Downstream	7.8	0.1	7.8	0.1	7.9	0.1
	Upstream	7.6	0.2	7.6	0.2	7.7	0.2

Although the overall levels of turbidity were low, there were some unique differences between the upstream site and the downstream site. In general, for these point samples, the turbidity levels were higher for the downstream during the wet season than the upstream location and turbidity levels for the upstream site were higher in the dry season the downstream location. Within 72 hours after the rain event, the downstream site displayed a higher standard deviation than the upstream one. This difference in standard deviation may suggest that the turbidity levels downstream take longer to return to base flow levels than upstream. Furthermore, there was no significant difference in Total Solids (TS) between the upstream and downstream sites.

Additionally, the standard deviation of turbidity for the samples collected within 72 hours was slightly greater for upstream than downstream, 0.129 NTU. There was only a 0.61 NTU difference in average turbidity between the upstream and downstream sites collected within 72 hours, respectively. Even though the average turbidity levels were higher downstream, both the upstream and downstream had nearly the same standard deviation. This small difference suggests that there is a high amount of washoff occurring at both upstream and downstream sites.

Since the continuous Water Quality Sonde data has been recorded from August 2013 to March 2015, select events are used to represent the characteristics of turbidity in the LCC. The following is a results and discussion on the turbidity levels caused by particular storm events.

The continuous measurements of turbidity revealed that the turbidity upstream and downstream of the interstate crossing indicated that LCC flows have relatively low turbidity. On average the flows were less than 10 NTU in the absence of recent rain events. The range of turbidity recorded was from 0.7 to 242.8 NTU. Turbidity results comparing three different events are shown in Figure 4.2.

The Water Quality Sonde turbidity results for the rain events on 12/8/2013 and 4/29/2014 exemplify that during some rain events the turbidity increase downstream from the road was more pronounced, with peaks up to 36% larger than the peak turbidity upstream in the mid spring. On average the downstream turbidity levels from the Water Quality Sonde were 20% greater than the turbidity levels at the upstream site, as shown in Table 4.2.

In the case of smaller rain events, some measurements of upstream turbidity were similar to or slightly exceeded the amount of turbidity recorded downstream. One can assume that contributing factors in the interstate (pavement, median) would be causing the turbidity to increase at the downstream end. This contribution may be from the interstate, the median, the tributary that connects to the LCC at the median, or some other unidentified factor. Overall, this relative turbidity increase across the interstate is not major in absolute terms, and in most cases is below 50 NTUs.

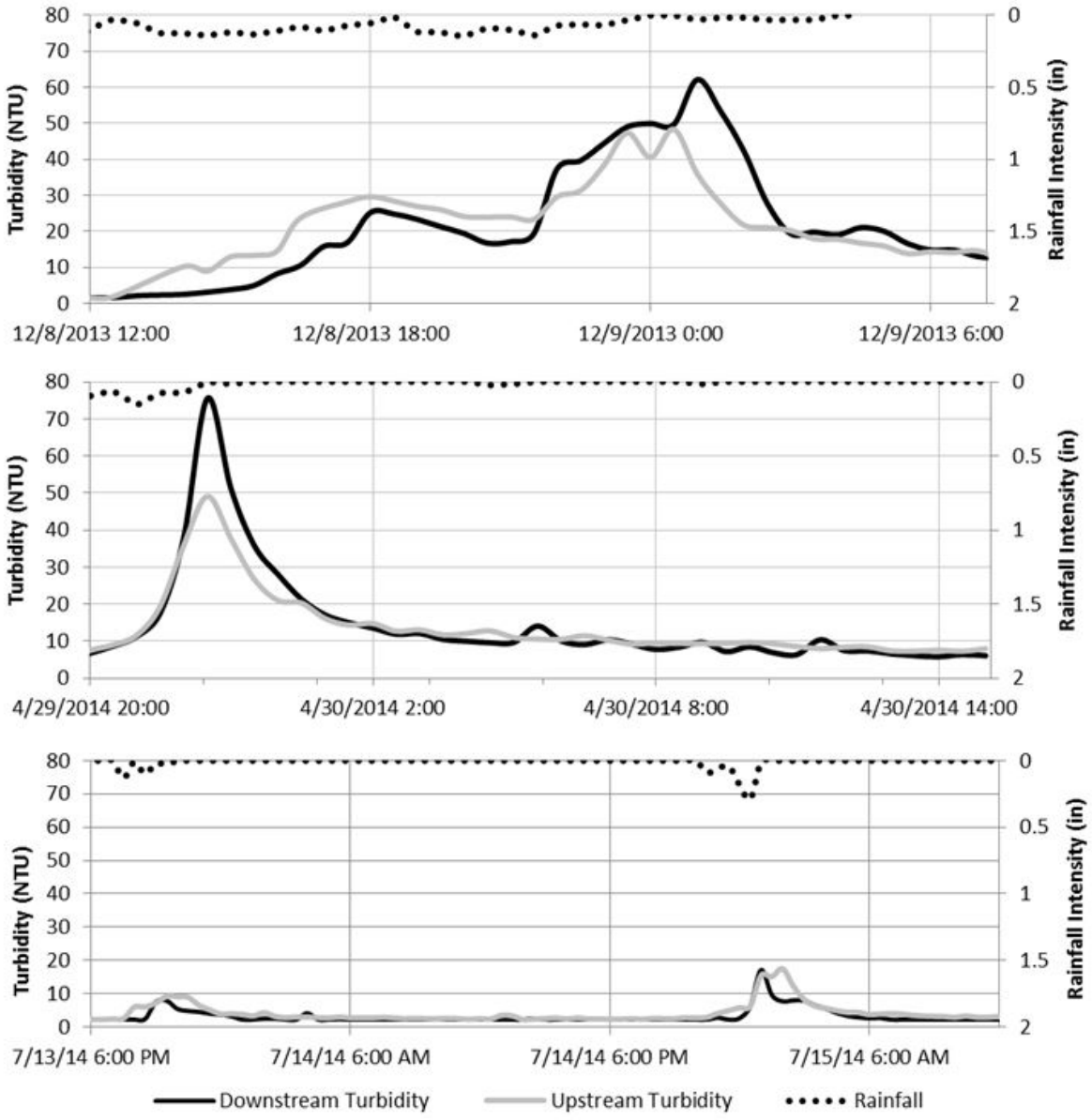

Figure 4.2: Turbidity results measured in LCC downstream from I-59 and upstream from I-59 and how this parameter was impacted by rain events.

In addition to the Water Quality Sondes, auto-samplers were deployed to help in event-based characterizations of the stream water, particularly how stream turbidity and TSS would vary during rain events. These results are presented in Figure 4.3.

Samples were collected between 10/1/2013 and 4/3/15 and used to derive a relationship between the total suspended solids (TSS) and turbidity measured from these samples. The results indicate that for the low TSS values (under 10 mg/L), the turbidity between downstream and upstream are comparable; however the turbidity is slightly larger downstream from the road. For larger TSS values, there is a relatively steady increase of turbidity for samples collected in upstream, up to the range of 34 NTUs. The results of turbidity for large range of TSS at the downstream site also increased, but the data points are much more scattered. Turbidity values reached 110 NTUs in one storm for a TSS value of 30.8 mg/L. In another rain event, for the same range of TSS (32.6 mg/L) a much smaller turbidity value (3.4 NTU) was recorded. This indicated that contributions from roadway runoff have a complex impact on the stream turbidity. Some events carry significant solids and increasing turbidity, while in other cases turbidity is only minimally impacted. Overall, the auto sampler turbidity results at the downstream site were on average 3.7 times greater than the upstream turbidity levels. On average the TSS levels at the downstream site were 4.6 times greater than the upstream TSS levels.

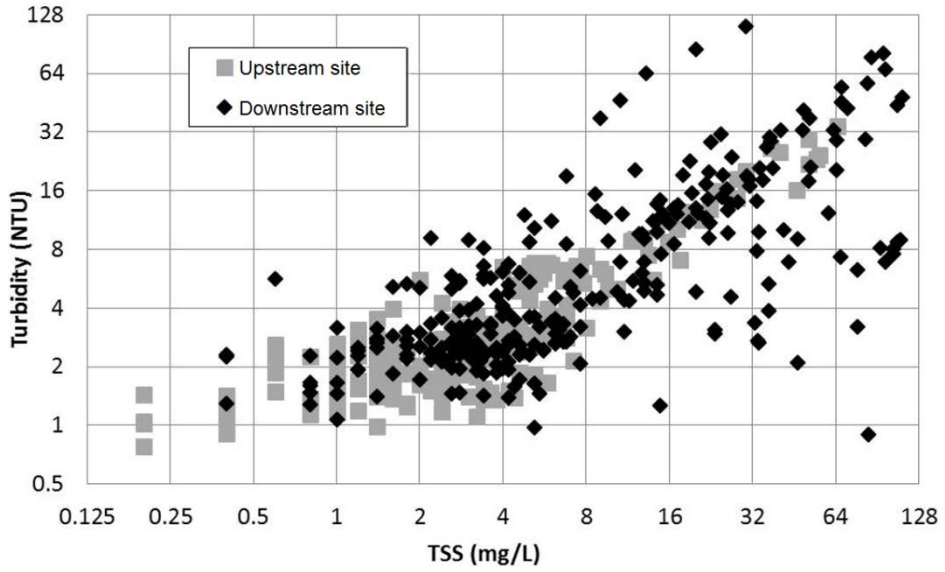

Figure 4.3: Total suspended solids and turbidity from samples obtained with the use of auto samplers downstream of I-59and upstream from I-59.

Once turbidity levels returned to base flow levels for the Water Quality Sonde, the values between the downstream and upstream sites were within 0.03 NTU of the point samples collected from April 2013 to April 2014. This second validation of turbidity results helped provide a great deal of insight into the characteristics in the LCC. Figure 4.4 shows the

comparison between TSS and Turbidity from the point samples (P.S.) and the TSS power relationship (POW) derived from Figure 4.3. Both relationships display a linear trend for Turbidity and TSS points under 5 NTU. This one-to-one relationship provided support for the low Water Quality Sonde readings that were at times obscure or faulty.

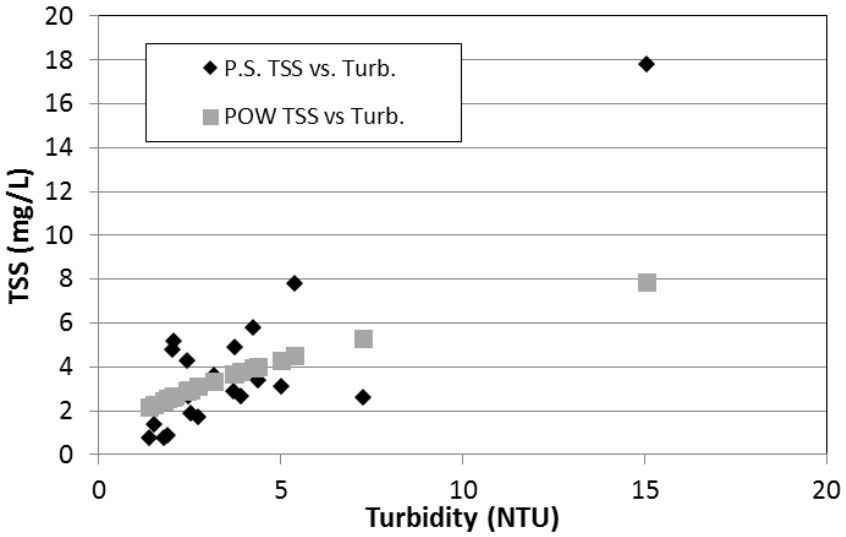

Figure 4.4: Comparing point sample (P.S.) TSS and turbidity collections to the power relationship derived from the Auto Sampler data.

Table 4.2 shows the difference in observed peak turbidity levels between upstream and downstream. There are inconclusive results supporting the whether or not there are continuously higher turbidity levels at the downstream level or at the upstream level. Nine events were available for comparison. There were more rain events for both sites; however, these are the events that possess the most confident results. From the nine events list in Table 4.2, three of the events show greater levels of turbidity at the upstream site. These are represented with a negative percent value. The percent difference for 6 events showed that there were greater peak levels of turbidity at the downstream site. Nonetheless, no conclusions can be drawn to whether or not more turbidity is present downstream or upstream without more supportive rain events.

Table 4.2: Percent differences between the upstream and downstream observed turbidity levels for nine rain events.

Dates	Upstream Observed Turbidity	Downstream Observed Turbidity	Percent Difference
8/3/2013	9.8	18.8	92%
8/4/2013	183.4	192.8	5%
11/25/2013	27.1	33.9	25%
12/8/2013	45.1	64.3	43%
4/28/2014	16.5	13.5	-18%
4/29/2014	51.3	77.8	52%
6/11/2014	189.4	170.6	-10%
7/13/2014	9.2	7.9	-14%
7/15/2014	15.5	17.1	10%
		Average	20%

4.1.2. Nitrogen and Phosphorus Species Measurements

Figure 4.5 through Figure 4.8 are a comparison of the upstream and downstream sites nutrient levels over 12 months: nitrate (NO_3), total nitrogen (TN), ammonia-nitrogen (NH_3-N), and total phosphorous (TP), respectively. The estimated detection limit (EDT) as well as the level of accuracy of the Hach test conducted is included in the caption. TN, TP and NH_3 all show no major seasonal variations. The level of NO_3 rose from August to January by approximately 1 ppm.

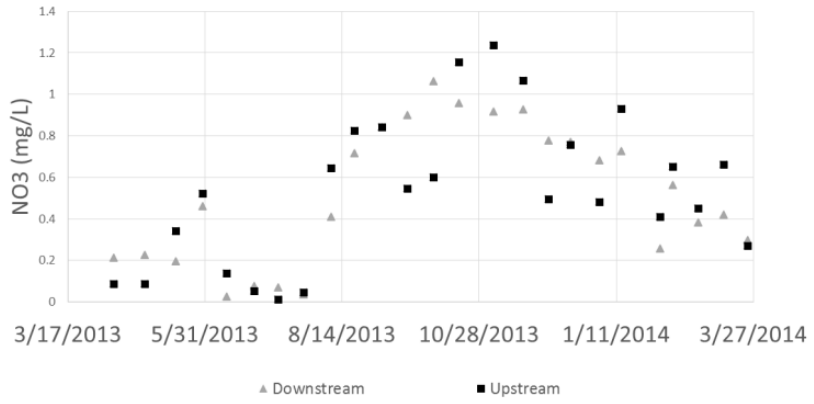

Figure 4.5: Upstream and downstream sites NO3 results expressed as N (EDT: 0.01 ppm NO3-N; accuracy: ±0.03 mg/L).

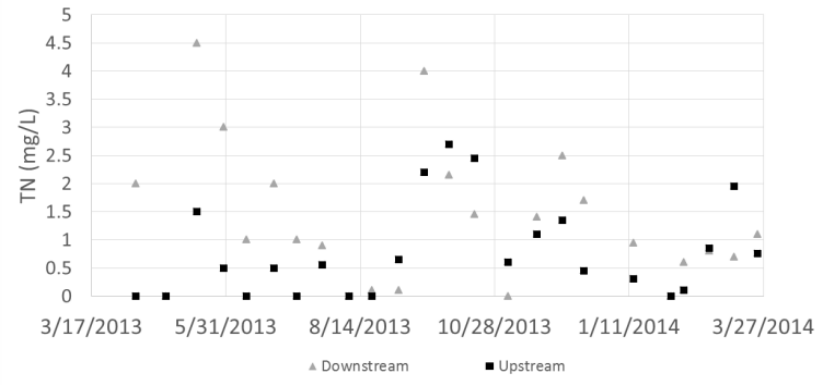

Figure 4.6: Upstream and downstream sites total nitrogen results (EDT: 2 ppm N; accuracy: ±0.05 mg/L).

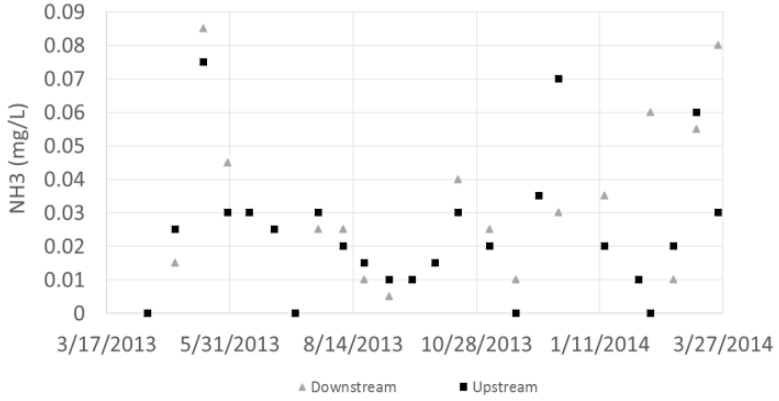

Figure 4.7: Upstream and downstream sites NH_3–N results expressed as N (EDT: 0.07 ppm N; accuracy: ±0.02 mg/L).

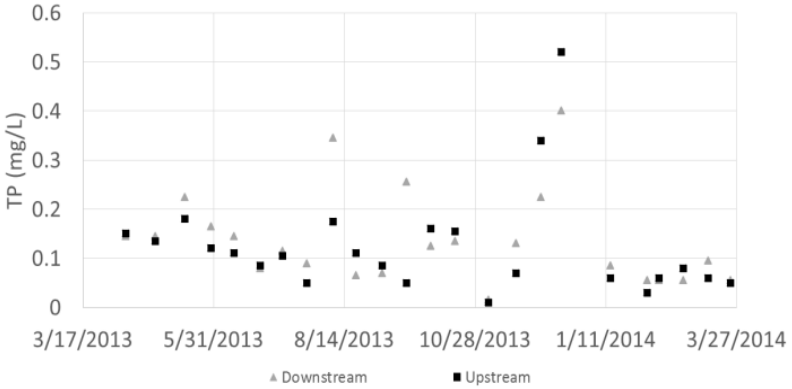

Figure 4.8: Upstream and downstream sites total phosphorus results (EDT: 0.07 ppm PO_4; accuracy: ±0.07 mg/L).

There is no significant increase of nutrients when upstream and downstream samples were compared. The downstream site had a 29% average increase of NO_3 from the upstream site. The downstream site also experienced a 33 % average increase in TP. Although these increases seem noticeable, these nutrient levels are already at low levels, even close to the detection limit of the Hach colorimeter. Additionally, the downstream nutrient results were for some events lower than the upstream site. Due to these facts and the accuracy of the testing instruments, these differences are deemed insignificant.

There was however a significant difference in TN, which tended to have higher levels at downstream than upstream. This increase in TN could be caused by atmospheric deposition in the paved area, or by vehicular exhaust. Since vehicle exhaust contains nitrogen oxides, such as NO and NO_2, and NH_3 (AQEG, 2004), vehicle exhaust may be a contributing factor to this increase in nitrogen (Capea et al. 2004).

4.1.3. Discussion and comparison with related investigations

In order to further assess the measurements of solids and nutrient levels for the LCC at the upstream and downstream sites, these results are compared to the National Stormwater Quality Database (NSQD) by Pitt et al. (2004). According to the NSQD, from observing the TSS event mean concentrations from both the Water Quality Sonde and the turbidimeter are significantly below the national average for freeways and residential areas (including seasonal trends), as well as for EPA Zone 3.

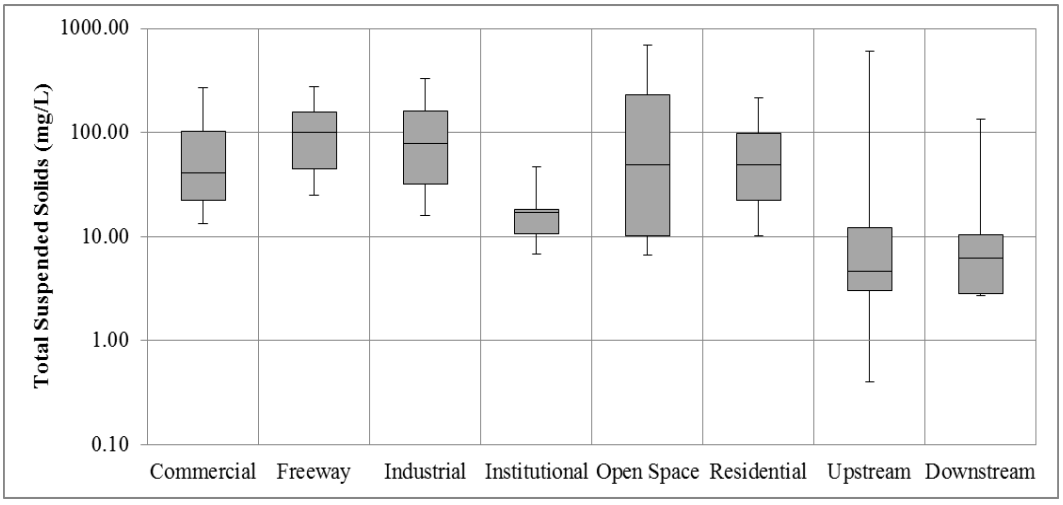

Figure 4.9 presents a whisker plot taken from NSQD database for stormwater data for different land uses, and compared to LCC measured results for the upstream and downstream

sites. In these plots, the top error bar represents the maximum value, while the bottom error bar represents the minimum value recorded. The top of the box represents the 3rd quartile value, the value in the middle of the box represents the average and the bottom of the box represents the 1st quartile value.

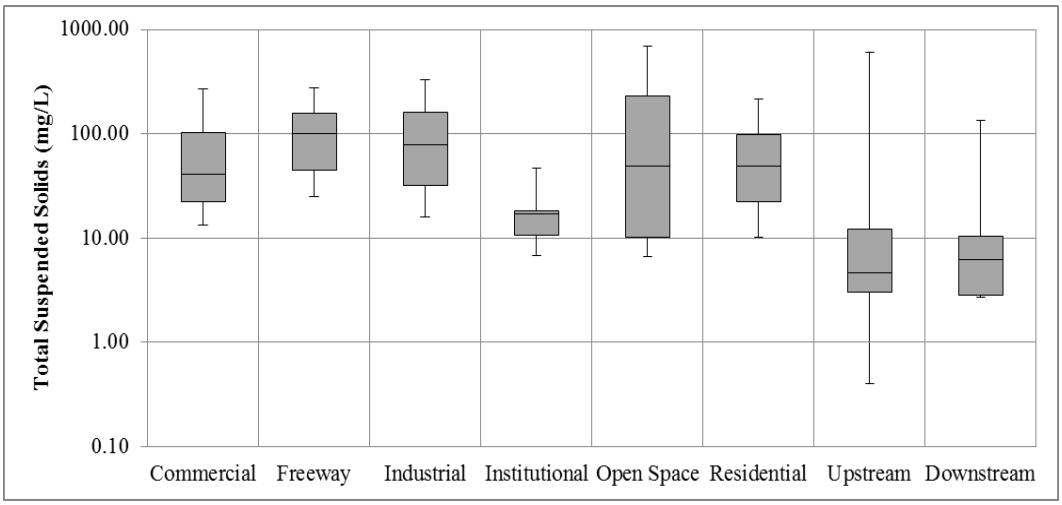

Figure 4.9: Example TSS stormwater data sorted by land use (no mixed land use data in plots).

In addition to the TSS levels being below the national average for land use and seasonal the nutrient levels were also below the first Quartile of other land uses. The national standard deviation of Total Phosphorus (TP) for open space is significantly greater than the standard deviation for freeway land use. Although the TP levels coming from the specific land uses cannot be determined, the TP levels in the LCC are on average 0.13 mg/L with a maximum recording of 0.96 mg/L for the downstream site, Figure 4.10. The average and maximum levels of TP for the upstream site were 0.11 mg/L and 0.95 mg/L, respectively. The only land use where the LCC was above average for NO_3+NO_2 values was Freeway land use. The average NO_3+NO_2 for the upstream and downstream 0.5 and 0.46 mg/L, respectively, and the average NO_3+NO_2 for Freeways is 0.27 mg/L. However, the minimum NO_3+NO_2 value for the downstream were well below the minimum value for Freeway land use.

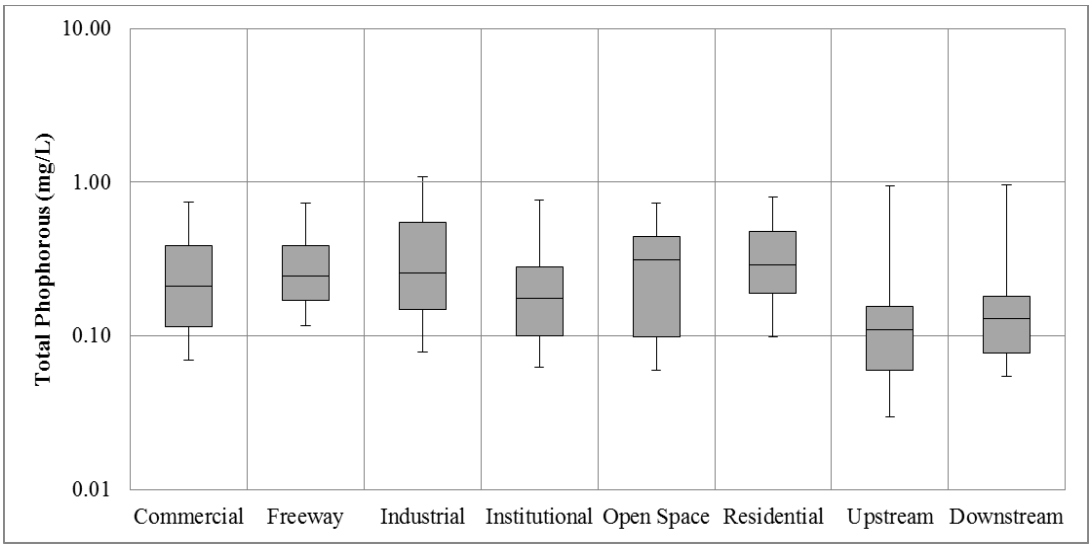

Figure 4.10: Example TP stormwater data sorted by land use (no mixed land use data in plots).

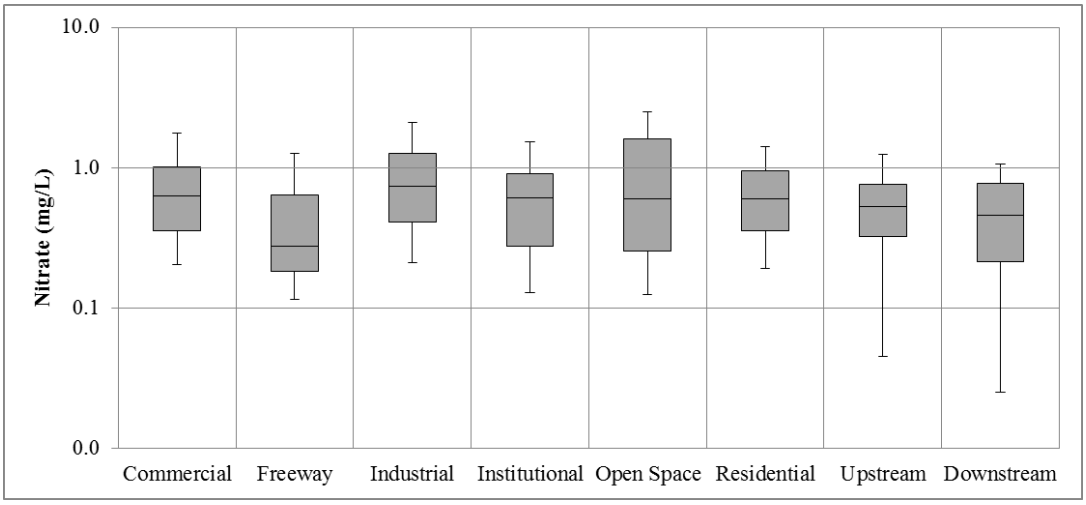

Figure 4.11: Example NO_3+NO_2 stormwater data sorted by land use (no mixed land use data in plots).

In context of the EPA rain region 3, which includes but is not limited to part of Mississippi, Alabama, Georgia, South Carolina, and Florida, the TP levels for this region are relatively much lower than the other regions of the United States. These below average total phosphorous and nitrate plus nitrite levels of the both the upstream and downstream sites suggest that the surrounding open space/farmland does not have a significant impact on the immediate area.

4.1.4. Groundwater Measurements

From the two shallow groundwater wells (~20 ft deep) installed at the upstream downstream, stations, a relationship between the surface water level loggers and groundwater level logger was observed. The results from Figure 4.12 are a typical representation of this interaction.

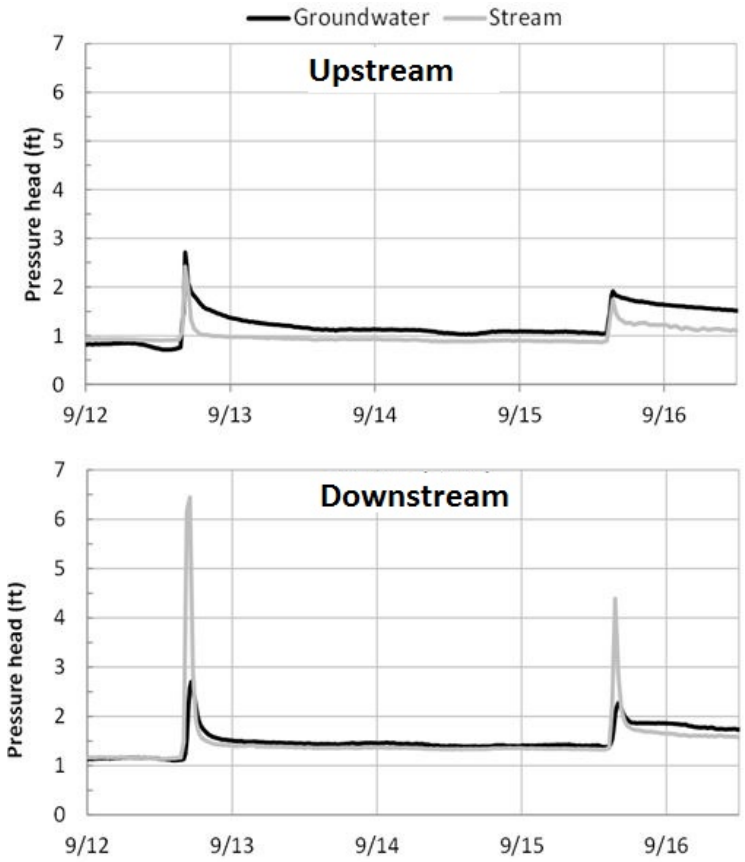

Figure 4.12: Pressure hydrograph for two rain events on Sep/14, with level logger changes upstream from the I-59 and downstream from the I-59.

There were steeper increases in stream depths upstream compared to downstream. The same conclusion is drawn when comparing the surface water upstream to the groundwater downstream. As expected, there is more runoff produced from the road than from the residential and undeveloped areas upstream of the interstate. The upstream site typically showed the same increase in magnitude of pressure for both the stream water and groundwater. This suggested that the upstream location is mainly fed by groundwater, or a receiving stream. This suspicion was

confirmed when there was water visibly pouring into the stream at the upstream site from several places in the ground.

The recession curves upstream for the surface water and groundwater were very different. The surface flow quickly returned to original stream flow levels, while the groundwater at site returned very slowly to the original groundwater levels. The recession curves downstream for surface water and groundwater had a closer relationship than upstream. However, the groundwater downstream had a more gradual recession curve than the surface water before returning to base levels.

Compared to the dry season, as shown in Figure 4.12, there was a faster recession for both surface water and groundwater at both sites. During the wet season in December, there was overall a slower recession for both surface water and groundwater rain events. This was more than likely due to the increase in stored groundwater and the increase in stream baseflow during this time period. However, the surface still receeded more quickly than the groundwater.

The magnitude of the groundwater peaks in the wet season (October to April) and dry season (May to September) were similar at the downstream location. The only difference in peak magnitudes between the dry and wet seasons was seen when comparing the difference in surface water and groundwater at the downstream site. The surface water peaks were up to five times larger than the groundwater peak magnitudes in the dry season than during the wet season at the downstream location. Therefore, a majority of runoff was conveyed as overland flow. The surface water and groundwater peak magnitudes upstream were similar for both dry and wet seasons. The differences between surface water and groundwater peak magnitudes were also similar for both the wet and dry season.

On the other hand, the magnitude of the rise in groundwater for both sites were similar. This similarity indicates that there may be limited impact from the interstate on the underlying aquifer betweenthe upstream and downstream.

4.2. PCSWMM simulation results of LCC

Hydrological Comparison

Modeling tools are useful in estimating the effects of rain events in watershed in terms of flow rate hydrographs and water quality changes, among others. Once the temporal characteristics of the hydrograph peak and recession are determined through field measurements,

modeling parameters can be better adjusted to fit the observed data. Figure 4.13 through Figure 4.18 are the result of several calibration and sensitivity radio tuning calibration tool (SRTC) in PCSWMM. These periods include both dry and wet weather situations in the hydrological calibration period (6/12/2014- 12/31/2014) and the validation period (1/1/2015-3/26/2015).

Figure 4.13: Flow hydrograph comparison for upstream (top) and downstream (bottom) simulated and respective measurements (9/12/2014).

Overall, the simulated flow matched fairly well with the observed hydrographs. Some smaller summer rain events were more difficult to represent (rainfall < 0.1in/hr). These small summer events eventually improved through the calibration process. For the larger summer events, such as in Figure 4.13, the simulated peaks were larger than the observed data for upstream. The downstream observation site produces more runoff and the peaks measured downstream were more sufficiently matched than those upstream. For the most part, the timing of the peak flows for the simulated results agreed with the observed peak flows for both summer and winter events.

During the winter season or the wet season, measured groundwater levels were higher, resulting in a more gradual recession curve for the stream. The simulation was able to replicate this gradual decent in water levels in the stream. However, in some cases in the model there is a gap among the simulated and observed recession curves for Figure 4.14, Figure 4.15, and Figure

4.16. This noticeable difference between water levels suggests that there are additional sources, possibly aquifers that are not properly represented by the PCSWMM modeling of LCC.

Additionally, the slow release observed in Figure 4.14, Figure 4.15 and Figure 4.16 is not produced by the median or interstate since the slow release is also observed upstream. This slow recession of stream water suggests that the LCC has a very slow return of groundwater to base levels, which may be the main reason for the perennial characteristic of the LCC.

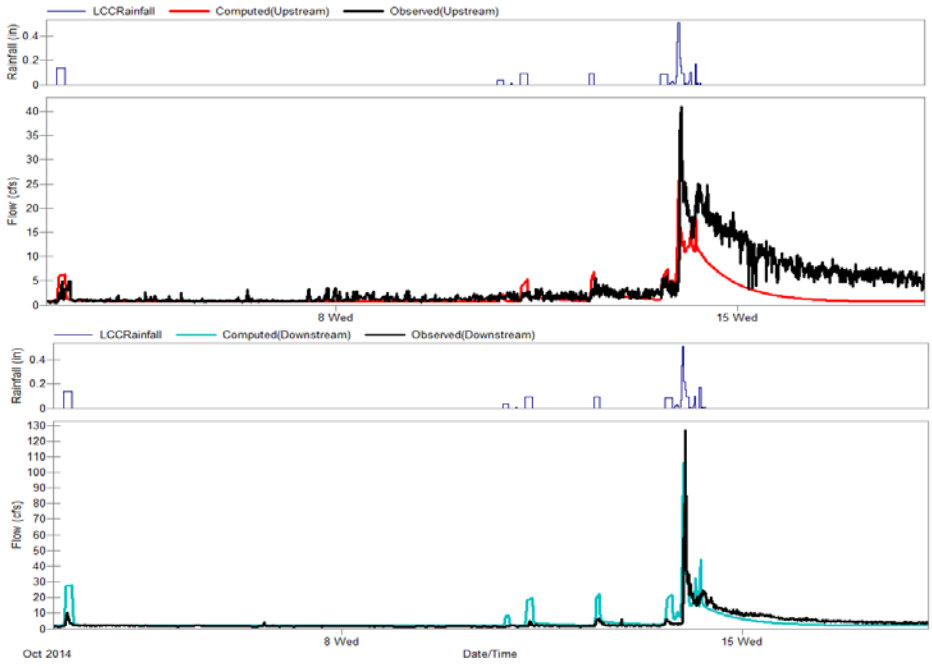

Figure 4.14: Hydrograph comparison of upstream (top) and downstream (bottom) for simulated and observed stream flow data (10/14/2014).

Another difference in rainfall events was observed through the comparison of Figure 4.15 and Figure 4.16. In January of Figure 4.16, these events performed differently than the events represented in December of Figure 4.16 , even though the first two rain events in December produced the same amount of rainfall if not more rainfall than the rain event in January. There is a significantly greater peak flow observed from the event in January than the previous events, both upstream and downstream. Since the difference in flow is observed at both sites, this missing flow could originate further upstream. There was no surveying data available from the two waterbodies further upstream of I-59, and a lack of precise representation of these large physical structures of the LCC watershed could be influencing this discrepancy in observed and modeled flows.

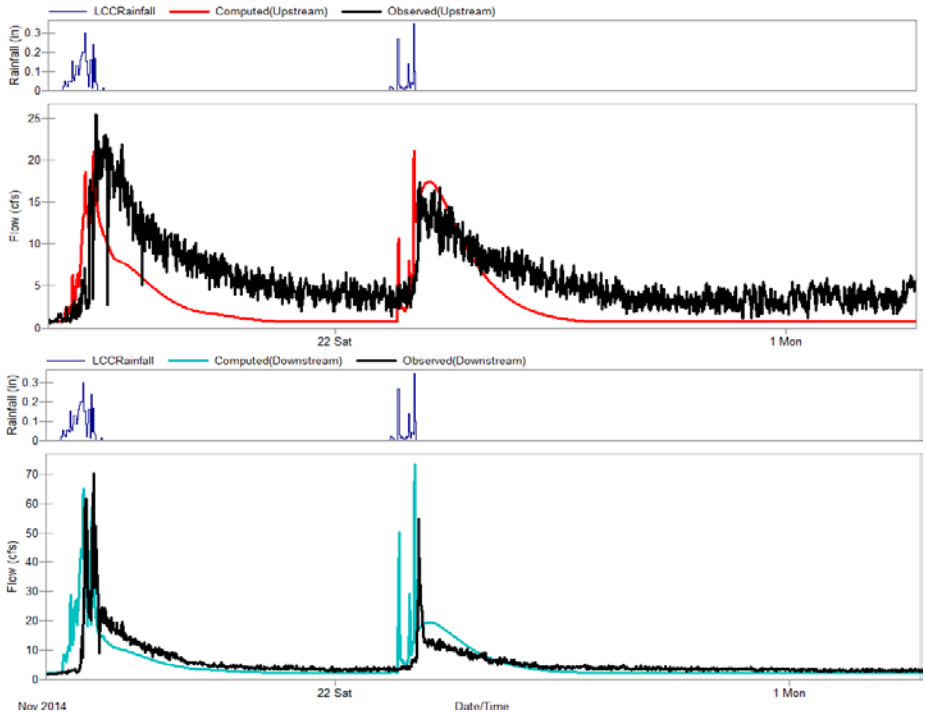

Figure 4.15: Hydrograph comparison of upstream (top) and downstream (bottom) for simulated and observed stream flow data (11/17/2014).

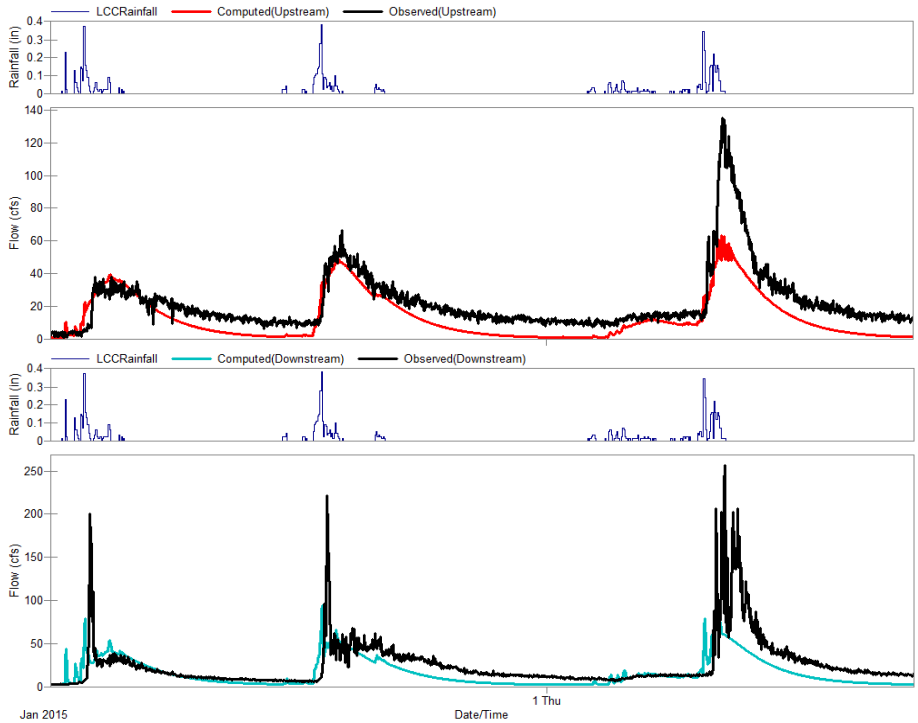

Figure 4.16: Hydrograph comparison of upstream (top) and downstream (bottom) for simulated and observed stream flow data (12/14-1/15).

The results for the validation period were sufficient. A key objective behind the calibration period was to represent the observed peak flows. While not all the flows matched up perfectly with the peak flows, the overall results were considered satisfactory to good according to the criteria by Moriasi et al. (2007). In

Figure **4.17** and Figure 4.18, the peaks were replicated, except the first flush at the upstream site on 3/22/2015.

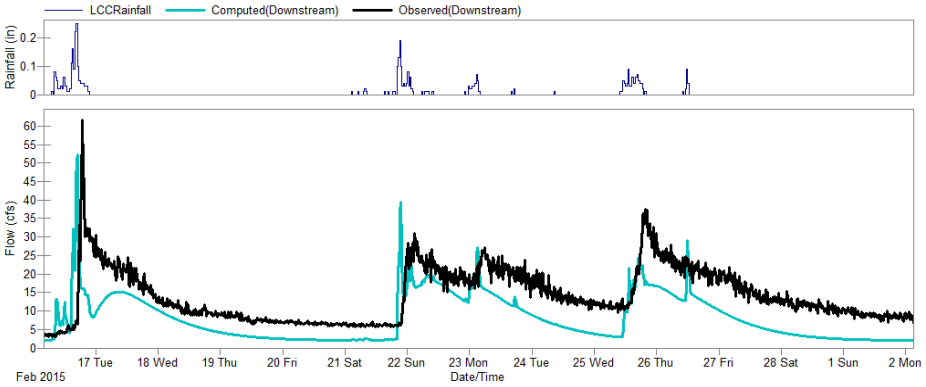

Figure 4.17: Hydrograph comparison of downstream for simulated and observed stream flow data (2/17/2015) (No data available at upstream location).

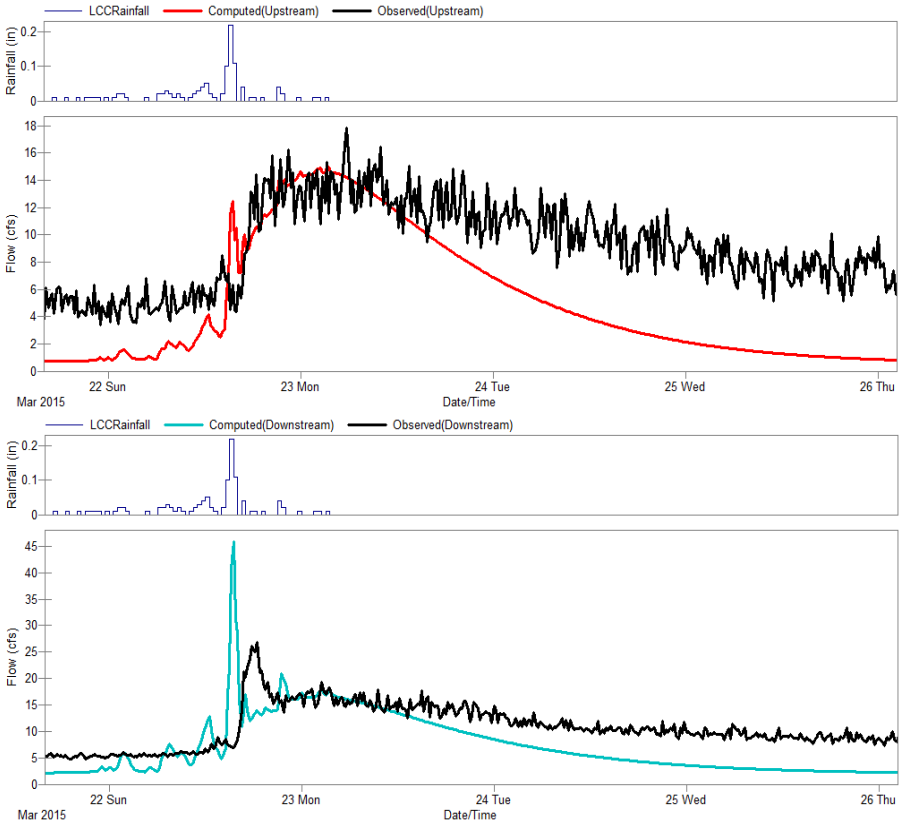

Figure 4.18: Hydrograph comparison of upstream (top) and downstream (bottom) for simulated and observed stream flow data (3/22/2015) (validation period).

Table 4.3 compares the AV sensor observed peak flows for the same events between the upstream and downstream. The percent difference was calculated between 23 peak flow events for both the upstream and downstream sites. Those events were then categorized by: less than 0%, between 0% and 25%, between 25% and 50%, and greater than 50% difference. 78% of the downstream peak flows were 50% or greater than the peak flow values at the upstream site. This increase in peak flow downstream during storm events could possibly be from the impervious area from the surrounding area. The peak flow downstream was on average 1.7 times greater than the peak flows at the upstream site. However, there is approximately a 30% increase in subcatchment area for the downstream site. This increase in area along with the difference in land use influences this increase in peak flows downstream.

Table 4.3: Percent difference between the AV sensor observed peak flows for both the downstream and upstream site.

Percent difference between observed peak flows for the downstream and upstream sites	
Diff in Flows ≤ 0%	9%
0% < Diff in Flows ≤ 25%	9%
25% < Diff in Flows ≤ 50%	4%
Diff in Flows > 50%	78%

In order to compare the post-development conditions of the existing I-59, a second version of the LCC model was created to account for the pre-development conditions. This new pre-development model included changing the land use, imperviousness, channel bed roughness, and the channel bed geometry. With these changes the post-development stream flow was compared to the pre-development flow. The percent difference was calculated between 23 post- and pre-development peak flow events for both the upstream and downstream sites, as shown in Table 4.4 and Table 4.5. When the percent difference in flows were less than zero, the value from the pre-development was greater than the post-development model. Those events were then categorized by: less than 0%, between 0% and 2%, between 2% and 5%, and greater than 5% difference. Therefore, the percent shown in the right-hand column are the percentage of peak flow levels that fell into the specified category.

The most common difference in flows for the upstream site ranged between 0 and 2 %. The same was true for the downstream site. However, only 13 % of the upstream flows for pre-development were larger than the post-development, while for the downstream site, 39% of pre-development flows were larger than the post-development. The conduits may have been acting as a control structure, lowering the flow downstream of the interstate.

Table 4.4: Percent difference between the peak flows of the post- and pre-development LCC models at the upstream site.

Percent Difference between Peak Flows of Post- and Pre-Development Conditions at Upstream Site	
Diff in Flows ≤ 0%	13%
0% < Diff in Flows ≤ 2%	48%
2% < Diff in Flows ≤ 5%	22%
Diff in Flows > 5%	17%

Table 4.5: Percent difference between the peak flows of the post- and pre-development LCC models at the downstream site.

Percent Difference between Peak Flows Post and pre-development conditions at Downstream Site	
Diff in Flows ≤ 0%	39%
0% < Diff in Flows ≤ 2%	43%
2% < Diff in Flows ≤ 5%	4%
Diff in Flows > 5%	13%

Groundwater Comparison

The groundwater results from the SWMM5 model are compared to the groundwater levels from the HOBO level loggers deployed at both downstream and upstream locations. Four events were chosen to display the similarities and differences between the groundwater levels: 9/12/2014, 10/17/2014, 12/24/2014, and 2/22/2015 (from the hydrological validation period). The HOBO level logger data is represented in pressure head (ft) with respect to a reference point at the bottom of the well, and the simulated results are represented by elevation (ft) with respect to sea level. The pressure hydrographs by both the level logger and SWMM5 are in general consistent as further elaborated in a later section.

Figure 4.19 through Figure 4.22 present different seasonal patterns and ground water characteristics. For late summer events, such as in

Figure **4.19**, SWMM5 tends to overestimate the groundwater levels. During the winter events in October, Figure 4.20, and December, Figure 4.21, and even late February, Figure 4.22, the spikes in groundwater are more adequately represented by the SWMM5 model. There is speculation that the differences in groundwater levels between the model and measurements may be linked to the choice of modeling parameters defining soil and infiltration characteristics in the PCSWMM model.

Another reason for the difference in groundwater results could originate from the approach SWMM5 uses to calculate groundwater elevation. The groundwater elevation of a subcatchment represents the average groundwater level that subcatchment is experiencing and not at a specific point. The process implemented by SWMM of the infiltration and percolation of stream water to groundwater through the interaction with nodes, could be a limited representation of a specific point within that subcatchment, since lateral infiltration from stream into the nearby banks is not represented.

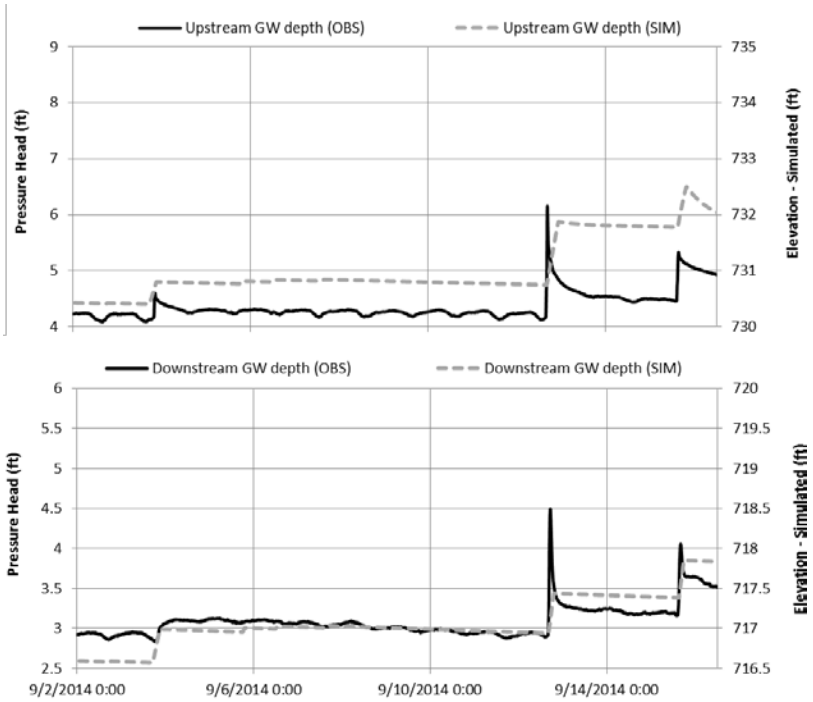

Figure 4.19: Groundwater level comparison of hobo level logger and PCSWMM results for 9/12/14-9/15/14.

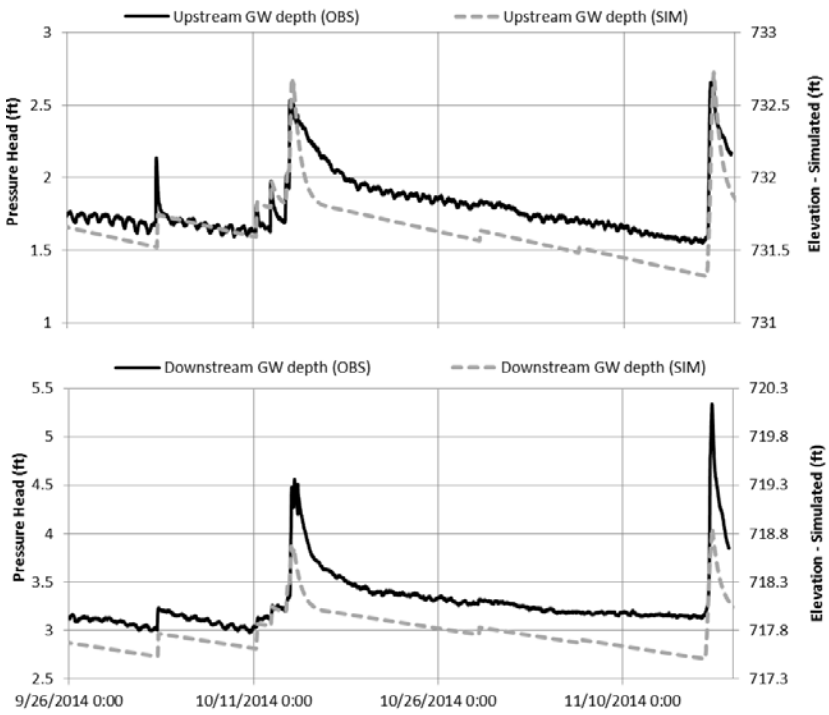

Figure 4.20: Groundwater level comparison of hobo level logger and PCSWMM results for 10/17/2014.

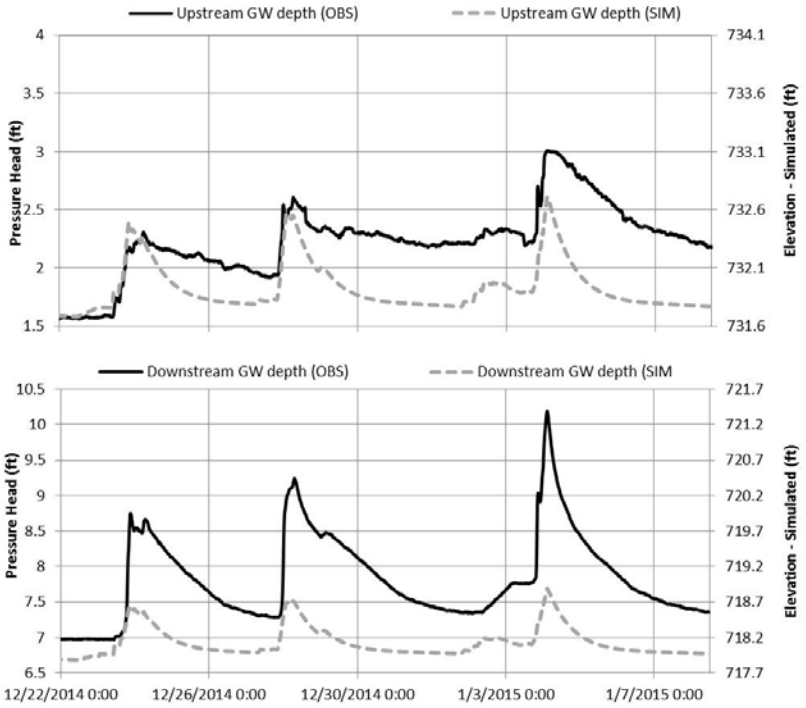

Figure 4.21: Groundwater level comparison of hobo level logger and PCSWMM results for 12/24/14-1/8/15.

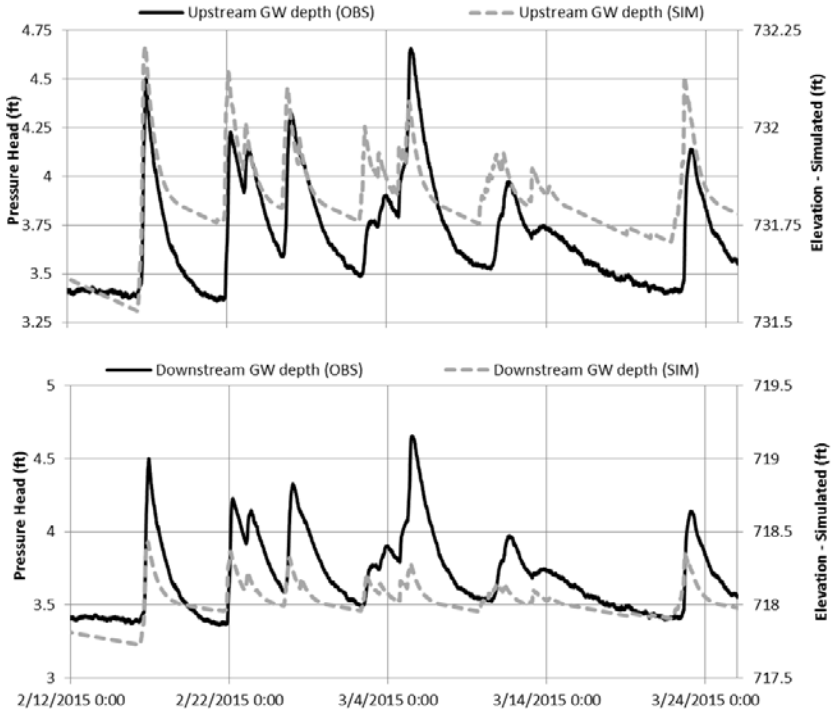

Figure 4.22: Groundwater level comparison of hobo level logger and PCSWMM results for February 2015 rain events (hydrological validation period)

Pollutant Comparisons: TSS

Figure 4.23 through Figure 4.27 are the pollutographs used to calibrate the Total Suspended Solids (TSS) in the LCC watershed. The simulated pollutographs are plotted in comparison to how well each event represents the observed TSS flow (mg/L). Due to issues with the Water Quality Sonde data collection, there were not as many dates available for comparison during the calibration period (6/12/2014-3/26/2015). The dates compared are rain events that occurred on 7/13/2014, 7/15/2014, 8/24/2014, 9/12/2014, 9/15/2014, and 12/27/2014. Only events on 7/13/2014, 7/15/2014, and 12/27/2014 had available data for the downstream site. Among the pollutant calibration dates, 7/13/2014, 7/15/2014 and 9/12/2014 provided the best results for calibration of the upstream site. The peaks for these dates came within approximately 10 cfs of the observed peaks. In some cases the observed flow was underestimated, though for the most part the observed TSS peaks were overestimated, such as on 9/15/2014 for the upstream site. Calibration was attempted for both the dry and wet seasons. However, this limited data posed significant difficulties for a thorough calibration of TSS simulated results.

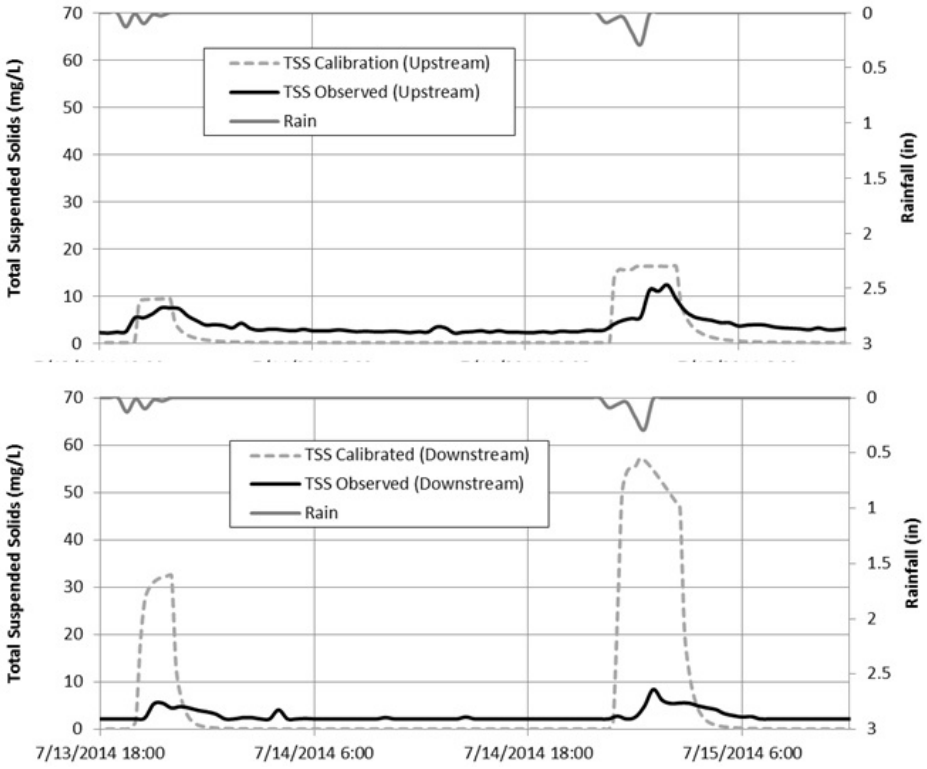

Figure 4.23: Comparison of TSS measured and modeled results for rain event in 7/13/2014-7/15/2014.

From the events provided in Figure 4.23 through Figure 4.27 there is no simple relationship between the summer events and the winter events. The only winter date available, 12/27/2014, shows a significant underestimation of observed TSS. During the same winter events, the flow hydrograph sufficiently replicated the peak flows. Due to the preceding rain event, the TSS that should be available for washoff during the 12/27/2014 event may have been depleted from the previous event on 12/24/2014.

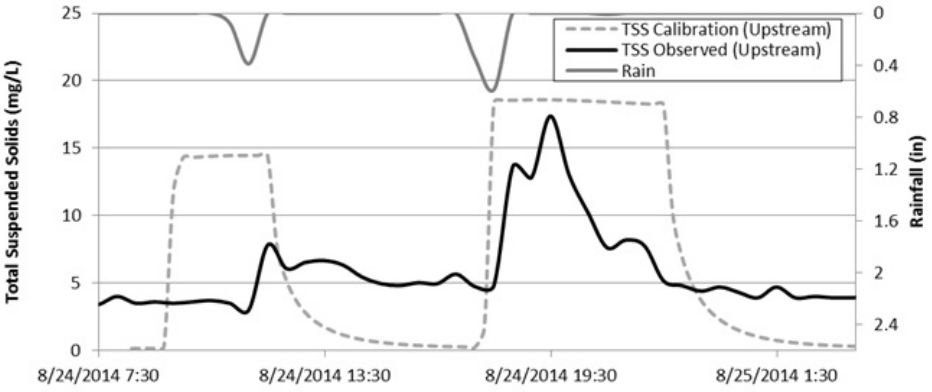

Figure 4.24: Comparison of TSS measured and modeled results for rain on 8/24/2014.

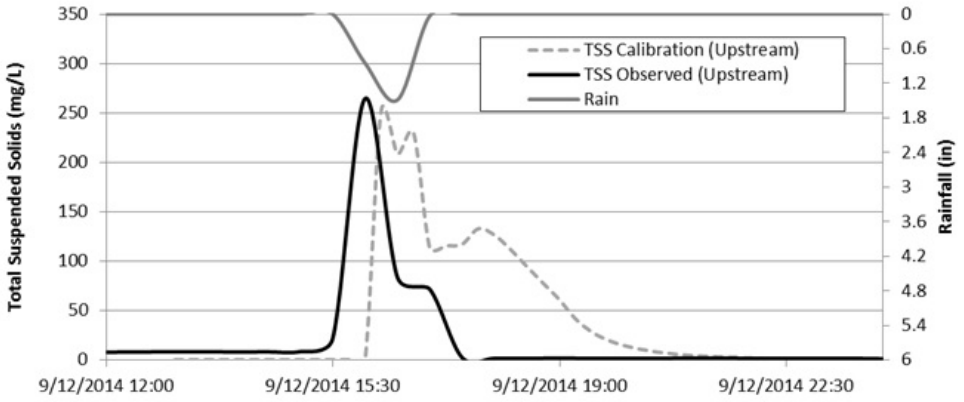

Figure 4.25: Comparison of TSS calibration modeled results for rain on 9/12/2014.

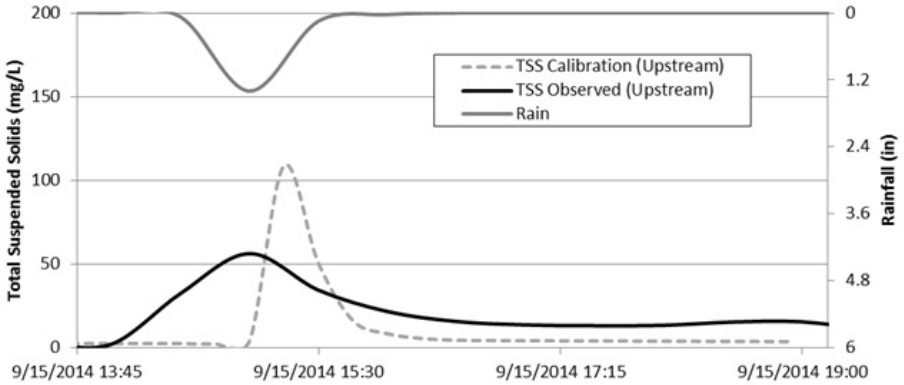

Figure 4.26: Comparison of TSS measured and modeled results for rain on 9/15/2014.

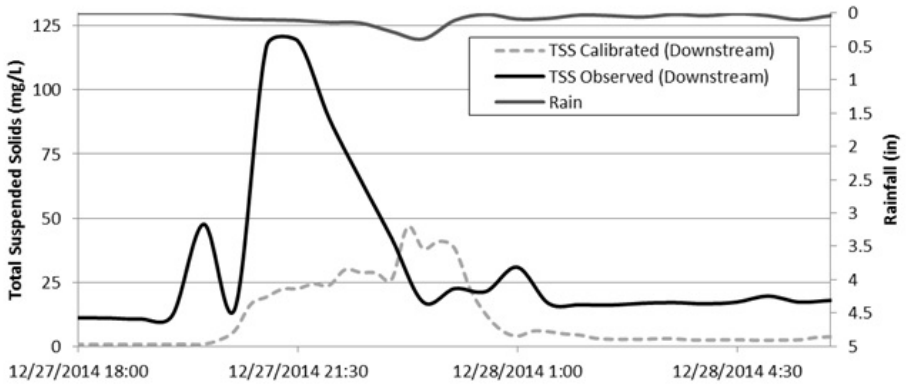

Figure 4.27: Comparison of TSS measured and modeled results for rain on 12/27/2014.

Figure 4.28 through Figure 4.31 display the validation results from the TSS simulation. This validation period is from 6/1/2013 to 6/11/2014. Compared to the accuracy of the calibration results for TSS, the modeling results from the validation period represented fairly

well the observed TSS values. The simulated validation results were also more accurate for the upstream location when compared to the downstream. The reason for the less efficient calibration of TSS at the downstream site may be a result of the limited observed events available for the calibration of the downstream. The runoff characteristics downstream are very different from the upstream location in respects to the amount of impervious area directly surrounding the site.

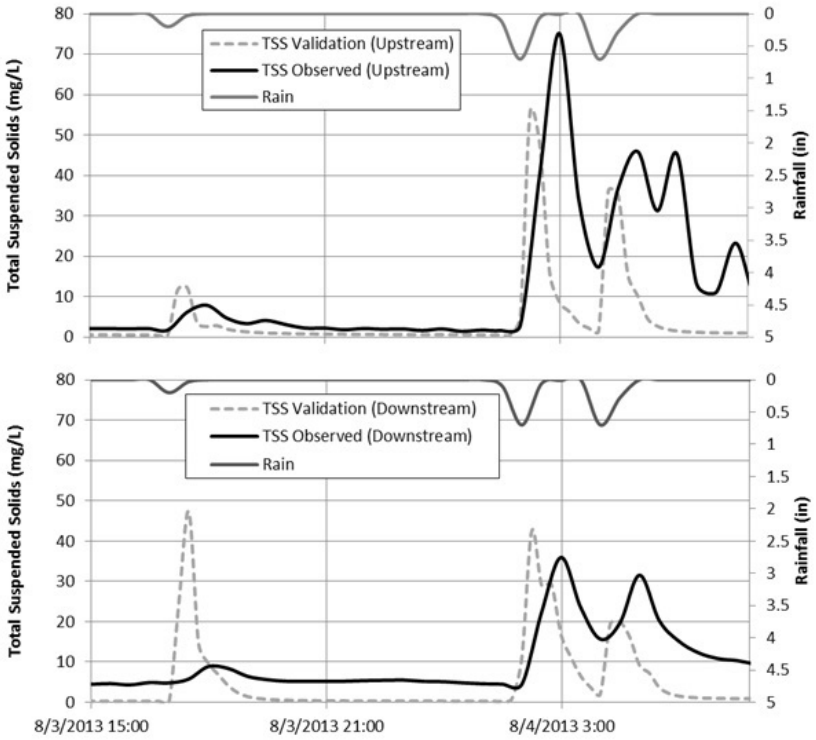

Figure 4.28: Comparison of TSS measured and modeled results for rain on 8/3/2013.

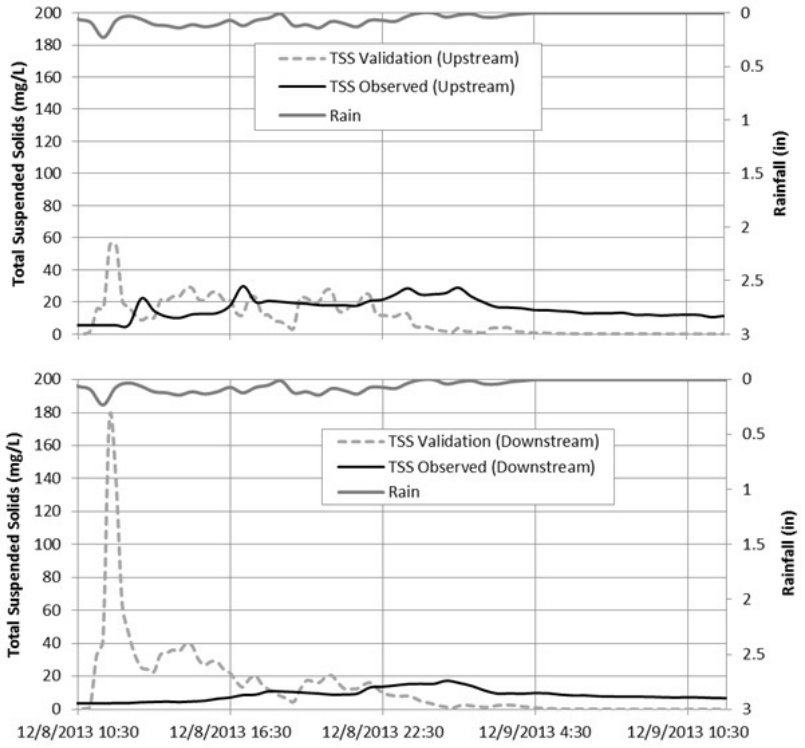

Figure 4.29: Comparison of TSS measured and modeled results for rain on 12/8/2013.

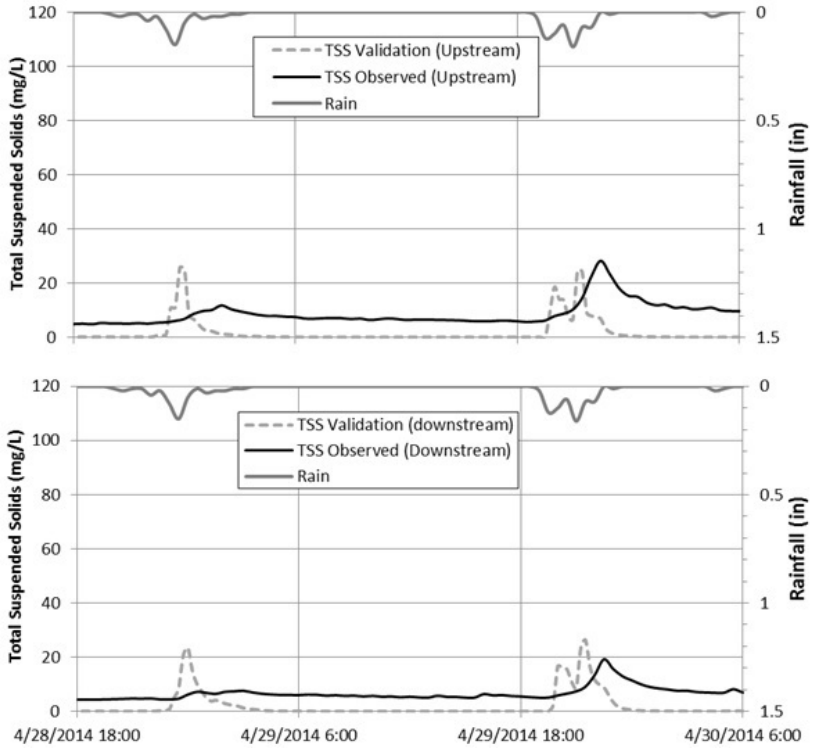

Figure 4.30: Comparison of TSS measured and modeled results for rain on 4/28/2014.

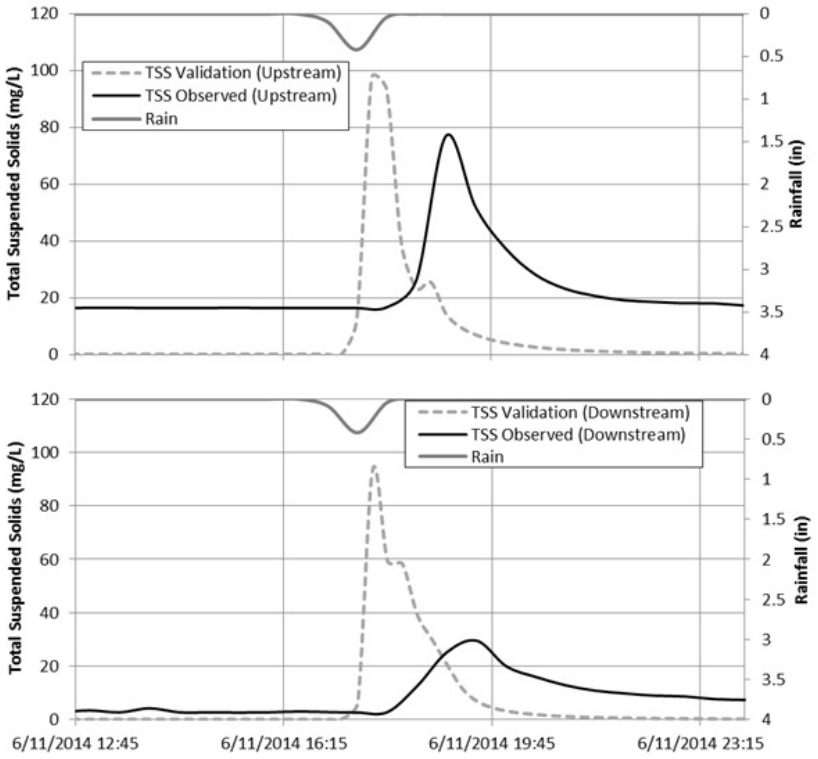

Figure 4.31: Comparison of TSS measured and modeled results for rain on 6/11/2014.

Flow Duration Curves

The following section presents the flow duration exceedance curves comparing the simulated and observed flows for both upstream and downstream. These figures provide a representation of the model's ability to replicate different flows, such as peak flows, recession flows and base flows. In Figure 4.32, the dotted line represents the simulated flow for the downstream location and the solid black line represents the observed flow from the AV sensor at that site. The goal for calibration of the LCC was to replicate the peak flows. As shown in Figure 4.32, the two curves depict a convergent relationship at the higher flows, which are less frequent. The under prediction of the recession curves at low flow rates and the base flow is depicted by the steeper drop at a high exceedance. The poorly represented low flows denote the limitations on the modeling of the aquifer component, which need to be adjusted to more accurately represent the base flow.

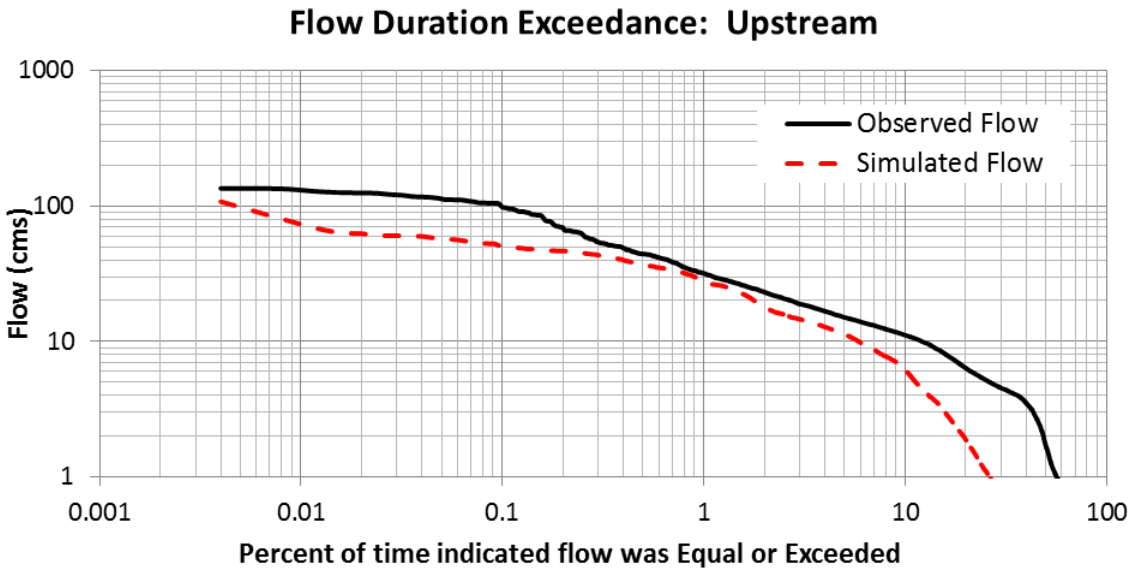

Figure 4.32: Flow duration exceedance-upstream for post-development.

For the downstream location, there is an improved relationship between the simulated and observed peak flows than those represented upstream. In Figure 4.33, the peak flows show an excellent relationship between the two flows. There is not as well of a defined relationship for the flows for 0.01 to 0.15 % exceedance or for the 10 to 30 % exceedance. The reason for this may be a poor representation of the rising and falling limb of the hydrograph. The downstream site also shows a better relationship for lower flows and base flow (~ 2.2 cfs).

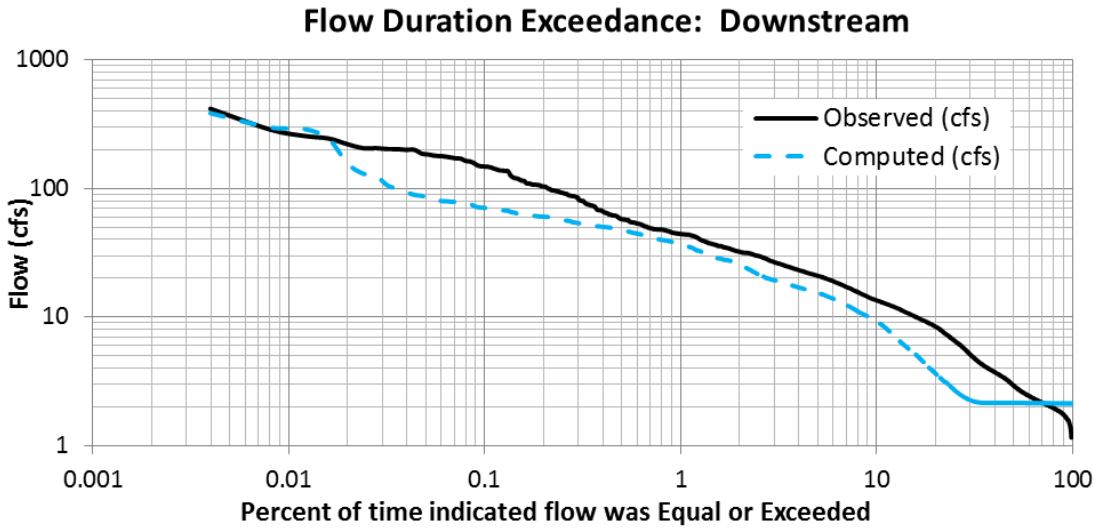

Figure 4.33: Flow duration exceedance- downstream for post-development.

These FDC curves are compared with the simulated flows from the pre-development LCC model results. As shown in Figure 4.34 and Figure 4.35, there is no significant difference between the post- and pre-development LCC models for both the upstream and downstream.

However, there is a difference in the base flow for the upstream site. The base flow results of the pre-development upstream site are lower. For instance, at 10% exceedance, the pre-development model will have a 4.4 cfs, where the post-development results show a 6.5 cfs at the same percent exceedance. There is also some fluctuation between the pre-and post-development results for the larger flows at the downstream site. The change in land use and impervious surface has influenced this peak flow relationship of the LCC model.

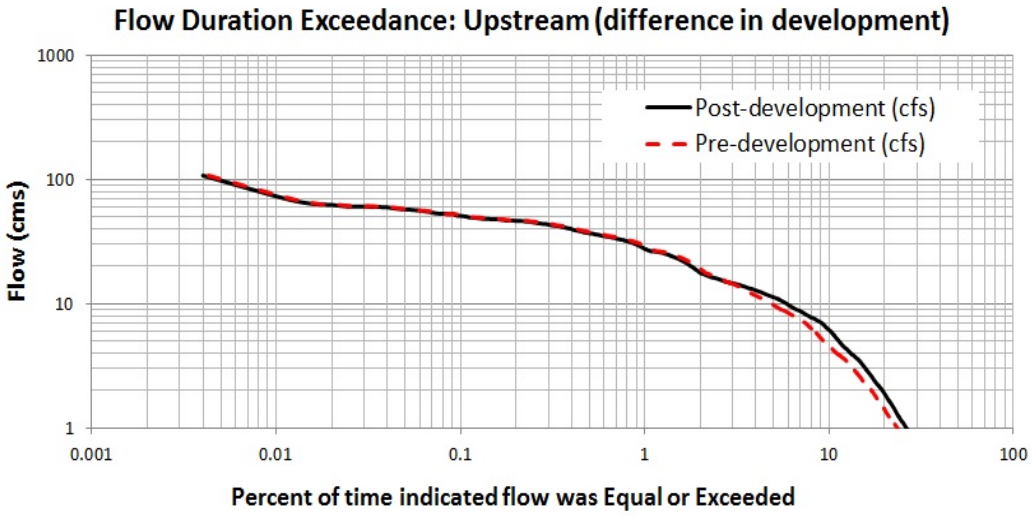

Figure 4.34: Flow duration exceedance-upstream for pre-development.

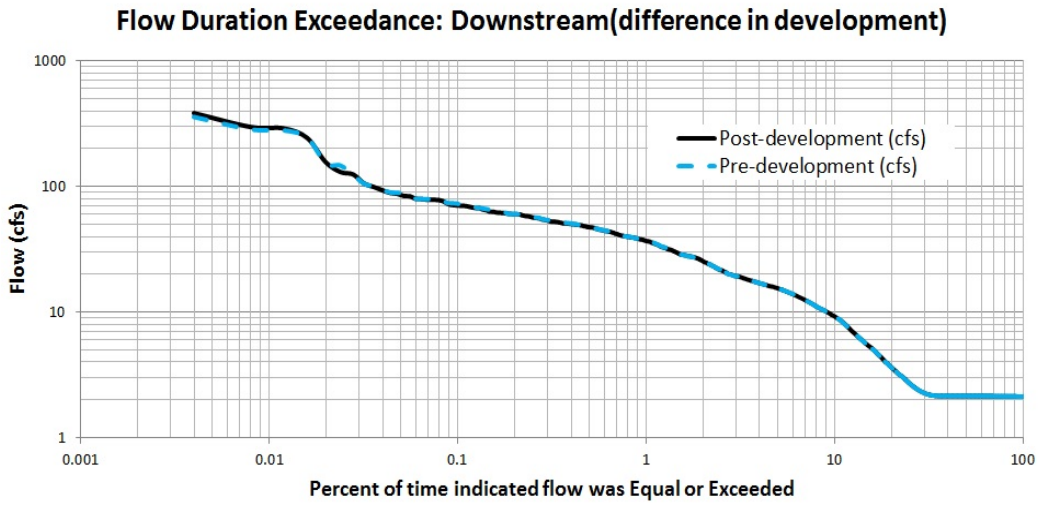

Figure 4.35: Flow duration exceedance-downstream for pre-development.

All of the simulated flows for the upstream and downstream were compared to the corresponding observed flow in Figure 4.36 and Figure 4.37, respectively. A 1:1 linear regression line was plotted to measure the performance of how well the simulated flows replicated the corresponding temporal flow. Overall, upstream manifested a well-defined trend in simulated to observed flow. There were a few outliers represented by the over-prediction of simulated flows; however the large linear cluster of points that show the underrepresented simulated flows, all occurred from the same event 1/4/2015. This event was also shown in Figure 4.36, which depicted a group of flow points that was completely misrepresented by the model. This misrepresentation of observed flow was larger for upstream than for downstream.

Figure 4.37 depicts a more scattered trend between simulated and observed flow rates of the downstream location. The overestimated simulated flow in the 60-100 cfs range is developed from the misrepresentation of small summer events. The LCC model failed to replicate the smaller rain events (rainfall < 0.1 in/hr) and consequently reported large flows when there were none. This misrepresentation could be due to poor calibration of runoff characteristics, particularly during the summer months. On the other hand, the storm event on 1/4/2015 as well as the event on 9/12/2014 produced the underestimated flows that spread from 75 cfs to 256.5 cfs of observed flow. As discussed previously, the event on 1/4/2015 showed a distinct wedge between the observed and simulated flow. This difference could originate from incorrectly calibrated aquifer parameters or even issues with the rain gauge results. As for the underestimated flow on 9/12/2014, this difference in peak flows could be caused by the poorly calibrated runoff characteristics for the summer. Improvement in runoff characteristics for the LCC would benefit both the overestimated and underestimated flows.

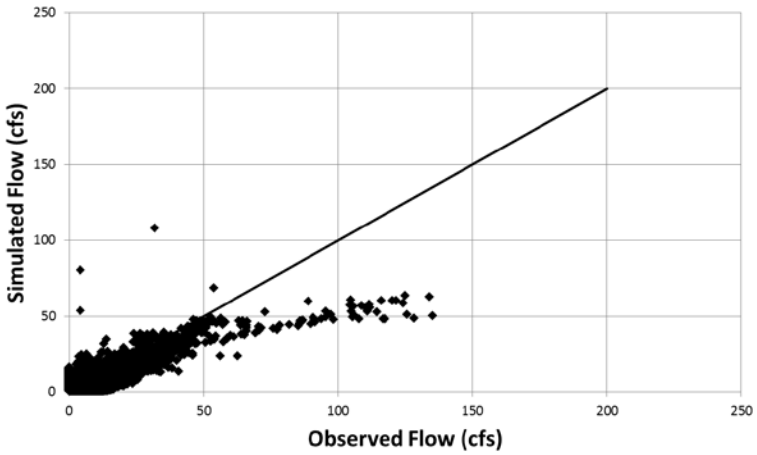

Figure 4.36: Upstream hydrograph error analysis.

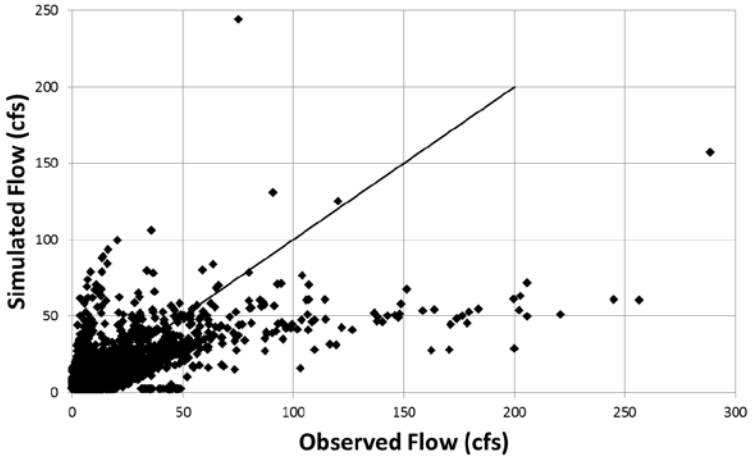

Figure 4.37: Downstream hydrograph error analysis.

In order to further analyze the downstream and upstream locations, a configuration of the specific calibrated and validation peak flows events were analyzed using the SRTC tool in PCSWMM. Figure 4.38 through Figure 4.41 show the linear regression of the plotted events for both sites. Percent envelopes were included to display a 10% and 30% range of values from the 1:1 regression line. Figure 4.38 shows the peak discharge comparison between the observed and simulated flows downstream. As shown, most of the calibration events were within the 30% envelope. The outlier events that underestimated the flow were on 12/23/2014 and 12/27/2014. These events were not able to simulate the groundwater flow accurately. This may be a reason for the underestimation in peak flow.

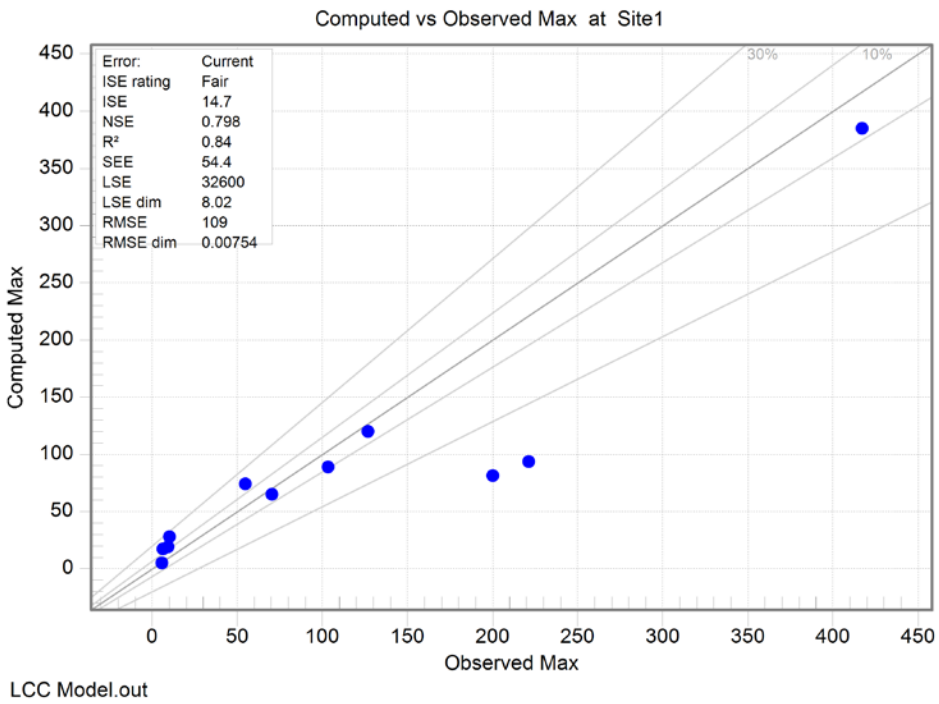

Figure 4.38: Calibration error analysis for max flow at downstream site.

Figure 4.39 shows the simulated and observed flow upstream for all the calibration events. The calibrated flow relationship for the upstream site was not as satisfactory as the relationship downstream; however, there are also only two points that lie outside of the 30% envelope: 10/13/2014 and 11/16/2014. According to Figure 4.39 each event outside the 30% envelope underestimated the peak flow by roughly 15 cfs, which is 37 % of the observed flow that is not being replicated by the simulated result.

The validation error analysis was not as adequate in replicating the observed flow downstream but was more successful in replicating the validation events upstream. These statistics are shown in Figure 4.40 and Figure 4.41. The outlier event for both sites was the rain event on 1/4/2015. As discussed previously, this event significantly underestimated the peak flow at both sites. The reason for this difference in flow may be due to an unobserved or poorly calibrated characteristic of the LCC watershed.

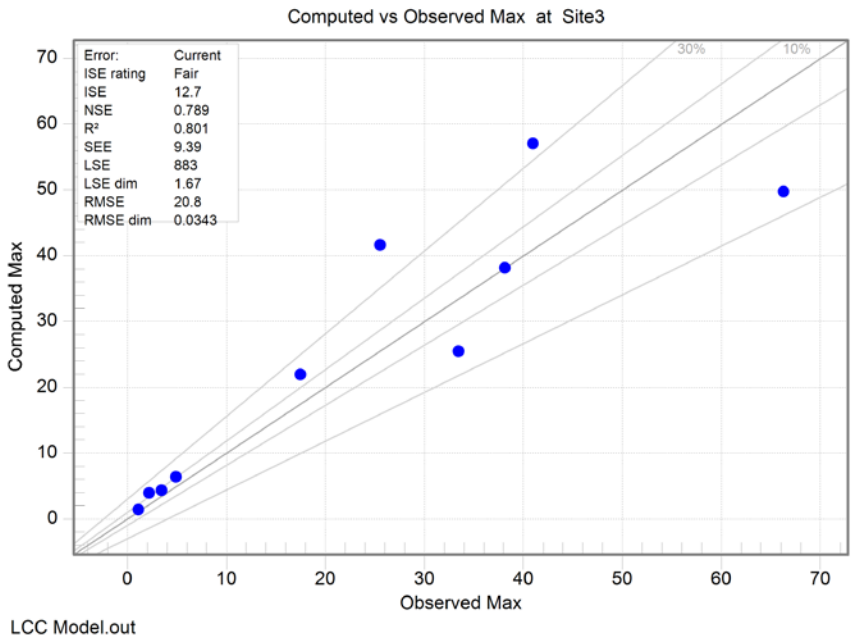

Figure 4.39: Calibration error analysis for max flow at upstream site.

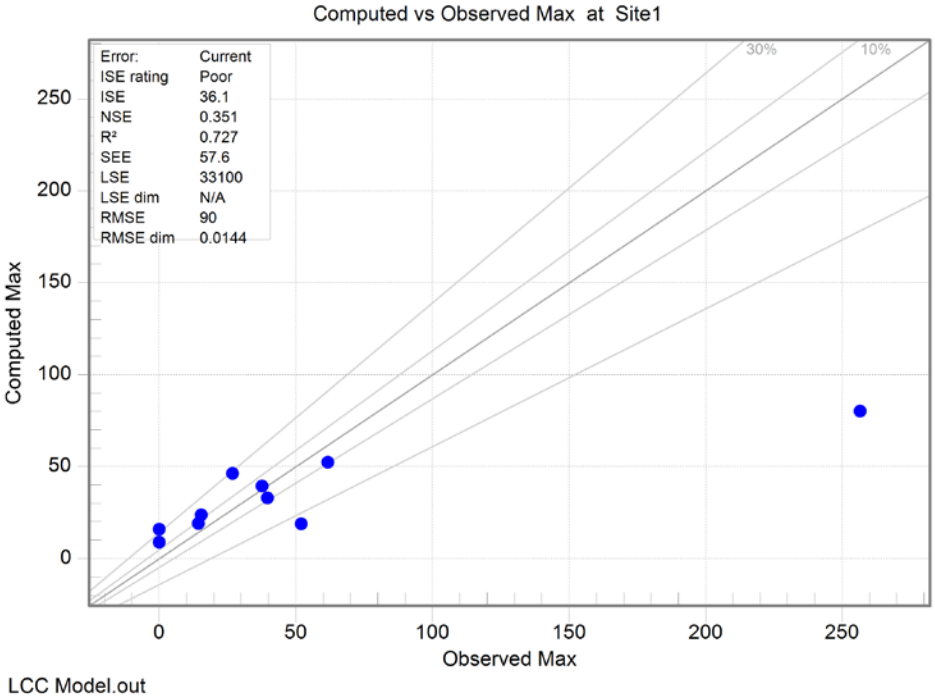

Figure 4.40: Validation error analysis for max flow at downstream site.

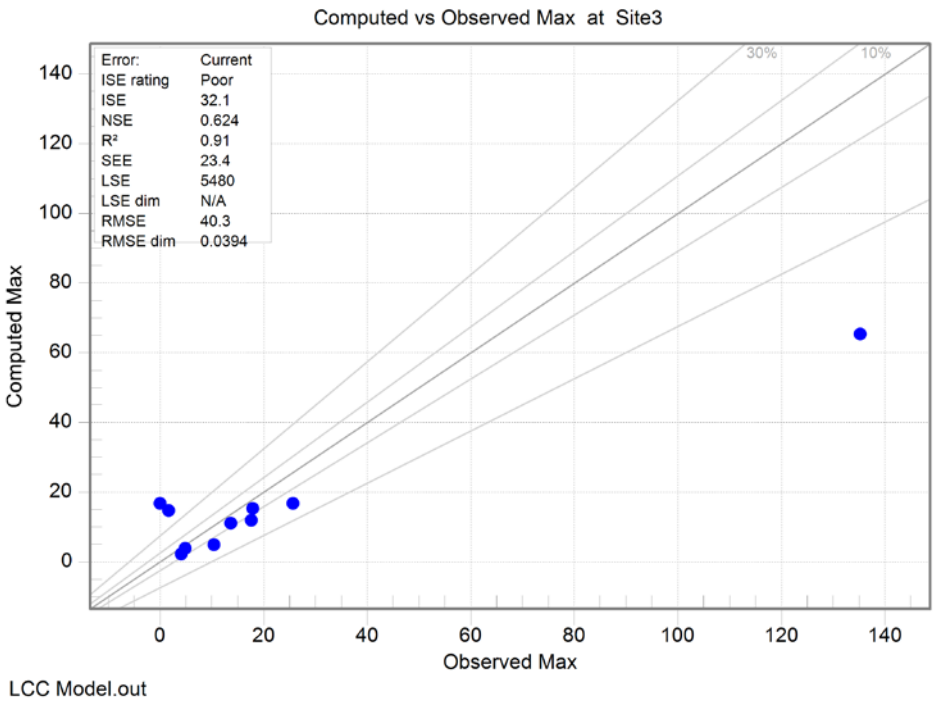

Figure 4.41: Validation error analysis for max flow at upstream site.

Statistical Summary

Following the study conducted by Moriasi et al. (2007), the performances of the hydrographs were evaluated. For this study, the Nash-Sutcliff efficiency (NSE), root mean square error (RMSE), and the coefficient of determination (R^2) are analyzed. When examining R^2 values, values at or values that fell below 0.5 were considered unsatisfactory, and values above 0.5 were considered satisfactory. Since R^2 statistics are oversensitive to high extreme values (outliers) and insensitive to additive and proportional differences between model predictions and measured data (Moriasi et al. 2007), results solely based off of R^2 results can be misleading as there may not actually be a good agreement between the simulated and observed flow. Therefore, NSE values were examined to determine the relative magnitude of residual variance or "noise" compared to the measured data variance (Nash and Sutcliffe 1970; Moriasi et al. 2007). NSE ranges from -∞ to 1, where the latter is the optimal value when agreement is perfect. Table 4.6 presents the performance ratings assigned to the NSE values based on the collaborative study by Moriasi et al. (2007). Also evaluated was the RMSE commonly used for model evaluation statistics, where values approaching zero are more desirable.

Table 4.6: Performance ratings for NSE, (Moriasi et al., 2007)

Performance Rating	NSE
Very Good	0.75<NSE ≤ 1.00
Good	0.65<NSE ≤ 0.75
Satisfactory	0.50<NSE ≤ 0.65
Unsatisfactory	NSE ≤ 0.50

The calibrated peak flows downstream had satisfactory performance ratings for R^2 and NSE, as shown in Table 4.7. However, the RMSE value for the downstream calibrated events was unsatisfactory. The calibrated peak flow upstream had a very good relationship to the available observed TSS data according to Moriasi et al. (2007) NSE performance ratings. The magnitude oscillation from the observed flow was acceptable, but this value should be further improved.

Table 4.7: Calibration error analysis for all calibrated simulations

	Max Flow (ft3/s)		
Station	**R2**	**NSE**	**RMSE**
Site 1	0.727	0.351	90
Site 3	0.91	0.624	40.3

Table 4.8 shows the performance ratings of the validation period for both downstream and upstream sites. The overall performance of the upstream validation worsened. The RMSE value more than doubled. The NSE value representing the "noise" in the system was decreased; however, the value is still within the satisfactory performance ratings. Nonetheless, with the large RSME value, these results did not meet expectations.

Downstream validation results worsened as well. The NSE value dropped to 0.351 and the R^2 value dropped to 0.727. The RMSE decreased. Although RMSE was decreased, since this is a measure of the absolute error, the improved value does not mean necessarily the overall relationship between simulated and observed flow improved. Therefore the validation results for the downstream site were unsatisfactory. The outlying events that may be causing this poor validation relationship occurred on 1/4/2015 and 1/22/2015. As mentioned before, the event on 1/4/2015 showed a gap between simulated and observed flow for both upstream and downstream locations. Excluding these two events from the downstream statistical analysis, the results were

satisfactory. R^2 was 0.662 and NSE was 0.575. Since there was only validation data available mainly during the wet season, there is not a validation of the model's relationship to storm events in the dry season. A longer validation period could potentially improve the statistical results.

Table 4.8: Validation error analysis for all calibrated simulations

	Max Flow (ft3/s)		
Station	**R2**	**NSE**	**RMSE**
Site 1	0.727	0.351	90
Site 3	0.91	0.624	40.3

4.3. Chapter Summary

Within this Results chapter, the difference in upstream and downstream flows and water quality levels were presented and discussed. Starting with the point samples collected in April 2013 to April 2014, there was at most a 33% increase in values between the downstream and upstream sites for turbidity, pH, TSS, NO_3, and TP levels. This is an insignificant increase for nutrients due to the low results and the range of accuracy of the testing instrument. Compared to the NSQD the TSS, NO_3, and TP values were all low.

The Water Quality Sonde and auto-sampler showed that there were increases in peak turbidity and TSS values at the downstream site, averaging 3.7 times larger for turbidity and 4.6 times larger for TSS. The area-velocity sensor showed that on average the downstream peak flows were 1.7 times larger than the upstream peak flows. This increase in flow is most likely from the increase in roadway runoff due to the increase in impervious land use and the 30% increase in subcatchment area flowing into the downstream site.

In order to better quantify the impact of the roadway on the LCC post-development model, a pre-development model was created. The difference in the post- and pre-development model for the upstream and downstream sites were mainly in the smaller range of percent difference as well as the pre- development peak flows being larger than some of the post-development flows. This small difference in flows is verified by the FDCs comparing the pre- and post-development scenarios for both the upstream and downstream sites.

Comparing the upstream pre- and post-development values for TSS, 89% of the differences in flows had less than a 2% difference. However, there was a noticeable difference

between the downstream pre- and post-development TSS levels. 78% of the peak flows downstream showed a difference greater than 5%, ranging as high as 47%.

Overall, the post-development LCC model on average overestimated the upstream and downstream peak calibration flows by 47% and 123%, respectively. During the validation period the upstream peak flows were on average underestimated by 34%, and the downstream peak flows were on average overestimated by 2%.

Chapter 5
Conclusion

Through the investigation of the lower portion Little Cahaba Creek watershed, approximately 2.6 mi^2, which is intercepted by Interstate 59 (ADT of 26.5k to 32.9k), results show that this roadway is not a critical source of water quality impacts in terms of physical, and chemistry parameters such as nutrients. However, on average the observed stormwater peak flows downstream of the interstate were 1.7 times larger than the upstream site, with episodes of very rapid stream flow change, which is expected in the headwater regions of a stream. Monitoring and modeling the LCC has led to the following findings:

Hydrological Behavior

- The LCC is perennial due to the upstream reservoirs through surface water and groundwater supplies.
- During the dry season in the late spring and summer (April to September), high peak flows were observed with little to no recession limb.
- Small rain events (rainfall< 0.2 in) did not produce peak flows higher than 10 cfs.
- Upstream location displays characteristics of a receiving or gaining stream.
- Both sites exhibited a quick surface water and groundwater response to large rain events (> 0.1 in/hr). However, the groundwater level at both sites takes longer to return to the base flow levels.
- The majority of runoff in the LCC is conveyed as overland flow, with little to no hard-piping, therefore abstractions are relatively higher than in more urban watersheds.
- The downstream peak flow from rain events is on average 1.7 times larger than the peak flows upstream. 78% of the rain events had a 50% or greater increase in peak flow downstream. This is a resultant of the 30% increase in subcatchment area flowing into the downstream site as well as the difference in land use.
- There is speculation that there is no overland flow from the forested areas in the LCC; thus the water in the LCC may infiltrate and slowly travel through subsurface flow to the stream.
- Increases in groundwater and base flow were observed in late fall to early spring. Rain events during this period produced peak flows from 50 to 256 cfs with long recession limbs lasting approximately a day.

- Since the LCC, particularly upstream, lies on a fault line, water can easily travel through cracks more quickly than through the clay soils that make up most of that region.

Water Quality Measurements

- Changes in water quality parameters across the intersection between I-59 and LCC, including solids (33% increase), nutrients (approximately a 30% increase), and pH (2% increase), are relatively low. During rain events, these parameters change more dramatically due to runoff, but the impacts of the road runoff to the parameters selected in this investigation are relatively minor. Ongoing studies aim to assess this statement with respect to metals, oil and grease parameters.
- Larger rain events in the summer (>0.4 in total) produced significant spikes in wash-off for TSS and Turbidity.
- There were more significant spikes in washoff occurring during the wet season compared to the dry season runoff.
- The secondary tributary upstream of the interstate, located 2050 ft from the upstream site, is an ephemeral stream that does not display the same characteristics as the upstream location. There is an increase in finer sediment deposited at this site that is causing higher levels of turbidity throughout the year. The momentary increase in turbidity during large storm events, occurring during the fall through winter, may be affecting the turbidity levels downstream. This tributary is typically active from November to May.
- The culvert may also be influencing the TSS levels, causing the larger sediment, such as gravel and large rocks, to be deposited at the upstream site, and the finer sediment, such as clays and silts, to be deposited at the downstream site.
- The overall turbidity and TSS levels recorded at downstream site were not high enough to negatively affect the surrounding ecological habitat, according to EPA regulations. The turbidity ranged on average from 0.5 NTU to 401.

Modeling

- The most sensitive parameters for the LCC were the subcatchment flow length width, % impervious, Horton's maximum and minimum infiltration rates, and channel roughness.
- Hydrological comparison between measured and modeled results showed that the downstream experienced more runoff than upstream, and the TSS pollutographs showed that overall the upstream location showed smaller concentrations of TSS (mg/L) than downstream.
- Additionally, the base flow and recession limbs were not adequately replicated by the simulated flow for both upstream and downstream. This underestimation of base flow from groundwater

leads to the conclusion that the groundwater system of the LCC is more complicated than the proposed LCC model.

- Although observed data is taken from continuous monitoring devices, observed data still needs to be analyzed and consistency verified through support of surrounding monitoring devices. There may be an error in calibration or a drift in data due to a mechanical error in the monitoring device.
- The placement and frequency of rain gauges are a vital role in the performance of any hydrological model. The poor placement of a rain gauge can inhibit a hydrological model from adequately replicating the observed data.
- Applying the SWMM model provided keen insight into the processes and characteristics of the LCC. Through PCSWMM features, the parameters most relevant to this watershed hydrology were quickly detected. Realizing there may be different combinations of the calibrated parameters that yield the same results, the range and applicability of each parameter was assessed as the model was calibrated. In general, the peak flows were well replicated at the upstream site but further calibration needs to be applied to the runoff relationship downstream.
- The processes behind infiltration of the LCC were best replicated with Horton's infiltration model.
- This investigation confirmed the perception that an effective calibration can be achieved with proper delineation, quantification of infiltration and runoff parameters and aquifer material, and deployment of continuous monitoring devices

Not included in the results section of this paper, the macroinvertebrate results obtained on 3/26/2015, confirm that the impact from the interstate and surrounding areas is limited. Overall, the findings listed above, point to the fact that there is no significant impact of the interstate on the specified water quality parameters of the branches monitored in the LCC watershed. However, there was a difference in groundwater characteristics between the upstream and downstream site as well as an increase in the amount of runoff downstream of the interstate that is influenced by the increase in subcatchment area and the difference in land use.

Practical application of these results will serve as a baseline for the post-development stormwater management following the roadway construction phase of the BNB. An additional application of these findings and research on water quality will allow for a more thorough analyzation of the LCC as well as serve as a possible guide to related investigations for characterizing streams in the path of the proposed BNB project. Nevertheless, in order to better characterize the LCC, future studies intend to include present and future results on metals, oils, and greases. Future work in the LCC watershed may also attempt to include more traffic measurement between rain events, correlating with measured pollutants.

Bibliography

Acheampong, M.A., Paksirajan, K., and Lens, P.N. (2012). *Assessment of the effluent quality from a gold mining industry in Ghana*. Environmental Science Pollutant Research, Vol. 10.1007/s11356-012-1312-3.

Angermeier, P. L., Wheeler, A. P., and Rosenberger, A. E. (2004). *A conceptual framework for assessing impacts of roads on aquatic biota*. Fisheries, Vol. 29: 19–29

APHA. (1992). *Standard methods for the examination of water and wastewater*. 18th ed. American Public Health Association, Washington, DC.

American Society of Testing and Materials (ASTM). (1996). *Annual Book of ASTM Standards*. West Conshohocken, PA: ASTM, Vol. 04.08, 1996.

AQEG. (2004). *Nitrogen Dioxide in the United Kingdom*. Air Quality Expert Group. Department for Environment, Food and Rural Affairs.

Arnold Jr., C. L. and Gibbons, C. J. (1996). *Impervious Surface Coverage: The Emergence of a Key Environmental Indicator*. Journal of the American Planning Association, 62:2, 243-258, Vol. 10.1080/01944369608975688.

Barrett, M.E., Malina, J.M., Charbeneau, R.J., and Ward, G.H. (1995a). *Characterization of Highway Runoff in the Austin, Texas Area*. CRWR 263. Center for Research in Water Resources, Austin, Texas.

Barrett, M.E., Zuber, R.D., Collins, E.R., Malina, J.F., Charbeneau, R.J., and Ward, G.H. (1995b). *A Review and Evaluation of Literature Pertaining to the Quantity and Control of Pollution from Highway Runoff and Construction*. Austin, Texas.

Bian, B. and Zhu, W. (2008). *Particle size distribution and pollutants in road-deposited sediments in different areas of Zhenjiang, China*. Environmental Geochem Health, Vol. 31, No. 4, pp. 511-520.

Borris, M., Viklander, M., Gustafsson, A.M. and Marsalek, J. (2014). *Modelling the effects of changes in rainfall event characteristics on TSS loads in urban runoff*. Hydrologic Processes, Vol. 28, 1787–1796.

Bumgardner, J., Ruby, A., Walker, M. (1984). *Discharge Characterization of Urban Stormwater Runoff Using Continuous Simulation*. CRC Press. Inc. 1-5667 0,052-3194

Cambez1, M.J., Pinho1, J., David, L.M. (2008). *Using SWMM 5 in the continuous modelling of stormwater hydraulics and quality*. 11th International Conference on Urban Drainage, Edinburgh, Scotland, UK. pp 1 -10.

Capea, J.N., Tanga, Y.S., van Dijka, N., Lovea, L., Suttona, M.A., Palmer, S.C.F. (2004). *Concentrations of ammonia and nitrogen dioxide at roadside verges, and their contribution to nitrogen deposition*. Environmental Pollution, Vol. 132 (2004) 469–478.

Chin, D.A. (2006). *Water Resources Engineering, 2nd edition*. Upper Saddle River, New Jersey: Prentice Hall.

Chow, V.T. (1973). *Open-Channel Hydraulics*. McGraw-Hill International Editions. Ch. 5. pp 115-126.

Chua, L.H.C., Lo, E.Y.M., Shuy, E.B., Tan, S.B.K. (2009). Nutrients and suspended solids in dry weather and storm flows from a tropical catchment with various proportions of rural and urban land use. Journal of Environmental Management 90 3635–3642.

Chui, T. (1981). *Highway Runoff in the State of Washington: Model Validation and Statistical Analysis*. Master's thesis. University of Washington, Seattle, Washington.

Cole, R. A. (1973). *Stream Community Response to Nutrient Enrichment*. 3. Water Pollution Control Federation, Vol. 45(9): 1874-1 888.

Davis, J., Rohrer, C., and Roesner, L. (2007). *Calibration of rural watershed models in the North Carolina piedmont ecoregion*. In Proceedings of the 2007 World Environmental and Water Resources Congress: Restoring Our Natural Habitat. Reston: ASCE, pages 1-10.

Driscoll, E.D., Shelly, P.E. and Strecker, E.W. (1990). *Pollutant loadings and impacts from highway stormwater runoff volume III: analytical investigation and research report*. Federal Highway Administration Publication No. FHWA-RD-99-008.

Duncan, H.P. (1995). *A review of urban stormwater quality processes*. Cooperative Research Centre for Catchment Hydrology, Melbourne, Australia. Report No. 95/9.

Duncan, R.S., Elliott, C.P., Fluker, B.L. and Kuhajda, B.R. (2010). *Habitat use of the watercress darter (estheostoma nuchale): An endangered fish in an urban landscape*. American Midland Naturalist, Vol. 164, pp. 9-21.

Dupuis, T.V., Kaster, J., and Bertram, P. (1985). *Effects of Highway Runoff on Receiving Waters* - Vol. II Research Report, Federal Highway Administration, Office of Research and Development Report No. FHWA/RD-84/063.

Dussart, G.B.J. (1984). *Effects of Motorway Runoff on the Ecology of Stream Algae*. Water Pollution Control, Vol. 83, No. 3, pp. 409-415.

Finney, K. and Gharabaghi, B. (2011). *Using the PCSWMM 2010 SRTC Tool to Design a Compost Biofilter for Highway Stormwater Runoff Treatment*. Cognitive Modeling of Urban Water Systems. 978–0–9808853–4–7.

Finney, K., James, R., James, W. and Xiao, T. (2013). *Efficiency and Accuracy of Importing HEC-RAS Datafiles into PCSWMM and SWMM5*. CHI Journal of Water Management Modeling. R246-0.

Gassman, P.W., Reyes, M.R., Green, C.H., and Arnold, J.G. (2007). *The Soil and Water Assessment Tool: Historical development, applications, and future research directions*. Transactions of the ASABE. Vol. 50(4): 1211-1250.

Gironàs, J., Roesner, L.A. and Davis, J. (2009). *Stormwater Management Model Applications Manual*. National Risk Management Research Laboratory, Office of Research and Development, US Environmental Protection Agency.

Gould, J.J., Irvine, K.M., Perrelli, M.F., Reth, K. (2010). *Exploring Impacts of Land Use Change on Sediment Erosion in the Cayuga Creek Watershed, Niagara Falls, New York, using BASINS SWAT*. CHI Journal of Water Management Modeling 2010; R236-14.

Gregory M. and Cunningham. (2004). *Improved Parameter Estimation Techniques for Soil Storage Capacity*. Journal of Water Management Modeling 2004; R220-03. pp 1-23.

Grottker, M. (1987). *Runoff quality from a street with medium traffic loading*. Science of the Total Environment, Vol. 59, 457 -466.

Gubernick, B., Clarkin, K. and Furniss, M.J. (2003). "Design and construction of aquatic organism passage at road-stream crossings: site assessment and geomorphic considerations in stream simulation culvert design", In: 2003 Proceedings of the International Conference on Ecology and Transportation (Irwin, C.L., Garrett, P. and McDermott, K.P., Eds.). Center for Transportation and the Environment. Raleigh, NC: North Carolina State University, pp. 30-41.

Haile, T.A, and Rientej, T.H.M. (2005). *Effects Of Lidar Dem Resolution in Flood Modelling: A Model Sentitivity Study For The City of Tegucigalpa, Honduras*. WG III/3, III/4, V/3. pp 1-6.

Hannouche, A., Ghassan, C., Ruban, R., Tassin, B., Lemaire, B. (2011). *Relationship between turbidity and total suspended solids concentration within a combined sewer system*. Water Science and Technology, IWA Publishing, Vol. 64 (12), pp.2445-52.

Harned, D.A. (1988). *Effects of highway runoff on streamflow and water quality in the Sevenmile Creek basin, a rural area in the Piedmont Province of North Carolina, United States Geological Survery*. Water supply paper 2329.

Herrera Environmental Consultants, (2007). *White Paper – Untreated highway runoff in western Washington.*

Hopkinson, C., Hayashi, M., and Peddle, D. (2009). *Comparing alpine watershed attributes from LiDAR, Photogrammetric, and Contour-based Digital Elevation Models*. Hydrological Processes. Vol. 23, 451–463.

Huynh-Ba, G., Williams, C., McGee, C., Orlins, J. (2005). *Measurement and Modeling of Hydrologic Response in a Southern New Jersey Watershed*. Managing Watersheds for Human and Natural Impacts.: pp. 1-11. Vol. 10.1061/40763(178)160.

Irish, L.B., Barrett, M.E., Malina, J.F., and Charbeneau, R.J. (1998). *Use of Regression Models for Analyzing Highway Storm-Water Loads*. Journal of Environmental Engineering Vol. 124(10):987–993.

James, W. (2005). *Rules for Responsible Modeling, 4th edition*. CHI Journal of Water Management Modeling 2006;R184. http://www.chiwater.com/Files/R184_CHI_Rules.pdf.

Jones, T., Johnston, C. and Kipkie, C. (2003). *Using Annual Hydrographs to Determine Effective Impervious Area*. Stormwater and Urban Water Systems Modeling Conference. Practical Modeling of Urban Water Systems, Toronto, Ontario, Canada. Monograph 11. pp. 291-306.

Jones, A.F., Brewer, P.A., Johnstone, E., Macklin, M.G. (2007). *High-resolution interpretative geomorphological mapping of river valley environments using airborne LiDAR data*. John Wiley & Sons, Ltd. Earth Surface Processes and Landforms. pp 1574–1592.

Kayhanian, M., Singh, A., Suverkropp, C. and Borroum, S. (2005). *Impact of Annual Average Daily Traffic on Highway Runoff Pollutant Concentrations*. Journal Environmental Engineering. Vol. 10.1061/(ASCE)0733-9372(2003)129:11(975).

Kim, L.H., Kayhanian, M., Zoh, K.D., Stenstrom, M.K. (2005). *Modeling of highway stormwater runoff*. Science of The Total Environment. Vol. 348, Issues 1-3. pp 1-18.

Line, D.E., Shaffer, M.B., and Blackwell, J. (2009) *Effects of Highway Construction in Sedgefield Lakes and Kings Mill Continued*. Final Report. Raleigh, NC: NC State University, Biological and Agricultural Dept, 9 January 2009. 3-5. Web. Report No. FHWA/NC/2008-17.

Maestre, A., and Pitt, R. (2004). *Nonparametric Statistical Tests Comparing First Flush and Composite Samples from the National Stormwater Quality Database*. Tuscaloosa, AL: University of Alabama Department of Civil and Environmental Engineering.

Malik, U. and James W. (2007). *Reliability of Design Storms used to Size Urban Stormwater System Elements*. CHI Journal of Water Management Modeling 2007;R227-16.

Manning, M.J., Sullivan, R.H. and Kipp T.M. (1977). *Nationwide Evaluation of Combined Sewer Overflows and Urban Stormwater Discharges – Vol. III: Characterization of Discharges*. U.S. Environmental Protection Agency, Cincinnati, OH. EPA-600/2-77-064c (NTIS PB-272107).

Meierdiercks, K.L., Smith, J.A., Baeck, M.L., Miller, A.J. (2010). *Analyses of Urban Drainage Network Structure and its Impact on Hydrologic Response*. JAWRA-09-0149-P. pp 1-12.

Moriasi, D., Arnold, J., Van Liew, M., Bingner, R., Harmel, R., and Veith, T. (2007). *Model evaluation guidelines for systematic quantification of accuracy in watershed simulations*. Transactions of the ASABE, Vol. 50(3):885{900}.

Motiee, H., Motiei, A., Hejranfar, A., and Delavar M. R. (2006). *Assessment of Unaccounted-for Water in Municipal Water Networks Using GIS and Modeling.* Power and Water University of Technology; Inergi LP; Water Distribution Company of Ghazvin; Tehran University. CHI Journal of Water Management Modeling 2006; R225-24

Moynihan, K. (2013). *Field Investigations and SWMM Modeling of an Undeveloped Headwaters Catchment Located in the Lower Coastal Plain Region of the Southeast USA*. M.S. thesis, Auburn Univ., Auburn, AL.

Muleta, M. (2012). *Uncertainty Analysis and Calibration of SWMM Using a Formal Bayesian Methodology*. World Environmental and Water Resources Congress 2012: pp. 562-568.

Nash, J. E., and J. V. Sutcliffe. (1970). *River flow forecasting through conceptual models: Part 1. A discussion of principles*. Journal of Hydrology Vol. 10(3): 282-290.

National Oceanic and Atmospheric Administration (NOAA). (2002). *Climatography of the United States, No. 81: Monthly Station Normals of Temperature, Precipitation, and Heating and Cooling Degree Days 1971–2000*. Asheville, NC: National Oceanic and Atmospheric Administration; National Environmental Satellite, Data, and Information Service; National Climatic Data Center. http://nsstc.uah.edu/aosc/files/ALnorm.pdf

Natural Resources Conservation Service (NRCS). (2011). *United States Department of Agriculture*. Custom Soil Resource Report for Jefferson County, Alabama, and St. Clair County, Alabama. Accessed June 2014.

J. J. Packman, K. J., Comings, and D. B. Booth, (1999). *Using turbidity to determine total suspended solids in urbanizing streams in the Puget Lowlands*. Managing Change in Water Resources and the Environment, Canadian Water Resources Association annual meeting, Vancouver, BC, 27–29 October 1999, p. 158–165.

Peart, J. and Bradford, A. (2007). *Ecological Flow Assessment Techniques for Headwater Reaches*. World Environmental and Water Resources Congress 2007: pp. 1-10, Vol. 10.1061/40927(243)116

Perrelli, M., and Irvine, K. (2013). *Planning Level Modeling of E. Coli Levels in a Suburban Watershed Using PCSWMM.* Pragmatic Modeling of Urban Water Systems, Monograph 21. 423-435.

Peterson, S.A., Miller, W.E., Greene, J.C., and Callahan, C.A. (1985). *Use of Bioassays to Determine Potential Toxicity Effects of Environmental Pollutants*. Perspectives on Nonpoint Source Pollution, pp. 38-45.

Pitt, R., Maestre, A., Morquecho, R. (2004). *The National Stormwater Quality Database (NSQD, version 1.1).* Tuscaloosa, AL: University of Alabama Department of Civil and Environmental Engineering. Ver. 1.1.

Pitt, R. (2007). Water Sample Collection Methods. Module 3 of Experimental Design and Field Sampling. Tuscaloosa, AL: University of Alabama Department of Civil, Construction, and Environmental Engineering.

Pouraghniaei, M.J. (2002). Effects of urbanization on quality and quantity of water in the watershed. MSC of Watershed Management, Natural Resources Research Center of Semnan, Semnan Province, Iran.

Rabalais, N.N., W.J. Wiseman, Jr., and R.E. Turner. (1994). *Comparison of continuous records of near-bottom dissolved oxygen from the hypoxia zone of Louisiana*. Estuaries, Vol. 17:850–861.

Rabalais, N.N., R.E. Turner, and W.J. Wiseman. (2001). *Hypoxia in the Gulf of Mexico*. Journal of Environmental Quality, Vol. 30:320–329.

Rees, P. and Schoen, J. (2009). *PCSWMM Evaluation. Project # 08-08/319 Final Technical Report*. Water Resources Research Center and the Massachusetts Department of Environmental Protection. Amherst MA. pp 1-76.

Rice, Eugene W. (2012). *Standard Methods for the Examination of Water and Wastewater*. 22nd ed. Washington, D.C.: American Public Health Association. Print.

Rossman, L. A. and Supply, W. (2005). *Stormwater management model user's manual, version 5.0*. National Risk Management Research Laboratory, Office of Research and Development, US Environmental Protection Agency.

Sabouri, F., Gharabaghi, B., Perera, B., and McBean E. (2013). *Evaluation of the Thermal Impact of Stormwater Management Ponds*. CHI Journal of Water Management Modeling 2013; R246-12.

Sansalone, J.J. and Buchberger, S.G. (1997). *Partitioning and First flush of Metals in Urban Roadway Stormwater*. Journal of Environmental Engineering, Vol. 123:134-143

Sansalone, J.J., J.M. Koran, J.A. Smithson, and S.G. Buchberger. (1998). *Physical Characteristics of Urban Roadway Solids Transported During Rain Events*. Journal of Environmental Engineering, Vol. 124(5):427–440.

Sansalone, J., Raje, S., Kertesz, R., Maccarone, K., Seltzer, K., Siminari, M., Simms, P., Wood, B. (2013). *Retrofitting impervious urban infrastructure with green technology for rainfall-runoff restoration, indirect reuse and pollution load reduction*. Environmental Pollution, Vol. 183 204-212.

Schmitt, T.G., Thomas, M., Ettrich, N. (2005) *Assessment of urban flooding by dual drainage simulation model RisUrSim*. Water Science Technology, Vol. 52(5):257–264

Selvakumar, A., O'Connor, T.P. and Struck, S.D. (2010). *Role of stream restoration on improving benthic macroinvertebrates and in-stream water quality in an urban watershed: case study*. Journal of Environmental Engineering, Vol. 136, pp. 127-139.

Shamsi, U.M. (2012). *Modeling Rain Garden LID Impacts on Sewer Overflows*. CHI Journal of Water Management Modeling 2012; R245-07.

Stephenson, D. (1989). *Selection of Stormwater Model Parameters*. Journal Environmental Engineering, 1989; Vol. 115:210-220.

Stephenson, J.B., Zhou, W.F., Beck, B.F. and Green, T.S. (1999). Highway stormwater runoff in karst areas – preliminary results of baseline monitoring and design of a treatment system for a sinkhole in Knoxville, Tennessee. Engineering Geology, Vol. 52, pp. 51-59.

Strecker, E., Mayo, L., Quigley, M., Howell, J. (2001). Guidance Manual for Monitoring Highway Runoff Water Quality. FHWA-EP-01-02.

Sun, N., Hall, M., Hong, B., and Zhang, LJ., (2014a). *Impact of SWMM Catchment Discretization: Case Study in Syracuse, New York*. Journal Hydrologic Engineering, Vol.19:223-234.

Sun, B., Ahmed, F., Retiz, F., Qian, Q. (2014b). *Development and Implementation of Wireless Sensor Networks (WSNs) for Measuring Water Quality*. Water Environmental and Water Resources. pp 836-845.

Sutherland, R.C., Minton G.R., and Marinov, U. (2006). *Stormwater Quality Modeling of Cross Israel Highway Runoff*. CHI Journal of Water Management Modeling 2006; R225-08.

Teledyne. (2012). *ISCO 2150 AV Installation and Operation Guide*. Revision DD, June 2012.

Thomson, N. R., McBean, E. A., and I. B. Mostrenko. (1994). *Characterization of Stormwater Runoff from Highways*. CRC Press. Inc. 1-56670-052-3/94.

Thomson, N.R., McBean, E.A., Snodgrass, W. and Monstrenko, I.B. (1996). *Highway stormwater runoff quality: Development of surrogate parameter relationships*. Water, Air, and Soil Pollution, Vol. 94, pp. 307-347.

Tobio, J., Maniquiz-Redillas, M., and Kim, L. (2015) *Application of SWMM in Evaluating the Reduction Performance of Urban Runoff Treatment Systems with Varying Land Use*. International Low Impact Development Conference 2015: pp. 11-20, Vol. 10.1061/9780784479025.002

Trimble, S.W. (1997). *Contribution of stream channel erosion to sediment yield from an urbanizing watershed*. Science, Vol. 278, pp. 1442-1444.

Tsihrintzis, V.A., Hamid, R. (1998). *Runoff quality prediction from small urban catchments using SWMM*. Hydrological Processes, VOL. 12, 311±329.

Turner, R.E. and Rabalais, N.N. (1994). *Coastal eutrophication near the Mississippi river delta*. Nature 368: 619-621.

US Environmental Protection Agency (EPA) (1983). *Results of the Nationwide Urban Runoff Program*. United States Environmental Protection Agency. Water Planning Division, Washington, DC, December 1983.

US Environmental Protection Agency (EPA) (2005). *Stormwater Phase II Final Rule: Small MS4 Stormwater Program Overview*. United States Environmental Protection Agency. Fact Sheet 2.0- 2.10. Revised December 2005.

US Environmental Protection Agency (EPA) (2012). *Water: Monitoring and Assessment*. United States Environmental Protection Agency, Fact sheet 5.5 Turbidity, Revised March 2012.

Vanoni, V.A. (1975). *Sedimentation Engineering, ASCE Manual and Report on Engineering Practice.* No. 54, New York, NY.

Vaze, J. and Chiew, F.H.S. (2002). *Experimental study on pollutant accumulation on an urban road surface*. Urban Water, Vol. 4, pp. 379-389.

Vaze, J. and Chiew, F.H.S. (2004). Nutrient loads associated with different sediment sizes in urban stormwater and surface pollutants. Journal of Environmental Engineering, Vol. 130, No. 4, pp. 391-396.

Vieux, B., and Vieux, J. (2007). *Continuous Distributed Modeling for Evaluation of Stormwater Quality Impacts from Urban Development*. Journal of Water Management Modeling 2007; R227-13.

Viklander, M. (1998). *Particle size distribution and metal content in street sediments.* Journal of Environmental Engineering, Vol. 124, No. 8, pp. 761-766.

Wan, B. and James, W. (2002) *SWMM Calibration Using Genetic Algorithms*. Global Solutions for Urban Drainage: pp. 1-14.

Wheeler, A.P., Angermeier, P.L. and Rosenberger, A.E. (2006). *Impacts of new highways and subsequent landscape urbanization on stream habitat and biota*. Reviews in Fisheries Science, Vol. 13, No. 3, pp. 141-164.

Wilson, C., Papanicolaou, A., Denn, K., and Abban, B. (2014) Quantifying Sediment Sources to the Suspended Load of an Agricultural Stream Using Radioisotopes. World Environmental and Water Resources Congress 2014: pp. 1243-1252, Vol. 10.1061/9780784413548.125

Wu, J., Allan, C., Saunders, W., and Evett, J. (1998). *Characterization and Pollutant Loading Estimation for Highway Runoff*. J. Environ. Eng., Vol, 124(7), 584–592.

Yonge, K.G., Stein, S., Cole, P., Kammer, T. Graziano, F., Bank, F. (1996).*Evaluation and Management of Highway Runoff Water Quality*. Federal Highway Administration. Washington DC.

Yonge, D. (2000). *Contaminant Detention in Highway Grass Filter Strips*. Washington State University, Pullman, Washington.

Yonge, D., A. Hossain, M. Barber, S. Chen, and D. Griffin. (2002). *Wet Detention Pond Design for Highway Runoff Pollutant Control.* National Cooperative Highway Research Program.

Zhang, Y. and Shuster, W. (2014). *The Comparative Accuracy of Two Hydrologic Models in Simulating Warm-season Runoff for two Small, Hillslope Catchments*. Journal of American Water Resource Association, Vol. 50, Iss. 2. 434-447.